University of Aveiro Department of Chemistry

Year 2012

Daniela Sofia Pereira Freitas

"Identifying chemoresistance targets in putative lung cancer stem cells"

"Identificação de alvos moleculares envolvidos em quimio-resistência em possíveis células estaminais cancerígenas de pulmão" (Portuguese)

Dissertation submitted to University of Aveiro to accomplish the requirements for Master of Science Degree in "Bioquímica Clínica", developed under the supervision of Doctor Gabriela Almeida (IPATIMUP) and co-supervision of Professor Doctor Pedro Domingues (Department of Chemistry) of University of Aveiro.

This work was funded by FEDER Funds through the *Programa Operacional Factores de Competitividade* - COMPETE and National Funds from FCT - *Fundação para a Ciência e a Tecnologia* under the project PTDC/EBB-BIO/099672/2008.

Dedico este trabalho à minha família pelos excelentes ensinamentos, conselhos e apoio incondicional. Obrigada por me ensinarem sempre a "ver para além de". A ti mãe por me teres acompanhado sempre muito atentamente e por me recarregares as baterias quando precisei. A ti Ricardo por me teres mostrado muitas vezes o caminho e me ajudares nas tomadas de decisão importantes. E a ti PAI, que embora hoje estejas ausente, estarás sempre presente em todos os meus passos.

Obrigada Ciro pelo acompanhamento diário, força, motivação e inspiração.

Aos meus bons amigos, um muito obrigada pelo grande apoio, especialmente nas alturas mais difíceis.

Agradeço à Doutora Helena Vasconcelos por me ter aceite no seu grupo de investigação e a todos os seus elementos que tão bem me acompanharam e ajudaram no desenvolvimento desde projeto.

À Doutora Gabriela Almeida pela excelente orientação, dedicação e acompanhamento durante toda esta caminhada.

Ao professor Pedro Domingues pelo bom apoio e orientação.

Obrigada Maria Inês Alvelos pela grande receção e pelo empenho com que me transmitiste os teus conhecimentos.

Um muito obrigado a todos os meus professores que contribuíram ativamente para a minha formação.

Agradeço ao IPATIMUP e à Universidade de Aveiro pela colaboração.

Agradeço à FCT e ao projeto COMPETE/QREN/UE (PTDC/EBB-BIO/099672/2008) pelo apoio financeiro.

The Jury

President

Doctor Luisa Helguero
Associated researcher from Department of Chemistry of University of Aveiro

Prof. Doctor Pedro Domingues
Auxiliary professor from Department of Chemistry of University of Aveiro

Doctor Gabriela Almeida
Researcher from Cancer Drug Resistance Group at IPATIMUP

Prof. Doctor Maria Madalena Marques Pedro de Oliveira
Auxiliary professor from ISCS-N

Palavras-chave – Células estaminais cancerígenas, cancro de pulmão, quimio-resistência

Resumo

A resistência tumoral é o maior problema relacionado com a eficácia do tratamento de cancro de pulmão, tipo de cancro com a maior taxa de mortalidade a nível mundial. Atualmente, acredita-se que uma subpopulação de células tumorais, as células estaminais cancerígenas (CECs) que possuem capacidade de autorrenovação e capacidade de sustentar o crescimento tumoral, seja parcialmente responsável pela resistência tumoral face à terapia. De facto, CECs pulmonares isoladas de tumores de pacientes com cancro de pulmão revelaram-se particularmente químio-resistentes. Embora os mecanismos subjacentes à resistência não serem completamente compreendidos, a sobre-expressão de bombas de efluxo, de proteínas anti-apoptóticas e alta eficiência na reparação do ADN parecem fazer parte das propriedades das CECs responsáveis pela resistência aos agentes químio-terapêuticos.

É pretendido, neste projeto, isolar e caracterizar populações de CECs pulmonares e, tendo em conta os seus mecanismos de resistência, identificar possíveis alvos terapêuticos de forma a sensibilizá-las aos fármacos atualmente utilizados clinicamente.

Linhas celulares pulmonares cancerígenas (NCI-H460, A549) foram incubadas com os fármacos cisplatina ou doxorrubicina durante três semanas, seguindo-se um período de recuperação, para isolar uma possível população de CECs. Durante este período, a morfologia celular foi acompanhada e registada. Para medir o efeito de fármacos foram feitos ensaios de crescimento/viabilidade celular (ensaio à base de resazurina e ensaio de sulforodamina B) tanto nas células parentais como nas selecionadas. Realizou-se, ainda, *qRT-PCR* e *Western blot* para averiguar a existência de possíveis mecanismos de resistência nas células selecionadas. Utilizou-se citometria de fluxo e *qRT-PCR* para procurar marcadores de estaminalidade (como, ABCG2 e Sox2) e o ensaio de formação de colónias para verificar o enriquecimento de CECs após uma exposição prolongada aos fármacos.

A exposição aos fármacos levou a uma alteração temporária da morfologia celular, onde as células apareceram com uma estrutura do tipo mesenquimal. A exposição à cisplatina conduziu a um aumento na capacidade das células NCI-H460 resistirem tanto ao agente de seleção como à gencitabina e à doxorrubicina, contudo o mesmo não se verificou

em relação ao 5-FU. Após o tratamento com cisplatina, registou-se um aumento das proteínas anti-apoptóticas, Bcl-XL e XIAP, e da glicoproteína-P, em comparação com as células NCI-H460 parentais. Houve um ligeiro aumento na percentagem de células a expressar ABCG2 e, com menor intensidade, CD133. Relativamente à expressão génica do *Bmi-1* e do *Sox2*, não foi registado nenhum aumento de expressão após o contacto com cisplatina. As células resistentes não demonstraram mais capacidade para formar colónias que as células parentais.

Possivelmente, o aumento da resistência das células após o tratamento com cisplatina deve-se ao aumento de expressão das proteínas Bcl-XL, XIAP e glicoproteína-P. Como trabalho futuro ir-se-á silenciar estas proteínas através de iRNAs, numa tentativa de sensibilizar as células resistentes e validar, assim, estas moléculas como possíveis alvos terapêuticos para ultrapassar a resistência das células pulmonares cancerígenas à quimioterapia.

Key words: Cancer stem cells; lung cancer; chemoresistance

Abstract

Tumour drug resistance is a major issue in the management of lung cancer, the worldwide leading cause of cancer-related deaths. It is currently believed that a small sub-population of tumour cells, the cancer stem cells (CSCs) that possess self-renewal capacity and are able to sustain tumour growth, are partially responsible for tumour drug resistance. Indeed lung CSCs isolated from patients' tumours have been shown to be particularly chemoresistant. Although the mechanisms underlying this resistance are not fully understood, over-expression of efflux pumps, over-expression of anti-apoptotic proteins and efficient DNA repair seem to be involved in resistance of CSCs to chemotherapeutic agents.

In this project we aim to isolate and characterize putative lung CSC populations taking into account the chemoresistance mechanisms of these cells and to identify potential therapeutic targets to render them more sensitive to the chemotherapeutic drugs used in the clinic.

Lung cancer cells (NCI-H460, A549) were incubated with the drugs cisplatin or doxorubicin, for three weeks followed by a drug-free recovery period, in order to isolate a putative CSC enriched population. Cell morphology was monitored and recorded throughout the experiment. Drug-selected and parental cells were incubated with chemotherapeutic agents and multiwell based cell growth/viability assays (resazurin-based and SRB assays) were performed. Western Blot and qRT-PCR were performed to identify possible chemoresistance mechanisms present in the putative CSC enriched populations. Flow cytometry analysis and qRT-PCR for stem cell markers (*e.g.* ABCG2 and Sox2) and colony-forming assay were performed in order to assess enrichment of putative CSCs upon prolonged drug exposure.

Drug treatment led to a transient alteration in cell morphology in both cell lines, whereby cells acquired a more mesenchymal-like structure. In NCI-H460 cells, cisplatin exposure led to increased resistance towards the selecting drug but also to doxorubicin and gemcitabine, although not for 5-FU. Increased expression of the apoptosis-related proteins Bcl-XL and XIAP and of the drug efflux pump P-glycoprotein was verified in the cisplatin-selected population, when compared to the parental NCI-H460 cell line. There was an apparent increase in the percentage of cells expressing the putative stem cell marker

ABCG2, and to a much lesser extent CD133, upon drug treatment. *Bmi-1* and *Sox2* gene expression do not appeared to be up-regulated in selected cells and colony-forming assay did not show any differences between NCI-H460 parental and resistant cells.

The verified increased drug resistance after cisplatin treatment is possibly due to overexpression of Bcl-XL, XIAP and P-glycoprotein. We will now perform RNAi approaches to inhibit the combined expression of these proteins, in an attempt to chemosensitize resistant cells and to validate these molecules as therapeutic targets for overcoming chemoresistance in lung cancer cells.

Table of Contents

1. Introduction 1
1.1 Cancer Stem Cell hypothesis 1
1.1.1. Niche and origin of cancer stem cells 2
1.1.2. The hierarchy model and cancer stem cells 3
1.1.3. Properties and regulation of CSCs 4
1.2. Isolation/Enrichment of CSCs 8
1.2.1. Isolation of CSCs by using cell surface markers 9
1.2.2. Functional assays for CSC isolation 10
1.2.3. CSC enrichment using *in vitro* assays 12
1.3. Mechanisms of CSC resistance to chemo- and radiotherapy and CSC-targeted therapies ... 13
1.4. Drug resistance in lung cancer 18
1.5. Aims 21
2. Materials and Methods 22
2.1. Chemicals and Reagents 22
2.2. Cell lines and culture conditions 22
2.3. Analysis of ABCG2 and CD133 expression by flow cytometry 22
2.4. Fluorescence activated cell sorting (FACS) 23
2.5. Cell growth/viability assays 23
2.5.1. Resazurin-based assay (PrestoBlue): 24
2.5.2. SRB assay: 24
2.5.3. Optimization of the starting conditions for the resazurin-based and SRB assays 25
2.5.4. Cell incubation with chemotherapeutic agents 25
2.6. Enrichment of putative CSCs upon treatment with chemotherapeutic agents 26
2.7. Colony-forming assay 26
2.8. Chicken embryo chorioallantoic membrane (CAM) assay 27
2.9. Western Blot 27
2.9.1. Cell lysates 28
2.9.2. Protein quantification assay 28
2.9.3. Sodium Dodecyl Sulfate-PolyAcrylamide Gel Electrophoresis (SDS-PAGE) 28
2.9.4. Western blotting 29
2.10. Gene expression analysis 30
2.10.1. RNA extraction 30
2.10.2. RNA Treatment with DNase 31

2.10.3. RNA quantification 31
2.10.4. cDNA synthesis 31
2.10.5. Real-Time quantitative PCR 32
2.10. Statistical analysis 33
3. Results 34
3.1. Isolation of putative lung CSCs ($ABCG2^{+}$) by fluorescence activated cell sorting 34
3.2. Chemosensitivity of NCI-H460 cells and $ABCG2^{+}$/$ABCG2^{-}$ sorted cell populations 35
3.2.1. Optimization of the starting conditions for the cell growth/viability assays 35
3.2.2. Cell growth/viability assays 39
3.2.3. Expression of ABCG2 in NCI-H460 cell sorted populations following *in vitro* expansion 40
3.3 Enrichment of putative lung CSCs by incubation with chemotherapeutic agents 41
3.3.1. Assessment of cell morphology 41
3.3.2. Assessment of drug response in the drug-selected populations 46
3.3.3. Assessment of chemoresistance upon novel drug exposure of the drug-selected cell variants 53
3.4. Assessment of expression of proteins involved in drug resistance 56
3.5. Stemness assessment of the cisplatin-selected cell variants 58
3.5.1. Analysis of ABCG2 expression by flow cytometry 58
3.4.2. Colony-forming assay 60
3.4.3. Tumourigenesis assay 60
3.6. Assessment of expression of stemness and drug resistance-related genes 62
4. Discussion 63
5. Conclusions and future perspectives 71
6. References 73

LIST OF FIGURES

Figure 1.1 - Two models for tumour heterogeneity and propagation. a | A normal cellular hierarchy, stem cells (at the apex) progressively generate common and more restricted progenitor cells, ultimately yielding all the mature cell types that constitute a particular tissue. b | In the clonal evolution model all undifferentiated cells have similar tumourigenic capacity. c | In the cancer stem cell (CSC) model, only the CSC can generate a tumour, based on its self-renewal properties and proliferative potential. d | Both models of tumour maintenance may underlie tumourigenesis. Initially, tumour growth will be driven by a specific CSC (CSC1). With tumour progression, another distinct CSC (CSC2) may arise due to clonal evolution of CSC1. This may result from the acquisition of an additional mutation or epigenetic modification. This more aggressive CSC2 becomes dominant and drives tumour formation [35]. 4

Figure 1.2 – CSCs and EMT process. Cancer cells undergoing EMT in primary tumour invade into tumour stroma and enter the circulation, allowing transport to distant organs. At metastatic sites, the cancer cells generate the new metastatic focus through MET (mesenchymal-epithelial transition) [46]. 6

Figure 1.3 - Principal pathways regulating CSCs. The Notch pathway (orange) allows the NICD to translocate to the nucleus and activates transcription. Different growth factors (*e.g.*, EGF, FGF) can activate receptor tyrosine kinases (RTKs, green) that subsequently promote the activity of phosphatidylinositol-3-kinase (PI3K), Akt and mammalian target of rapamycin (mTOR), among others, leading to enhanced protein translation, cell growth, and proliferation. Activation of Hedgehog (Hh, cyan) pathway promotes the translocation Gli into the nucleus and transcription of target genes. The Wnt pathway (yellow) leads to stabilization of β-catenin, which can proceed to activate gene expression. Specific factors in the CSC niches also play critical roles in regulating CSC self-renewal and differentiation, NO produced by endothelial nitric oxide synthase (eNOS, red) can stimulate the production of cyclic guanosine monophosphate (cGMP) and activate protein kinase G (PKG), resulting in enhanced Notch signaling. Low oxygen tension in the hypoxic CSC niche suppresses the activity of prolyl hydroxylase domain-containing proteins (PHDs, blue), leading to stabilization of hypoxia-inducible factors (HIFs) and the transcription of HIF target genes [42]. 8

Figure 1.4 - Mechanisms leading to CSC resistance to chemo and radiotherapy. Cancer stem cells have been found to exhibit a number of genetic and cellular adaptations that confer resistance to classical therapeutic approaches, including relative dormancy/slow cell cycle kinetics, efficient DNA repair, high expression of multidrug-resistance-type membrane transporters, resistance to apoptosis, and protection by a hypoxic niche environment [80]. 13

Figure 1.5 - Comparison of conventional and CSC-based anticancer therapies. A) Conventional therapies (brown flash) target the tumour bulk but are inefficient against CSCs (red), which can subsequently re-establish the original tumour. B) CSC-based anticancer therapies are expected to eliminate CSCs. One approach is either direct killing of CSCs or their differentiation into non-CSCs (orange flashes) that can be targeted in combination with standard treatments. Another strategy entails the disruption of CSC niches, such as hypoxic regions or perivascular regions, or niche-derived signals (blue flashes), which are required for CSC maintenance. Both approaches are additionally combined with conventional anticancer agents (brown flash) to destroy bulk tumour cells. Blood vessels are depicted in pink [42].15

Figure 3.1- Sensitivity of the cell growth/viability assays. Cells were seeded at different densities (from 250 to 16,000 cells/well) in a 96-well plate (four replicate wells per cell density) and incubated for 24 hours prior to processing for the resazurin-based (A) and SRB (B) assays.36
Figure 3.2 - Determination of the optimal starting cell density. Cells were seeded at different densities (from 250 to 16,000 cells) in a 96-well plate (four replicate wells per cell density) and left to adhere during 24 hours. After 48 hours resazurin-based assay was performed. 37
Figure 3.3 - Determination of the optimal starting cell density. Cells were seeded at different densities (from 250 to 16,000 cells) in a 96-well plate (four replicate wells per cell density) and left to adhere during 24 hours. After 48 hours SRB was performed. 38
Figure 3.4 - Cell survival upon incubation with chemotherapeutic drugs (cisplatin, gemcitabine, 5-FU and doxorubicin) in NCI-H460 parental cells and the ABCG2+ and ABCG2- sub-populations, was assessed by resazurin-based (A) and SRB (B) assays. Results are the mean ± SD of three independent experiments (each from an independent cell sorting experiment).39
Figure 3.5 – Fluorescence activated cell sorting for the ABCG2 marker was performed in NCI-H460 cell line. ABCG2 was present in 16% of the NCI-H460 cells when compared with the IgG-PE control. Nine days upon cell sorting, the percentage of ABCG2 in each sorted sub-populations was assessed. The $ABCG2^{+}$ sub-population of cells possessed 15.7% of ABCG2 and the $ABCG2^{-}$ sub-population exhibited 12.2% of cells expressing this protein. Results shown were obtained from cell sorting experiment number 1. 40
Figure 3.6 - Cell morphology changes observed upon incubation of A549 cells with 10 μM of the chemotherapeutic drug cisplatin (for three weeks) followed by a drug-free recovery period (of several weeks). 42
Figure 3.7 - Cell morphology changes observed upon incubation of A549 cells with 0.1 μM of the chemotherapeutic drug doxorubicin (for three weeks) followed by a drug-free recovery period (of several weeks). 43
Figure 3.8 - Cell morphology changes observed upon incubation of NCI-H460 cells with 2 μM of the chemotherapeutic drug cisplatin (for three weeks) followed by a drug-free recovery period (of several weeks). 44
Figure 3.9 - Cell morphology changes observed upon incubation of NCI-H460 cells with 0.05 μM of the chemotherapeutic drug doxorubicin (for three weeks) followed by a drug-free recovery period (of several weeks). 45
Figure 3.10 – Percentage of cell growth following 48 hour incubation with doxorubicin (0 to 0.2 μM) in A549 parental cells and doxorubicin-selected (0.1 μM) A549 cells, was assessed by resazurin-based (A) and SRB (B) assays. Results are the mean of three replicate measurements per sample, performed in two independent experiments. 47
Figure 3.11 – Percentage cell growth following 48 hour incubation with doxorubicin (0 to 0.1 μM) in NCI-H460 parental cells and doxorubicin-selected (0.05 μM) NCI-H460 cells, was assessed by resazurin-based (A) and SRB (B) assays. Results are the mean of two independent experiments. 48
Figure 3.12 – Cisplatin-resistant cell variant A (derived from NCI-H460 when treated with 1 μM of cisplatin) and parental cells (NCI-H460) were incubated with different concentrations of cisplatin (0 to5 μM) for 48 hours. The percentage of cell growth was assessed with resazurin-based (A) and SRB (B) assays. Results are the mean ± SD of three independent experiments, * $P < 0.05$. 49
Figure 3.13 – Cisplatin-resistant cell variant B (derived from NCI-H460 when treated with 2 μM of cisplatin) and parental cells (NCI-H460) were incubated with different concentrations of

cisplatin (0 to 5 μM) for 48 hours. The percentage of cell growth was assessed with resazurin-based (A) and SRB (B) assays. Results are the mean ± SD of three independent experiments, * $P < 0.05$ and ** $P < 0.01$. 50

Figure 3.14 - Drug-selected and NCI-H460 parental cells were incubated with different concentrations of gemcitabine, 5-FU and doxorubicin. The percentage of cell survival was assessed with a resazurin-based (A) and the SRB (B) assays. Results are the mean ± SD of three independent experiments, * $P < 0.05$ and ** $P < 0.01$. 52

Figure 3.15 – Cisplatin-resistant cell variant C (derived from cisplatin-resistant cell variant B when treated with 5 μM of cisplatin), cisplatin-resistant cell variant B and parental cells (NCI-H460) were incubated with different concentrations of cisplatin (0 to 10 μM) for 48 hours. The percentage of cell growth was assessed with resazurin-based (A) and SRB (B) assays. Results are the mean ± SD of three independent experiments, * $P < 0.05$, *** $P < 0.001$ and **** $P < 0.0001$ (calculated between cisplatin-resistant cell variant c and parental cells). 54

Figure 3.16 – Doxorubicin-resistant cell variant A (derived from doxorubicin-treated cells when treated with 0.1 μM of doxorubicin) and parental cells (NCI-H460) were incubated with different concentrations of doxorubicin (0 to 0.2 μM) for 48 hours. The percentage of cell growth was assessed with resazurin-based (A) and SRB (B) assays. Results are the mean ± SD of three independent experiments, * $P < 0.05$ and ** $P < 0.01$. 55

Figure 3.17 – Western blot to XIAP, Bcl 2, Bcl-XL and to Pgp were performed using two independents extractions of total protein from each population of cells (A – cisplatin-resistant cell variant A; B – cisplatin resistant cell variant B). Actin was used as a loading control. 56

Figure 3.18 – Quantification of Pgp, XIAP and Bcl-XL expression using actin as a loading control. Each value represents the mean of two independent samples tested at least in two different occasions. 57

Figure 3.19 - Western blot was perfomed to P53 and Pgp proteins in CRCVA, CRCVB and NCI-H460 parental cells. After 24 hours of cisplatin exposure, all the treated populations up-regulated P53, althuogh a higher overexpression was found between the NCI-H460 parental cells. Only the CRCVA population was capable to up-regulate Pgp protein after 24 hours of drug exposure. Ctr – control cells; Trt – treated cells. Results represent one single experiment. 58

Figure 3.20 - Flow cytometry analysis for ABCG2 was performed in NCI-H460 parental cells (A), cisplatin-resistant cell variant A (B) and in cisplatin-resistant cell variant B (C). Results shown are representative of three independent experiments. 59

Figure 3.21 – Percentage of cells expressing ABCG2 was assessed by flow cytometry analysis in NCI-H460 parental cells and in cisplatin-resistant cell variants A and B, when compared to cells labelled with IgG-PE of each population. Results are the mean ± SD of three independent experiments, * $P < 0.05$. 60

Figure 3.22 – Tumour formation in CAM tissue. Seven days after $1x10^6$ cells from NCI-H460 parental cells (A) and CRCVB (B) being inoculated on CAM, tissue was dissected and fixed and tumours observed. Images are representative of the results obtained in condition 1. 61

LIST OF TABLES

Table 1.1 - Markers used in isolation and identification of CSC from different cancers. Adapted from [35, 42]. 11

Table 2.1 - List of antibodies used. 30

Table 2.2 - Primer sequence and expected PCR product length. 33

Table 3.1 - Cell sorting performed in NCI-H460 cell line using ABCG2 antibody. Three independent cell sorting experiments were performed. 35

Table 3.2 - Tumourigenesis of CRCVB and NCI-H460 parental cells. The capacity of CRCVB and parental cells to generate tumours *in vivo* was assessed by CAM model. The number of chicken embryos presenting a CAM tumour 7 days after cell inoculation is represented relatively to the final numbers of surviving chicken embryos. Results are representative of one single experiment. 61

Table 3.3 - Quantifications of gene expression through RT-PCR. *ABCG2*, *Sox2*, MDR1 and *Bmi-1* genes expression was quantified in CRCVA and CRCVB relatively to the amount of all tested genes in NCI-H460 parental cells. *Hprt1* gene was used as a loading control. Results are the mean ± SD of three independent experiments. 62

LIST OF ABBREVIATIONS

5-FU - 5-Fluorouracil

ABC - ATP-binding cassette

ABCG2 - ATP-binding cassette sub-family G member 2

AND - Ácido desoxirribonucleico

ALDH - Aldehyde dehydrogenase

ALL - Acute lymphoblastic leukemia

AML - Acute myeloid leukemia

AML - Acute myeloid leukemia

APS - Ammonium persulfate

Bcl 2 - B-cell lymphoma 2

Bcl-XL - B-cell lymphoma extra-large

BCRP - Breast cancer resistance protein

BSA - Bovine serum albumin

CAM - Chorioallantoic membrane

cGMP - Cyclic guanosine monophosphate

Chk 1/2 Kinase - Checkpoint kinase 1/2

CRCVA - Cisplatin resistant cell variant A

CRCVB - Cisplatin-resistant cell variant B

CRCVC - Cisplatin-resistant cell variant C

CSC - Cancer Stem Cell

dFdCDP - Gemcitabine diphosphate

dFdCTP - Gemcitabine triphosphate

DIABLO - Direct inhibitor of apoptosis binding protein

DNA - Deoxyribonucleic acid

dNTPs - Deoxyribonucleotides triphosphate

DOX - Doxorubicin

DRCVA - Doxorubicin-resistant cell variant A

ECL - Electrochemiluminescence

EDTA - Ethylenediaminetetraacetic acid

EGF - Epidermal growth factor

EGFR - Epidermal growth factor receptor

EMT - Epithelial-mesenchymal transition

eNOS - Endothelial nitric oxide synthase

FACS - Fluorescence activated cell sorting

FBS - Foetal bovine serum

FC - Fold changes

FGF2 - Fibroblast growth factor 2

FZ - Frizzled

Gli - Glioma-associated oncogene homologue

HCl - Hydrogen chloride

Hh - Hedgehog

HIFs - Hypoxia-inducible factors

HNSCC - Head and neck squamous cell carcinoma

IAP - Inhibitor of apoptosis

IG50 - Concentration corresponding to 50% of growth inhibition

LRP - Lipoprotein receptor-related protein

MDR1 - Multidrug resistance protein

MET – Mesenchymal to epithelial transition

mTOR - Mammalian target of rapamycin

MTT - 3-(4,5-dimethythiazol-2-yl)-2,5-diphenyl tetrazolium bromide

NICD - Notch intracellular domain

NSC - Normal Stem Cell

NSCLC - Non-small cell lung cancer

NTC - Non-template controls

OD - Optical density

PBS - Phosphate buffered saline

PCR - Polymerase chain reaction

PE - Phycoethrin

Pgp - P-glycoprotein

PHDs - Prolyl hydroxylase domain-containing proteins

PI3K - Phosphatidylinositol-3-kinase

PKG - Protein kinase G

PTCH - Patched

qRT-PCR - Real-time quantitative reverse transcription PCR

RPMI-1640 - Roswell Park Memorial Institute – 1640 medium

RT - Reverse transcription

RTKs - Receptor tyrosine kinases

SCC - Squamous cell carcinoma

SCID - Severe combined immunodeficiency

SCLC - Small cell lung carcinoma

SDS-PAGE - Sodium Dodecyl Sulfate-PolyAcrylamide Gel Electrophoresis

Smac - Second mitochondria-derived activator of caspase

SMO - Smoothened

Sox 2 - SRY (sex determining region Y)-box 2

SP - Side population

SRB - Sulforhodamine B

T0 - Time zero

TBS-T - Tris buffer saline - tween

TCA - Trichloroacetic acid

TEMED - Tetramethylethylenediamine

TS - Thymidylate synthase

XIAP - X-linked inhibitor of apoptosis protein

1. Introduction

Over the last decades, our understanding of human cancer development has greatly increased and much progress has been made regarding cancer therapy. Nevertheless, our ability to develop clinically effective therapies based on this knowledge has had limited success [1]. After an apparently successful initial therapy, many tumours often relapse in a more aggressive form than the original tumour [2]. It has been postulated that a small subpopulation of cells with self-renewing capacity, multipotent differentiation [3-6], tumourigenic potential [3, 5, 7], expression of stem cell markers [3-12], increased invasiveness [6, 7], radioresistance [3], chemoresistance [3-7], and resistance to apoptosis [2, 11] could sustain malignant growth, the cancer stem cells (CSCs) [13]. In order to totally eradicate the tumour, cancer therapies should target this specific population of cells [2]. Studies regarding this population of cells have emerged after John Dick's group demonstrated, in 1997, that acute myeloid leukaemia (AML) can contain a small population of cells that are capable to develop AML in immunodeficient mice after isolation and transference of these cells into the hosts [14]. The resulting leukaemia recapitulated the morphologic and immunophenotypic heterogeneity of the original disease [14].

In 2003, Michael Clarke's group was the first to isolate CSCs from a solid tumour. They isolated CSCs from breast cancer and only the cells sorted through $CD44^{+}/CD24^{low}$ phenotype were capable of transplanting disease into immunodeficient mice. This population, comprising about 11-35% of the cells constituting the tumour, gave rise to tumours in the mice that recapitulated the morphological and immunophenotypical features of the original tumour [15].

1.1 Cancer Stem Cell hypothesis

Cancer stem cells are also known as cancer initiating cells because of their capacity to re-establish part of the phenotype found in the primary tumour when transplanted into animal models [16]. The cancer stem cell hypothesis states that cancer stem cells have three defining features: they are able to self-renew, to generate all the heterogeneous cell types present in a tumour, and are the only cells within a tumour that can give rise to

secondary tumours [17]. The features of CSCs and their ability to resist conventional chemo and radiotherapy urge the need to find a specific therapy capable of destroying this subpopulation of cells [18]. CSCs have additional characteristic traits like a distinct surface marker expression profile, and the capacity of asymmetric/ symmetric cell division that allows the CSC population to maintain/expand itself and, at the same time, to give rise to a more differentiated progeny of tumour cells [17].

1.1.1. Niche and origin of cancer stem cells

Stem cells have a specialized microenvironment that surround them, such as nerves, mesenchymal cells and extracellular matrix, which regulate how these cells participate in tissue regeneration, maintenance and repair [19, 20]. The niche interacts with them and release factors to regulate stem cell self-renewal and differentiation, confining the normal stem cells expansion. CSCs are, possibly, originated from a normal stem cell that mutated and escaped the normal niche, and then expands and aberrantly differentiates into the cells that would comprise the bulk of the tumour [21, 22]. When CSCs are out of the niche control they can use mechanisms that enable them to commander alternative niches in order to benefit of self-renewal signals [2]. If aberrant niche microenvironments are responsible for the modulation of CSCs, this could be a good target for cancer therapy [2].

It is not clear if CSCs originate from normal stem cells or from differentiated cells [23]. For many types of leukaemia there are evidence which favours a stem cell origin for CSCs [24]. In solid tumours, the data suggests that CSCs can originate from a stem cell, but it has been also postulated that they can have an origin in cells that are already in the differentiation process [25]. In 2008, Rapp *et al*. have induced plasticity in differentiated cells by injecting a cocktail of oncogenes in the host, reprogramming a series of events. After this, they proposed a model of oncogene-induced plasticity for CSCs origin [1]. Li *et al*, in 2009, defended that CSCs originate from normal stem cells (NSCs) due to genomic instability, and they suggest that CSCs are possibly responsible for the heterogeneity found in tumours [26].

1.1.2. The hierarchy model and cancer stem cells

For more than a century, it has been acknowledged that tumours are composed of morphologically heterogeneous cells, and by the mid-twentieth century researchers understood that cancer cells also show functional heterogeneity both *in vitro* [27, 28] and *in vivo* [29, 30]. It has been documented that the vascular network around the tumour can, partially, dictate the phenotypic and behavioural heterogeneity found in tumour cells [31]. This includes non-cancer cells such as inflammatory cells, cancer associated fibroblasts and immature myeloid cells, all of them influencing tumour behaviour and often facilitating invasion and metastasis [32, 33]. The classical view of tumour formation is based on the "stochastic" or "clonal evolution" model [13], where the neoplasm, which results from one single cell, is seen as a mass of highly proliferative cells with similar potential for driving tumour growth. Tumour heterogeneity and progression are caused by microenvironment variations and genetic mutations in individual cells, followed by selection of mutant clones (clonal evolution) that are best adapted to support the further growth of the tumour [34]. An alternative concept that has been gaining increasing experimental support is the "hierarchy" or "cancer stem cell" model [35]. The cells within a tumour have heterogeneity and only a subpopulation of cells has the ability to initiate and perpetuate tumour growth. This model reports that cancer stem cells have stem cell-like properties, such as self-renewal and capacity to differentiate into the distinct cellular subtypes of the tumour (Figure 1.1). The heterogeneity found in the tumour is the result of the differentiation process from a stem cell precursor that sits on top of the tumour's "differentiation hierarchy" [36], which may also include some level of plasticity.

The CSC theory model tries to explain both the wide heterogeneity observed in the original neoplasm and tumour relapse after treatment, proposing that a sub-population of cells is especially resistant to therapy [37]. However, the identification, quantification and clinical relevance of cancer stem cells are still controversial issues. It has been difficult to associate the development of some types of cancer to this theory, including the origin of cancer stem cells in the tumour [38].

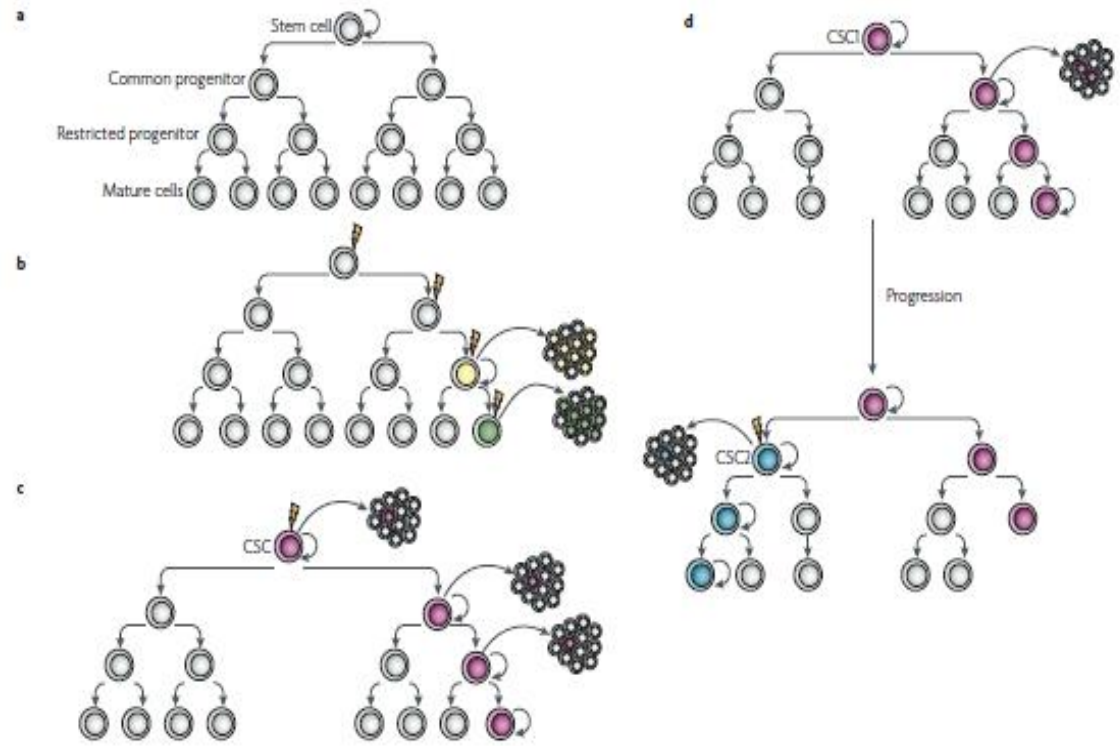

Figure 1.1 - Two models for tumour heterogeneity and propagation. a | A normal cellular hierarchy, stem cells (at the apex) progressively generate common and more restricted progenitor cells, ultimately yielding all the mature cell types that constitute a particular tissue. b | In the clonal evolution model all undifferentiated cells have similar tumourigenic capacity. c | In the cancer stem cell (CSC) model, only the CSC can generate a tumour, based on its self-renewal properties and proliferative potential. d | Both models of tumour maintenance may underlie tumourigenesis. Initially, tumour growth will be driven by a specific CSC (CSC1). With tumour progression, another distinct CSC (CSC2) may arise due to clonal evolution of CSC1. This may result from the acquisition of an additional mutation or epigenetic modification. This more aggressive CSC2 becomes dominant and drives tumour formation [35].

1.1.3. Properties and regulation of CSCs

Different properties of CSCs, such as self-renew potential [3-5], multipotent differentiation [3-6], tumourigenic potential [3, 5, 7], expression of stem cell markers [3-12], increased invasiveness [6, 7], proliferation as tumour spheres [3-5], radio-resistance [3], chemo-resistance [3-7], quiescence [2], resistance to hypoxia [39-41] and resistance to apoptosis [2, 11] have been documented. The self-renewal potential allows the cells to go through unlimited cycles of cell divisions, giving origin to a wide range of differentiated/specialized cells, while maintaining the undifferentiated state [2]. These characteristics are responsible for the tumourigenic ability and heterogeneous phenotype found in tumours, being considered the key properties of CSCs [2]. CSCs express some

stem cell markers like CD133, a 5-transmembrane glycoprotein which function is still unknown, or ATP-binding cassette (ABC) transporter proteins, which are believed to be associated with therapy-resistant phenotype, making these surface markers a good target to find and isolate CSCs [12].

According to the hierarchy model, CSCs are required for the initiation and growth of primary tumours. These capacities make them a possible cause for tumour relapse and metastasis [42]. Metastasis consist of a series of sequential transforming events involving invasion of tumour cells from primary neoplasms, followed by their dissemination through lymphatic or blood vessels, culminating in the establishment of metastasis at distant sites [37]. Recent data have supported the concept of metastatic CSCs, whereby a subpopulation of colorectal CSCs was found to possess exclusive metastatic potential and appeared to be the cause of distant metastasis in colon cancer patients. In addition, they exhibited enhanced chemoresistance [43]. It is possible that a tumourigenic CSC can acquire a migrating phenotype during an epithelial to mesenchymal transition process (EMT), whereby epithelial cells acquire mesenchymal features, occurring in the primary tumour [37]. This process would then allow these CSCs to spread to distant sites due to the loss of cell-cell and cell-extracellular matrix adhesion mediated by E-cadherin repression. A similar phenotype has been found between CSCs and cells which have undergone EMT in mammary carcinoma CSCs [44]. EMT is associated to tumour cell invasion and metastasis, and the process initiates with cell to cell adhesion disintegration and, consequently, loss of epithelial markers (such as E-cadherin) and gain of mesenchymal markers (such as vimentin). Subsequently, there is loss of basoapical polarization and the acquisition of front-rear polarization. Then, the cytoskeleton undergoes remodelling, with changes in cortical actin and actin stress fibres. Finally, cell-matrix adhesion is changed, with activation of proteolytic enzymes such as matrix metalloproteases [45]. These multiple steps result in detachment of cells from primary tumour, invasion of the surrounding stroma, which allows them to enter into circulation and reach new metastatic sites (Figure 1.2) [46].

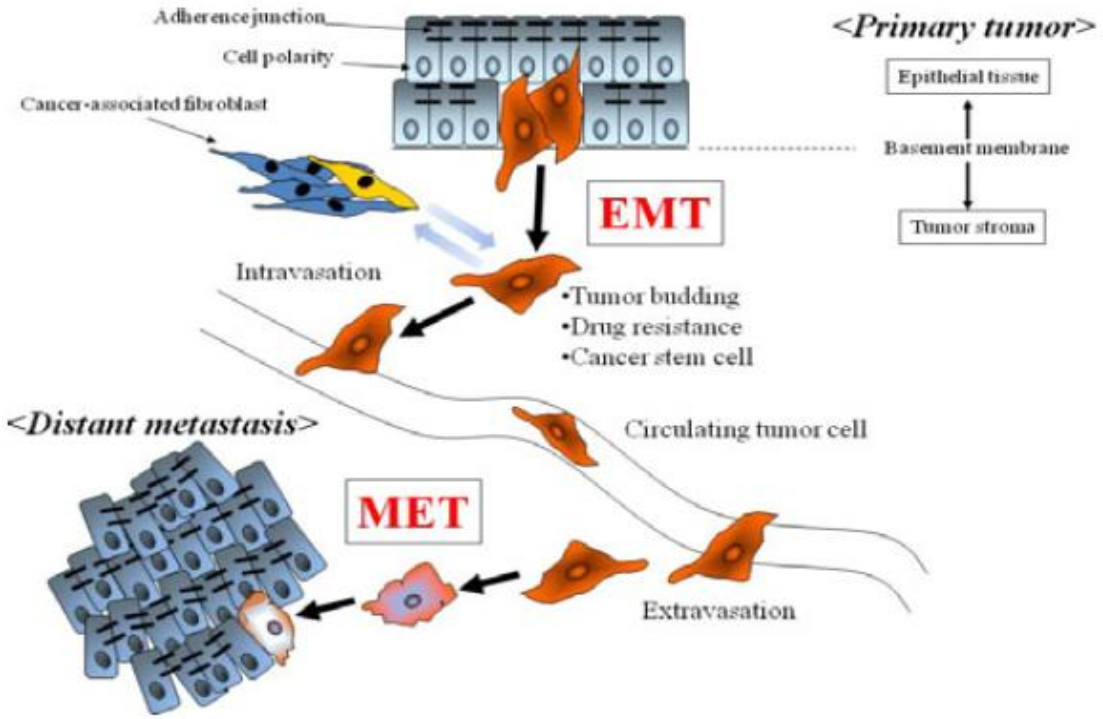

Figure 1.2 – CSCs and EMT process. Cancer cells undergoing EMT in primary tumour invade into tumour stroma and enter the circulation, allowing transport to distant organs. At metastatic sites, the cancer cells generate the new metastatic focus through MET (mesenchymal-epithelial transition) [46].

To better understand the characteristics of CSCs it is essential to study their regulation, being reported that signalling pathways involved in self-renewal and differentiation reveal substantial overlaps between CSCs and normal stem cells [42]. The Notch pathway is involved in the stem cell maintenance and differentiation and has been implicated in CSC function. This pathway is activated by the binding of transmembrane ligands (Delta/Delta like proteins or Jagged) to the membrane receptor Notch. This induces the proteolytic cleavage of Notch by γ-secretase, promoting the release of Notch intracellular domain (NICD), which enters the cell nucleus and modifies gene transcription (Figure 1.3) [42]. It has been documented that Notch receptors and ligands are overexpressed in breast cancer, leading to transformation of normal breast epithelial cells into more resistant cells towards drug-induced apoptosis [47]. The Notch pathway has been correlated with CSCs. The activation of Notch signalling in glioma cells increases the expression of stem cell markers and enhances self-renewal [48, 49].

The Wnt signalling is crucial for the control of multi/pluripotency, proliferation and differentiation in embryonic and adult stem cells and it is stated has necessary for CSC self-renewal and tumourigenicity [42]. This pathway is initiated when Wnt ligands link to transmembrane complex of receptors, the Frizzled (FZ) and lipoprotein receptor-related protein (LRP). A series of signalling steps are then activated, leading to stabilization of β-catenin, which can modify gene expression (Figure 1.3) [42]. Malanchi *et al* proved that in skin CSCs the activation of β-catenin is enhanced, and when they removed the β-catenin gene in mouse skin cancer models a loss of CSCs was evident leading to complete tumour regression [50].

Another signalling pathway playing a key role in regulation of stem cells of various tissues and in CSCs is the Hedgehog pathway [42]. Usually the receptor Patched (PTCH) inhibits Smoothened (a G protein coupled receptor), but when Hedgehog ligands bind to Patched receptor, the inhibition of Smoothened (SMO) protein is removed, which leads to the activation and translocation of Gli (glioma-associated oncogene homologue) transcription factor into the nucleus, providing transcription of its target genes (Figure 1.3) [42]. When this pathway is inhibited it is possible to suppress CSC proliferation and self-renewal and enhance apoptosis [51]. Since these pathways seem to be related with CSC self-renewal and maintenance of stem cell phenotype, they are a promising approach to therapy [31].

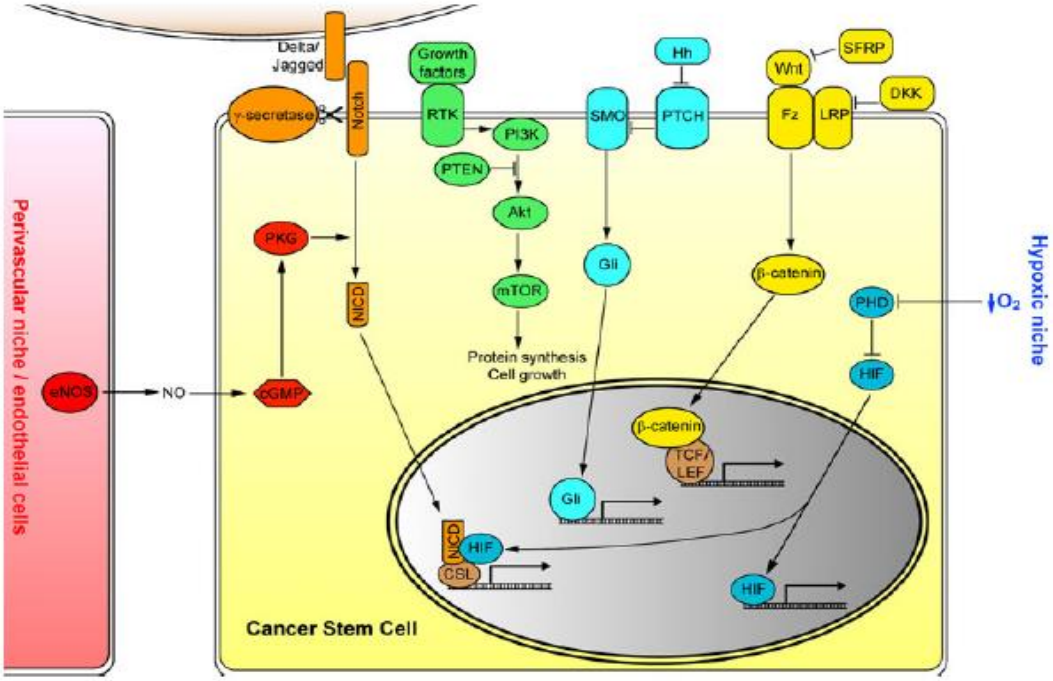

Figure 1.3 - Principal pathways regulating CSCs. The Notch pathway (orange) allows the NICD to translocate to the nucleus and activates transcription. Different growth factors (*e.g.*, EGF, FGF) can activate receptor tyrosine kinases (RTKs, green) that subsequently promote the activity of phosphatidylinositol-3-kinase (PI3K), Akt and mammalian target of rapamycin (mTOR), among others, leading to enhanced protein translation, cell growth, and proliferation. Activation of Hedgehog (Hh, cyan) pathway promotes the translocation Gli into the nucleus and transcription of target genes. The Wnt pathway (yellow) leads to stabilization of β-catenin, which can proceed to activate gene expression. Specific factors in the CSC niches also play critical roles in regulating CSC self-renewal and differentiation, NO produced by endothelial nitric oxide synthase (eNOS, red) can stimulate the production of cyclic guanosine monophosphate (cGMP) and activate protein kinase G (PKG), resulting in enhanced Notch signaling. Low oxygen tension in the hypoxic CSC niche suppresses the activity of prolyl hydroxylase domain-containing proteins (PHDs, blue), leading to stabilization of hypoxia-inducible factors (HIFs) and the transcription of HIF target genes [42].

1.2. Isolation/Enrichment of CSCs

All the studies regarding CSCs are dependent upon the successful isolation of this population of cells, making this a pivotal step in determining the molecular pathways involved in the regulation of CSCs' biological behaviour, such as tumour initiating potential, recurrence, therapy-resistance and metastasis [18, 23]. If it were possible to efficiently isolate the CSC population from each tumour, we could study the nature of their features when compared to non-CSCs. We would then be able to understand the mechanisms underlying therapy resistance of these cells to conventional therapy and find a way to sensitize them, avoiding tumour relapse [18].

1.2.1. Isolation of CSCs by using cell surface markers

The most frequent method to isolate the CSC population from a patient's tumour is based on performing fluorescence activated cell sorting (FACS) for specific cell surface markers found in normal stem cells, such as CD44, CD133, CD24, CD34 or ABC transporter proteins [23, 42]. In most cases these markers are not specific to CSCs, *e.g.*, CD133 was previously found in immature progenitor cells in normal haematopoietic, neural, endothelial and epithelial tissues [52-54]. Even so, these markers are used because they provide enrichment in CSCs and it is possible to isolate a more tumourigenic population than the rest of the tumour cells [42]. Indeed, CSC markers and gene signatures are associated with cancer progression and clinical outcome, and tumours enriched with CSCs have been shown to be more aggressive [55].

Several stem cell markers for the isolation and identification of CSCs have been described in the literature. CD34 is used as a marker for CSCs in a wide types of leukaemias, such as, acute lymphoblastic leukaemia (ALL) [56] and AML [14, 16, 57] (Table 1.1). In solid tumours, the most reported markers for the isolation of CSCs are CD44 and CD133. CD44 has been used to identify CSCs in breast cancer [15], in head and neck squamous cell carcinoma (HNSCC) [58], in prostate cancer [59] and in pancreatic cancer [60]. The CD133 marker is the most frequently used marker to isolate CSCs in a wide spectrum of solid tumours and, unlike other markers that are usually used in combination, CD133 is most of the times used on its own (Table 1.1) [23]. CD133 has been used as a marker for CSCs in medullo-blastoma [61], glioblastoma [58], colon cancer [62-64], pancreatic cancer [65], non-small cell lung cancer [8] and others [23].

By labelling tumour cells with fluorescent antibodies for stem cell markers, it is possible to isolate the positive cells (those who express the marker, the population of cells thought to be the CSCs) and the negative ones (non-CSCs) from the same tumour, using FACS [18]. This approach allows the separation of distinct populations of cells that can be used to study tumour features, such as tumourigenicity, chemo/radio resistance, gene expression and others [11]. Eramo *et al.* identified a rare population of $CD133^+$ cells in lung cancer and a low number of these cells were able to reproduce the original tumour when transplanted into an immunocompromised mice, while the $CD133^-$ population did not present tumour-initiating activity [4]. Bao *et al.* demonstrated that $CD133^+$ cells in fresh glioblastoma specimens or glioma xenografts irradiated *in vivo* were more resistant to

ionizing irradiation than $CD133^-$ cells [66]. They observed that in this model, $CD133^+$ cells activated the DNA damage checkpoint response more efficiently than $CD133^-$ cells [66]. Tumour xenografts derived from $CD133^+$ and $CD133^-$ cells of pancreatic carcinoma were treated with gemcitabine (a drug commonly used in pancreatic cancer therapy) and the results revealed that $CD133^+$ population was more resistant than the negative population. Additionally, immunohistochemistry analysis revealed that the tumour xenografts derived from $CD133^+$ cells reproduced the primary tumour at histological level [65].

It is important to note that the frequency of cells expressing a specific marker may vary within the same tumour type (Table 1.1). In colon cancer, CD133 does not identify CSCs in all patient samples, suggesting that tumours arising from the same tissue may express different surface markers *e.g.*, CD44 and CD133 are co-expressed in colon cancer, but they identify different populations of cells [23]. Some researchers use a combination of markers in order to obtain a more purified population of CSCs, like Chen and colleagues who used $CD133^+CD44^+$ cells to enrich a population of stem-like cells in a colon cancer cell line (HCT116) [67].

1.2.2. Functional assays for CSC isolation

Due to the variation of CSC surface phenotypes in tumours of the same type, some groups tried to isolate CSCs based on their functional activity.

High aldehyde dehydrogenase (ALDH) activity has been described in murine and human hematopoietic, neural stem and progenitor cells [68-70]. Some investigators have used ALDH to isolate CSCs and found these cells in AML [71, 72], in primary breast [73] and colon cancer [74].

Another method to isolate CSCs by FACS is based on their capacity to efflux the fluorescence dye Hoechst 33342, which is due to overexpression of ABC transporter proteins such as ATP-binding cassette sub-family G member 2 (ABCG2) [75]. The cells that have this ability are called side population (SP) and show self-renewal activity, differentiated progeny production, tumourigenicity, expression of CSC markers and stem cell genes [76]. SP have a high capacity of resistance to chemotherapeutic agents and are crucial in tumour recurrence [76-78]. Considering these features are mainly attributed to ABCG2 and its expression is conserved in stem cells, it was consider as a novel biomarker of CSCs [75]. Although there are many markers that can be used to isolate CSCs, the

FACS methodology is not always the best approach, due to the low and variable marker expression. The isolated population is not always totally pure and/or the marker expression rapidly equals that of the tumour, before isolation [11].

Table 1.1 - Markers used in isolation and identification of CSC from different cancers. Adapted from [35, 42].

Cancer type	CSC markers	% of CSC cells in tumour
Acute lymphoblastic leukaemia (ALL)	$CD34^{+}CD10^{-}$ / $CD34^{+}CD19^{-}$	8 ± 4 / 3 ± 1
Acute myeloid leukaemia (AML)	$CD34^{++}CD38^{-}$	0.02 - 2.00
Breast	CD44+CD24low	11 - 35
	$CD44^{+}CD24^{-}ALDH1^{+}$	0.1 - 1.2
Head and neck	CD44	0.1 – 41.7
Prostate	$CD44^{+}\alpha_2\beta_1^{high}CD133^{+}$	0.1 – 0.3
Pancreas	$CD44^{+}CD24^{+}EpCAM^{+}$	0.2 – 0.8
Colon	CD133	1.8 – 24.5
	$EpCAM^{high}CD44^{+}$	0.03 – 38.0
Lung	$CD133^{+}$	0.3 – 22.0
Liver	$CD90^{+}CD45^{-}$	0.7 – 6.2
Brain	CD133	19 - 29
	SP	0.15 – 1.2
Ovarian	$CD44^{+}CD117^{+}$	0.1 – 0.2
	$CD133^{+}$	0.3 – 35.0

EpCAM: epithelial cell adhesion molecule; SP: Side Population.

1.2.3. CSC enrichment using *in vitro* assays

There are some alternative strategies to enrich a CSC population, using *in vitro* assays, which enable at the same time the discovery and the study of CSCs capacities. When a tumour is formed, the rapid expansion of cancer cells creates a hypoxic microenvironment followed by periods of re-oxygenation that allows tumour propagation. It has been postulated that hypoxia can lead to the development of more aggressive cancer by selecting the most resistant population, the one that could survive to adverse conditions like lack of oxygen and nutrients [39-41]. Some authors have explored environment changes that can lead to more aggressive tumours, *e.g.*, Louie *et al.* could enrich a CSC population with stem like properties and metastatic potential by exposing a human metastatic breast cancer cell line to cycles of hypoxia followed by re-oxygenation [79].

The non-adherent sphere and the colony-forming assays are based on the growth of cells from a stem or progenitor cell. However the cell culture conditions used are different. In the first method, cells are in a non-adherent condition and serum free media containing growth factors (*e.g.* EGF-epidermal growth factor and FGF2-fibroblast growth factor 2). In the second one, cells grow on a substitute of the basal membrane (*e.g.* matrigel) with appropriated media. In these *in vitro* assays, cells are in adverse environments, are separated from each other (and in the first assay mentioned they are also in non-adherent conditions); only a cell possessing stem properties will be able to survive and generate a tumour sphere/colony by itself [31, 35]. The non-adherent assay also forces the cells to grow in 3D structures and when the spheres are too big a real tumour could be partially simulated, making this assay a useful surrogate for the *in vivo* CSC assay [31].

All the approaches described above to isolate (such as FACS) or to enrich (like non-adherent sphere and the colony-forming assays) CSC populations usually require confirmation with an *in vivo* assay (or when this is not possible an *in vitro* assay*)* that they are indeed of CSCs. The gold-standard assay to evaluate the presence of CSCs is xenotransplantation, when a selected number of the tumour cells are injected, preferably in an orthotopic location, in immunocompromised mice [35]. With this assay it is possible to check the self-renewal and tumourigenic potential of the cells tested, verifying if they are capable to recapitulate the cellular composition of the primary tumour. [31]. Eramo *et al.* could produce a tumour xenograft by injecting 10^4 undifferentiated lung cancer cells in

severe combined immunodeficiency (SCID) mice, although $5x10^4$ differentiated cells injected were unable to generate tumours in the same tested mice [4].

1.3. Mechanisms of CSC resistance to chemo- and radiotherapy and CSC-targeted therapies

Current cancer therapy has not been sufficient to successfully eradicate tumour cells. Considering that it is now believed that many cancers could be driven by a subpopulation of cells with capacity to sustain tumour growth, the CSCs, a CSC-targeted therapy seems to be the best option to totally eradicate the tumour. In order to achieve this, it is imperative to understand the mechanisms behind CSC therapy resistance. It was suggested that CSCs have gained genetic and cellular adaptations capable of making them more resistant to therapy [80]. Many studies have been performed after an efficient isolation of CSCs in different tumours to try to explain and understand why these cells are chemo- and radioresistant. Although the mechanisms underlying this resistance are not fully understood, relative dormancy/slow cell cycle kinetics, efficient DNA repair, high expression of multidrug-resistance membrane transporters and resistance to apoptosis seem to be the mechanisms involved in CSC resistance to therapy (Figure 1.4) [80].

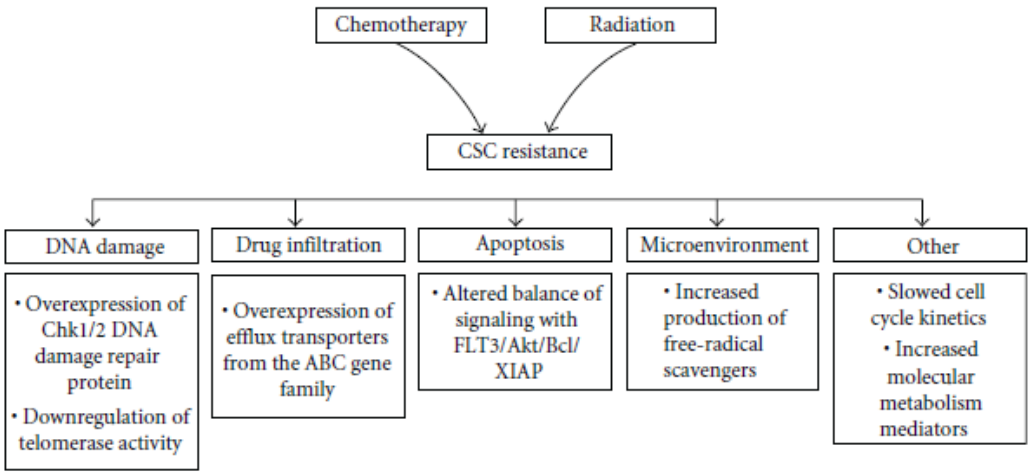

Figure 1.4 - Mechanisms leading to CSC resistance to chemo and radiotherapy. Cancer stem cells have been found to exhibit a number of genetic and cellular adaptations that confer resistance to classical therapeutic approaches, including relative dormancy/slow cell cycle kinetics, efficient DNA repair, high expression of multidrug-resistance-type membrane transporters, resistance to apoptosis, and protection by a hypoxic niche environment [80].

Conventional therapies appear to be capable of eliminating most of the cells in a tumour but not CSCs, which are less sensitive to chemotherapeutic drugs and have higher proliferation potential [13]. Thus, the neoplasm could initially shrink during the first rounds of therapy but, in time, CSCs would be able to re-establish the original tumour (Figure 1.5) [13]. By contrast, if clinical therapies were targeted against CSCs, the neoplasm reduction would be softer, but the cells would not be able to sustain tumour growth, leading to its degeneration (Figure 1.5) [13]. Generally it is believed that a high proportion of CSCs in a tumour are correlated with poor prognosis, *e.g.* high ALDH expression is assumed to be associated with poor prognosis in various tumour types, such as breast cancer [73], AML [71], prostate [81], head and neck squamous cell carcinoma [82] and early-stage lung cancer [6]. It is also believed that radiation and chemotherapy often serve to enrich the resistant CSC population and possibly promote more resistant clones within a heterogeneous CSC population, *e.g.* evidence of radiation-induced enrichment has been found in brain [83] and breast [84] CSCs. This feature has been utilized as a method to enrich the CSC population, as seen with gemcitabine treatment of pancreatic cancer [85], cyclophosphamide treatment of colorectal cancer [74] and with cisplatin, doxorubicin and methotrexate treatment of lung cancer [5]. This may indicate that only a specific and targeted therapy for CSC population would be a successful approach in fighting cancer [31]. It is now established that combination therapy helps preventing the development of cancer resistance. However the co-administration of chemo/radio therapy is not effective in all types of cancer and, in most cases, is much too toxic to be tolerated by the patient [80]. It would be important to test if CSC-targeted therapies combined with traditional cancer therapies is an appropriate strategy for fighting cancer [80].

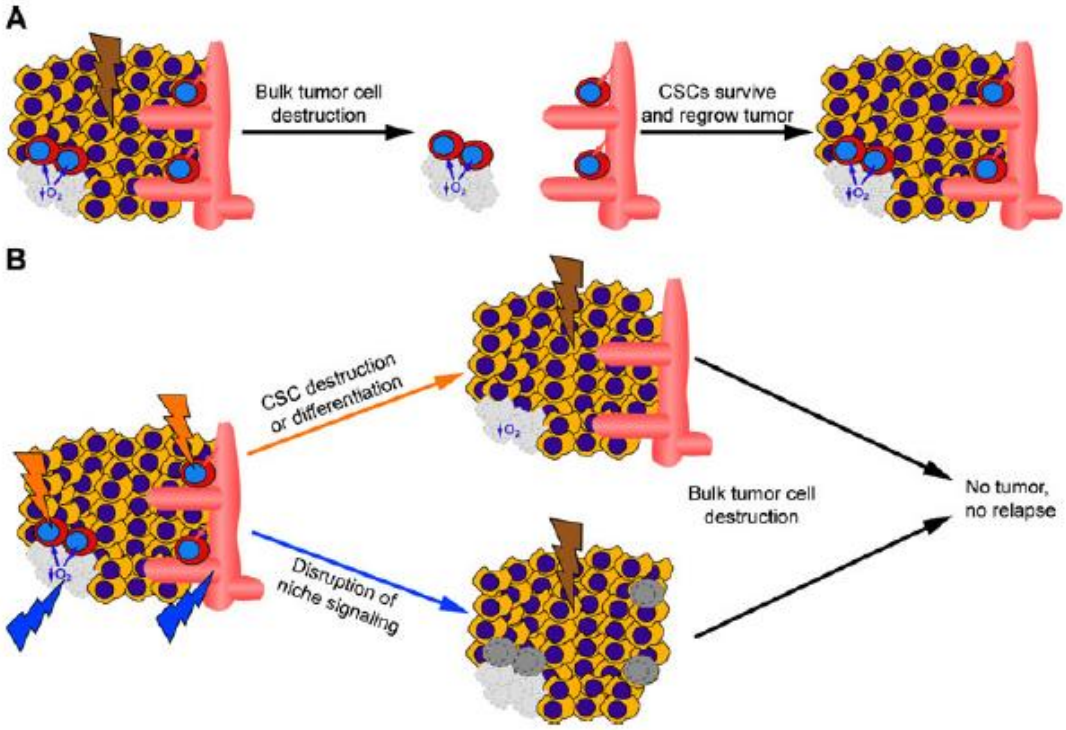

Figure 1.5 - Comparison of conventional and CSC-based anticancer therapies. A) Conventional therapies (brown flash) target the tumour bulk but are inefficient against CSCs (red), which can subsequently re-establish the original tumour. B) CSC-based anticancer therapies are expected to eliminate CSCs. One approach is either direct killing of CSCs or their differentiation into non-CSCs (orange flashes) that can be targeted in combination with standard treatments. Another strategy entails the disruption of CSC niches, such as hypoxic regions or perivascular regions, or niche-derived signals (blue flashes), which are required for CSC maintenance. Both approaches are additionally combined with conventional anticancer agents (brown flash) to destroy bulk tumour cells. Blood vessels are depicted in pink [42].

Radiotherapy and most type of chemotherapeutic agents act by disrupting the cancer cell DNA integrity and it is possible that CSC resistance is due to increased expression of DNA integrity-maintenance systems [86]. Normal stem cells have efficient DNA mutation defence systems but, if these cells mutate, can give rise to CSCs and then it is possible to find in CSCs high DNA damage repair potential [80]. Numerous experiments have demonstrated chemo/radio resistance in CSCs, *e.g.* when a tumour was a target of radiation all the cells showed equal levels of damage, but CSCs had the ability to recuperate quicker [83]. In pancreatic cancer, cell cycle analyses after gemcitabine treatment showed that $CD133^{+}$ cells stopped proliferating but did not undergo apoptosis. When gemcitabine was withdrawn, these cells immediately started to recapitulate the cancer cell pool. In contrast, the $CD133^{-}$ cells (the more differentiated cells, representing the majority of tumour cells) became apoptotic after gemcitabine treatment [37]. The

family of checkpoint kinase 1/2 (Chk 1/2 Kinase) is one potential modulator of CSC resistance to DNA-targeting agents, by arresting the cell cycle to allow DNA repair [66]. These Kinases have higher basal and inducible activities in CSCs than non-CSCs [66] and Chk 1/2 inhibitors can partially reverse the resistance of glioblastoma CSCs to radiation [66].

Radiotherapy depends on the production of oxygen free radicals to cause damage to DNA. It has been postulated that areas of low oxygen levels within a tumour create a microenvironment capable of partially protecting cells against radiotherapy-induced damage [87]. Another way to protect cells from radiotherapy is the presence of free radical scavengers. Vlashi *et al.* found this characteristic enhanced in breast CSCs [88]. It has also been found that CSCs are enriched around blood vessels, depending on signals derived from them [42]. This may explain why antiangiogenic therapies (targeting CSC niche) seem to have a good efficacy [80]. Theoretically, the antiangiogenic therapies may provide a hypoxic microenvironment, conferring radioresistance in cells, although the clinical relevance of this is still unknown. It is possible to speculate that radiation treatment may be more effective in cancer treatment before any antiangiogenic chemotherapy is applied [80].

Stem cells can also protect DNA integrity by preventing the action of mutagen chemicals in cellular DNA. This is possible due to high expression of efflux transporters from ABC gene family, that allows cells to preserve their genome more efficiently [89]. These drug efflux pumps were found in CSCs and they seem to be partially responsible for the chemotherapy resistance phenotype, since they are able to transport the drug out of the cell [90]. When CSCs can be separated from non-CSCs in the same cell line by their capacity to efflux the Hoechst 33342 fluorescent dye (due to the presence of ABC transporters) they are called side-population (SP) [75]. When tests of resistance to chemotherapeutic drugs were made, the SP cells showed higher percentage of cell viability than non-SP cells after 24 hours of drug exposure [7]. Although this mechanism of cell defence does not explain radiation resistance, a blockage of multidrug efflux pumps may provide an efficient method to make cells sensitive to clinical chemotherapeutic drugs already used [80].

Many authors have utilized Western blot assay to evaluate the protein levels of specific pathways, to find a possible cause for tumour-resistance therapy. The overexpression of apoptosis inhibitor proteins may also be behind of CSCs resistance to

therapy. The mitochondrial pathway of apoptosis is triggered by cytochrome c release and Smac (second mitochondria-derived activator of caspase) activation [91]. When Smac is associated with direct inhibitor of apoptosis binding protein (Smac/DIABLO) they promote apoptosis by neutralizing the inhibitor of apoptosis (IAP) [91]. Various human cancers have high levels of IAPs, including the XIAP (X-linked inhibitor of apoptosis protein) isoform, which is implicated in poor treatment responses [92, 93]. Vellanki *et al*. could alleviate radioresistance of glioblastoma CSCs by promoting apoptosis using a XIAP inhibitor [84], proving that XIAP is implicated in radioresistance of glioblastoma CSCs and perhaps suggesting a new CSC-targeted therapy [80]. Another approach that can be used is acting on RNA translation process, by silencing such proteins [94].

Self-renewal, which drives tumourigenesis, and differentiation capacity seem to be key properties of CSCs [2]. Targeting the molecular pathways behind the control of multi/pluripotency, proliferation and differentiation represent an attractive goal for drug discovery since they may provide positive strategies to eradicate CSCs [80]. The Wnt pathway, plays an important role in differentiation of normal stem cells and its activation promotes genomic instability, leading to transformation/mutation of the cells [83], *e.g.* Shiras proposed that this pathway possibly promotes conversion of NSC into CSCs in gliomas [95]. Genomic instability is seen as a way for tumour cells to both survive and develop additional adaptive mutations [80]. To overcome this possibility, Wnt inhibitors have been designed to specifically target this pathway [96]. In other cases, the effect of the inhibitors may not always eliminate the CSCs directly, but rather promote their differentiation, meaning that they are no longer able to self-renew and to support tumour growth [42]. It was reported that differentiation of glioma CSCs sensitized them to therapy, impaired the secretion of angiogenic cytokines, inhibited motility and reduced the CSC tumourigenicity [97].

Notch/γ-secretase/Jagged signalling pathway is defined as an important regulator of differentiation and helps to control cell fate [98]. It was found to be activated in breast cancer [99] and endothelial cells [100] in response to radiation. It was reported that inhibition of Notch signaling via γ-secretase inhibitors can potentially block CSC self-renewal, decrease tumour growth and prolong survival in medullo-blastoma and glioma [101, 102]. Significant efforts to downregulate Notch pathway are being studied, *e.g.* a γ-secretase inhibitor is in clinical development for treating leukaemia [80]. The hedgehog

signalling, being involved in proliferation and self-renewal of stem cells, may also provide a good approach for drug discovery, *e.g.* inhibition of this pathway with an antagonist of the hedgehog co-receptor SMO, eliminated CSCs in chronic myeloid leukaemia [103]. In glioma, tumour growth was suppressed when the same antagonist was co-administrated with a standard chemotherapeutic drug (temozolomide) [51].

1.4. Drug resistance in lung cancer

Lung cancer is the worldwide leading cause of cancer related deaths and one of the most intractable cancers [23]. In general, after an apparent good response to initial therapy, it has a particularly poor prognosis with five-year survival lower that 15% due to late presentation, disease relapse and low rate of curative therapy [8]. There are two main types of lung cancer, small cell lung cancer (SCLC) and non-small cell lung cancer (NSCLC). The latter includes three major histological types: adenocarcinoma, squamous cell carcinoma (SCC) and large cell carcinoma. About 15% of lung tumours are SCLCs and arise in the larger airways, grow rapidly and have a neuroendocrine component. Adenocarcinoma represents about 40% of NSCLCs and usually originates in peripheral lung tissue. SCCs represent 25% of NSCLCs and commonly start near a central bronchus. Large cell carcinomas are believed to derive from neuroendocrine cells and may be observed in combination with other types of NSCLC [2]. Lung cancer has been object of intense studies because of its association to chemotherapeutic drug resistance and lung cancer cell lines are widely used for drug resistance experiments. NCI-H460 and A549 are examples of the most utilized cell lines in lung cancer studies. NCI-H460 cell line is tumourigenic and was derived in 1982 from the pleural fluid of a patient with large cell lung carcinoma by A.F. Gazdar and associates. The A549 cell line was initiated in 1972 by D.J. Giard, *et al.* after an explant culture of lung adenocarcinoma from a 58-year-old Caucasian male. All of this cell lines were isolated from NSCLC patients, present adherent growth properties and have an epithelial morphology [104]. Several studies have been published with these cell lines, *e.g.* Almeida *et al* reported that A549 cell line showed to be significantly more resistant to cisplatin than NCI-H460 cell line and studied how these cell lines responded to drug treatment [105].

Drug resistance of malignant tumours is a very complex phenomenon, being the mechanisms behind chemoresistance probably acting in a combinatory way, making the understanding of resistance quite complicated. Apart from intrinsic resistance, the tumour cells can acquire resistance during chemotherapy treatment. The chemotherapeutic drugs, to be efficient, must reach the tumour cells through the blood vessels, however the vasculature of solid tumours is highly variable [106]. Such drugs usually act by disrupting the cell cycle process. Cisplatin, one of the most potent anticancer drugs is used in a wide range of tumour types. This drug interacts with DNA forming DNA adducts, activating signal transduction pathways that culminate in apoptosis [107]. Gemcitabine, another anticancer drug commonly used, is a cytidine analog. Following influx through the cell, gemcitabine undergoes complex intracellular conversion to the nucleotides gemcitabine diphosphate (dFdCDP) and triphosphate (dFdCTP) responsible for its cytotoxic actions. Incorporation of dFdCTP into DNA is most likely the major mechanism by which gemcitabine causes cell death. After this incorporation on the end of the elongating DNA strand, one more deoxynucleotide is added and thereafter, the DNA polymerases are unable to proceed and the cell will activate the apoptosis pathway [108]. Doxorubicin is an anticancer drug with a wide spectrum of activity, since it has the ability to intercalate the DNA helix and to bind proteins involved in DNA replication and transcription. Such interactions lead to inhibition of DNA, RNA and protein synthesis, resulting in cell death [109]. 5-Fluorouracil (5-FU) has played an important role in treatment of cancer and is usually administrated in combination therapy. It has been proposed to be incorporated into RNA and DNA, but the mechanism of action reported is the capacity to inhibit thymidylate synthase (TS). Inhibition of TS, a key enzyme of pyrimidine synthesis, will impair DNA replication and culminate in cell death [110]. The mechanisms underlying cancer drug resistance are normally associated with reduced drug uptake, increased drug inactivation, and increased DNA adduct repair [107].

In 2007, Ho *et al* isolated the SP of cells from lung cancer cell lines and discovered that SP cells display significantly increased invasiveness, when compared to non-SP, using an *in vitro* Matrigel invasion assay. These cells were also more tumourigenic than non-SP cells *in vivo, i.e.* only a small number of SP cells were required to induce tumour formation upon injection into mice. This study also showed that SP cells are more resistant to drugs commonly used in chemotherapy. Several drugs were tested, such as cisplatin, gemcitabine

and doxorubicin, in different lung cancer cell lines (*e.g.* NCI-H460 and A549) for 24 hours and SP cells exhibited higher resistance to chemotherapeutic drugs than non-SP cells [7]. Eramo *et al* reported, using MTT assay, that lung cancer stem cells are resistant to chemotherapy after 5 days of drug exposure, and also that lung cancer spheres are tumourigenic *in vivo* and can reproduce the human tumour when injected in immunocompromised mice [8].

As mentioned above, there CSCs and EMT cells share many common features. Indeed, EMT is associated with resistance to multiple drugs and allows rapid tumour progression. Clarifying this correlation may help clinicians to select an optimal anticancer drug treatment [46]. The concept of EMT was first developed in the field of embryology, but has been recently extended to cancer progression and metastasis [111]. Cells undergoing EMT become invasive and develop resistance to anticancer agents. It was also reported that EMT can be induced by chemotherapeutic agents and by stress conditions, such as exposure to radiation and hypoxic conditions [112]. The biology of EMT has been clarified in tumour samples through EMT-associated markers, such as mesenchymal specific markers (*e.g.* vimentin and fibronectin) [113], epithelial specific markers (*e.g.* E-cadherin and cytokeratin) [114] and transcription factors (*e.g.* Snail and Slug) [115].

Stable pancreatic cancer cell lines resistant to gemcitabine, due to continuous exposure to the drug, can undergo EMT with increased expression of Snail and Twist (EMT-regulatory transcription factors) [116]. On the other hand, EMT has been reported to confer resistance to chemotherapeutic drugs. Lung cancer cell lines that have undergone EMT (expressing vimentin and/or fibronectin) were insensitive to the growth inhibitory effect of EGFR (epidermal growth factor receptor) inhibition by erotinib both *in vitro* and in xenografts [117]. As EMT has been associated to resistance to multiple drugs and metastasis, clarifying such relation may help the development of optimal anticancer drug treatments [46]. Some molecular mechanisms seem to be involved with EMT in cancer progression. Diminished expression of E-cadherin can lead to tumour progression, metastasis and poor prognosis in various human carcinomas [114] and loss of the TGF-β signaling pathway results in the progression of cancer, once TGF-β is a strong growth inhibitor [118]. Some transcription factors, such as zinc finger proteins (ZEB1, ZEB 2), bH2H protein (twist) and the Snail family of zinc finger proteins (Snail, Slug) are known to repress E-cadherin, promoting EMT [119]. The involvement of small non-coding RNA

(microRNA) in the regulation of EMT-related genes as also been shown [120], for instance miR10b overexpression is associated with invasiveness and metastatic potential [121]. The correlation of these mechanisms with EMT may prove an important tool for future drug design [46].

1.5. Aims

It is currently believed that putative cancer stem cells (CSCs) (a small sub-population of tumour cells with self-renewing capacity that sustains tumour growth) are, in part, responsible for chemoresistance. CSCs seem to share some of the resistance mechanisms of NSCs. Although these mechanisms are not fully understood, over-expression of efflux pumps, over-expression of anti-apoptotic proteins and efficient DNA repair seem to be involved in resistance of CSCs to chemotherapeutic agents. Despite many advances in the CSC field, many progresses are needed in order to better understand such regulation and possibly identify potential therapeutic targets to overcome chemoresistance in these cells.

In this project we aim to isolate CSCs from lung cancer cell lines using FACS or by exposing cells to chemotherapeutic drugs. We then aim to study the resistance of the isolated populations against chemotherapeutic drugs used in the clinic (such as cisplatin, gemcitabine, 5-FU and doxorubicin). If we determine that the selected sub-populations of cells have increased chemoresistance, we aim to investigate the drug resistance mechanisms involved in order to identify potential therapeutic targets to overcome CSC resistance to the chemotherapeutic agents already used in the clinic.

2. Materials and Methods

2.1. Chemicals and Reagents

All chemicals were purchased from Sigma-Aldrich, unless stated otherwise. All tissue culture materials and reagents were purchased from Becton Dickinson or TPP and Lonza, respectively, unless otherwise stated.

2.2. Cell lines and culture conditions

Two human non-small cell lung cancer cell lines were used in this study: NCI-H460 and A549. Cell lines were kindly provided by Doctor George Don Jones (University of Leicester, United Kingdom). NCI-H460 is a large cell lung carcinoma cell line and A549 is an adenocarcinoma cell line. Both cell lines are epithelial and have wild type P53. Cells were grown as a monolayer in Roswell Park Memorial Institute – 1640 medium (RPMI-1640) supplemented with 10% (v/v) heat –inactivated foetal bovine serum (FBS), in a humidified atmosphere at 37 $^{\circ}$C and 5% CO_2. Cells were passaged twice a week using TrypLE™ Express.

2.3. Analysis of ABCG2 and CD133 expression by flow cytometry

Expression levels of the cell surface membrane proteins ABCG2 and CD133 were assessed by flow cytometry.

Single-cell suspensions were obtained using versene (Gibco) in order to protect the epitope recognized by the utilized antibodies, as initially obtained results using Tryple Express to detach cells showed that the protein was not being properly recognised by the ABCG2 antibody. Cell suspensions were washed twice with the labelling buffer, containing phosphate buffered saline (PBS), 0.2% ethylenediaminetetraacetic acid (EDTA), and 0.5% bovine serum albumin (BSA). Cells were then incubated with the specific antibodies: Bcrp1/ABCG2–phycoethrin (PE) antibody (R&D systems), CD133/1-PE antibody and IgG-PE (both from Miltenyi Biotec), diluted 1:10 in the labelling buffer

and incubated for 10 minutes at 4 °C in the dark. Unbound antibody was removed by washing cells with labelling buffer. Cells were then resuspended in an appropriate volume of labelling buffer and, kept on ice in the dark until flow cytometry analysis. Flow cytometric data acquisition was performed at IBMC's Advanced Flow Cytometry Unit using a FACS Calibur (Becton Dickinson). Acquired data, from a minimum of 30,000 events per sample, were analysed using Flow-Jo software (version 7.6.5, Treestar, Ashland, OR) and Microsoft Office Excel 7.0 (Microsoft, Redmond, WA).

2.4. Fluorescence activated cell sorting (FACS)

This approach allows the separation of distinct populations of cells that can be used to study tumour features, such as tumourigenicity, chemo/radio resistance, gene expression and others [11]. The tumour cells are labelled with fluorescent antibodies for stem cell markers and it is possible to isolate the positive cells (those expressing the marker, the population of cells thought to be the CSCs) and the negative ones (non-CSCs) from the same tumour, using fluorescence activated cell sorting (FACS) [18].

To perform cell sorting, 10^6 cells were labelled with the specific Bcrp1/ABCG2-PE antibody as described above, except that cells were incubated with the antibody for 30 minutes at 4 ^{o}C in the dark. The labelled cells were analysed and $ABCG2^+$ and $ABCG2^-$ sub-populations separated using a FACSAria cell sorter (BD Biosciences). Cell sorting efficiency was assessed immediately after cell separation by determining the % of cells expressing ABCG2 in each of the cell sub-populations by flow cytometry.

Upon cell sorting cells were plated in fresh RPMI-1640 medium supplemented with 10% (v/v) FBS and 0.1 % of gentamicin and expanded for at least 7 days.

2.5. Cell growth/viability assays

To investigate cell response towards chemotherapeutic agents (cisplatin, doxorubicin, gemcitabine and 5-FU), two different multiwell plate cell growth assays were performed: a resazurin-based assay and the Sulforhodamine B (SRB) assay.

2.5.1. Resazurin-based assay (PrestoBlue):

PrestoBlue reagent (Life Technologies) is a resazurin-based solution that functions as a cell viability indicator by using the reducing power of living cells to quantitatively measure the proliferation of cells. The PrestoBlue reagent contains a cell-permeant compound that is blue in colour and virtually nonfluorescent. When added to cells, the PrestoBlue reagent is modified by the reducing environment of the viable cell, turns red in color and becomes highly fluorescent.

Cells were seeded in 96-well plates, left to adhere for 24 hours, and incubated with chemotherapeutic agents for 48 hours. At the end of the incubation period, the media was removed, cells were washed once with PBS, 50 μL of PrestoBlue added to each well and incubated at 37 ºC for 45 minutes, in the dark. Fluorescence excitation and emission were measured at 560 and 590 nm, respectively using a multiwell plate reader (Synergy Mx, Biotek).

2.5.2. SRB assay:

The SRB assay is a colorimetric assay that measures biomass. SRB is a pink dye that directly binds to basic amino acids of cells that have been previously fixed by trichloroacetic acid (TCA). The incorporated dye is then solubilised in a Tris-Base solution (under basic conditions) and colorimetric evaluation (optimal wavelength for measurement of the optical density of SRB is 564 nm) provides an estimate of protein mass which is directly proportional to cell number [122].

The SRB assay was always performed following cell incubation with PrestoBlue, allowing analysing the same cells by two different cell growth/viability assays. Upon performing the PrestoBlue assay, cells were fixed in cold TCA (Merck) to a final concentration of 10% (v/v) and incubated on ice for 1 hour. The TCA was then removed, the wells washed with distilled water and allowed to dry. 50 μL of 0.4% SRB (w/v, prepared in 1% acetic acid) were added to each well and incubated at room temperature for 30 minutes. Afterwards, the SRB was removed, the wells were quickly washed three times with 1% acetic acid (v/v) (Merck), and allowed to air dry. The incorporated SRB dye was then solubilised by adding 100 μL of 10 mM Tris-Base solution, the plates were briefly shaken and the optical density (OD) of each well was measured spectrophotometrically in

a multiwell plate reader (Synergy Mx, Biotek) at a wavelength of 560 nm subtracting the background measurement at 655 nm.

2.5.3. Optimization of the starting conditions for the resazurin-based and SRB assays

Sensitivity of the cell growth/viability assays was tested by determining the linearity between the number of cells per well and the OD at 560 nm for the NCI-H460 cell line after 24 hours in culture. Cells were seeded at different densities (from 250 to 16,000 cells) in a 96-well plate (four replicate wells per cell density) and incubated for 24 hours prior to processing and fluorescence or absorbance reading as described above.

For determination of the optimal starting cell density, cells were plated in 96-well microplates at densities of 250 – 16,000 cells per well in quadruplicate. Cells were left to adhere for 24 hours and further incubated for 48 hours in a humidified chamber at 37 $^{\circ}$C and 5% CO_2. Cells were then processed for the PrestoBlue and SRB assays (as detailed above).

2.5.4. Cell incubation with chemotherapeutic agents

Cells were seeded at a density of 2.0 x 10^3 cells per well on 96-well microplates, left to adhere for 24 hours, and incubated with various concentrations of cisplatin (1 to 10 μM), doxorubicin (0.01 to 0.5 μM), gemcitabine (10 to 50 nM) and 5-FU (5 μM to 20 μM) for 48 hours. In addition, cells were also processed at time zero (T0) of drug incubation, i.e. 24 hours following cell seeding, in order to determine % cell growth. Background control wells, containing the same volume of complete culture medium with or without chemotherapeutic drugs were included in each experiment and used to correct the reading changes due to external factors (not to cells). Cells incubated with drug-free complete medium were used as controls, representing 100% cell growth/viability. The % of cell growth (taking T0 into account) or % cell survival (not taking T0 into account) in the cells treated with chemotherapeutic agents was determined in comparison to the control cells and the population of cells with increased drug resistance will have higher percentage cell survival, which can be measured by using different assays that provide us with an indirect measure of cell number. Three replicate wells were used for each condition. Cell growth/survival was assessed by the PrestoBlue and SRB assays. Results are shown as the mean ± SD of three independent experiments, except when stated otherwise. GI50

(concentration of drug that inhibits cell growth in 50%) of tested populations was calculated using GraphPad Prism 5.04.

2.6. Enrichment of putative CSCs upon treatment with chemotherapeutic agents

Cells were incubated with cisplatin (1 to 10 μM) or doxorubicin (0.01 to 0.2 μM), for three weeks followed by a drug-free recovery period, in an attempt to isolate cell populations enriched in putative CSCs. NCI-H460 and A549 cells were plated at T75 flasks, left to adhere during 24 hours and incubated with the drug. During three weeks, fresh medium with new drug was replaced every two days. After this time, drug was withdrawn and cells were left to recover.

Cell morphology was monitored and recorded throughout the experiment by optical microscopy (Olympus CK X 41).

2.7. Colony-forming assay

This approach was used in an attempt to test the ability of single parental and drug-selected resistant cells to survive and form colonies. In this assay, the cells are in an adverse environment because they are separated from each other and cells possessing stemness properties will be more prone to survive and generate a tumour cell colony by itself [31, 35].

Single-cell suspension of parental cells and cisplatin-resistant cell variant B were obtained using TrypLE™ Express. 300 cells were plated per 7cm Petri dish in triplicate. Cells were left to adhere for 24 hours, after which cells were either incubated with complete RPMI medium (controls) or with 1 μM of Cisplatin for 48 hours. Following this incubation, the media was replaced with drug-free complete RPMI medium until colonies containing at least 50 cells were visible (which took approximately 10 days). During this time period, medium was replaced twice a week. At the end of the assay, the medium was withdrawn, each Petri dish washed twice with PBS, cells fixed with methanol (Fisher Chemical) and 0.5% (w/v) crystal violet solution used to stain the colonies. The colonies

were visually counted and results are shown as mean ± SD of three independent experiments performed in triplicate.

2.8. Chicken embryo chorioallantoic membrane (CAM) assay

The chicken embryo chorioallantoic membrane (CAM) is an extra-embryonic membrane that serves as a gas exchange surface and its function is supported by a dense capillary network, which provides a uniquely supportive environment for primary tumour formation [123]. As the cchicken embryo is naturally immunodeficient and the CAM is easily accessible for manipulation and observation, this model provides an adequate environment to grow transplants from various cell lines.

The CAM in vivo assay was, therefore, performed to evaluate the tumourigenesis of cisplatin-resistant cell variant B versus NCI-H460 parental cells. Single cell suspensions of these cells were prepared and the CAM assay was performed by Marta Teixeira Pinto at the "*In vivo* Choriallantoic Membrane (CAM) Assays Unit" at IPATIMUP, as previously described with some modifications [124, 125]. Briefly, fertilized chick (*Gallus gallus*) eggs obtained from commercial sources were incubated horizontally at 37.8°C in a humidified atmosphere. After 3 days a square window was opened in the shell after removal of 1.5-2 mL of albumen to allow detachment of the developing CAM. The window was sealed with a transparent adhesive tape and the eggs returned to the incubator. On day 10, single cell suspensions of both populations were prepared and 1×10^6, 1×10^5 and 1×10^4 cells were inoculated into a silicone ring placed on top of the CAM. Six chicken embryos were used for each condition Tumours were allowed to grow for 7 days at which time the embryos were euthanized. The resulting tumours were then excised from the embryos, together with the surrounding CAM, and photographed *ex ovo* under a stereoscope (Olympus, SZX16 coupled with a DP71 camera) at 2x magnification.

2.9. Western Blot

Western blot is a technique by which specific antigens can be distinguished in a complex protein mixture. First, proteins are fractionated in polyacrylamide gels and the resulting pattern is then electrophoretically transferred to nitrocellulose sheets. An

antibody is used for the detection on the solid phase, and visualization is due to autoradiography [126]. Western blot was performed to identify possible targets involved in chemoresistance mechanisms present in the putative CSC enriched populations.

2.9.1. Cell lysates

Cell lysates were prepared using Lytic Cell M as lysis buffer solution, containing both protease (Roche) and phosphatase inhibitors to protect protein from degradation during the extraction procedure. After washing the cells twice with PBS, lysis buffer was added and incubated with plated cells during 15 minutes on ace. After this time the cells were scraped in the presence of the lysis buffer solution to help the lysing action.

2.9.2. Protein quantification assay

The cell lysates were then quantified using a quantification kit (BioRad) based on the Bradford dye-binding methodology, according to the manufacturer's instructions.

2.9.3. Sodium Dodecyl Sulfate-PolyAcrylamide Gel Electrophoresis (SDS-PAGE)

After quantification, 30 μg protein extracts were mixed with laemmli sample buffer that contains 1 M Tris-hydrogen chloride (HCl) pH 6.8, 40% glycerol, 5% sodium dodecyl sulphate (SDS), β-mercaptoethanol 14.3 M and 1% bromophenol blue. The prepared samples were then heated to 95 ºC during 5 minutes. The proteins were separated by their molecular weight by sodium dodecyl sulfate polyacrylamide gel electrophoresis (SDS-PAGE) through a 7% or 12% of polyacrylamide gel, depending on the molecular weight of the proteins of interest. The resolving gel was composed by 30% acrylamide mix (BioRad), 1.5 M Tris-HCl pH 8.8, 10% SDS, 10% ammonium persulfate (APS) and tetramethylethylenediamine (TEMED). The stacking gel had the same composition except for the Tris-HCl, 1 M Tris-HCl pH 6.8 was used in this case. The electrophoresis was performed with 10x Tris/Glycine/SDS buffer (BioRad) under 60-100 V during approximately 120 minutes.

2.9.4. Western blotting

After protein electrophoresis, the proteins were electrotransfered from the gel to a hybond-C nitrocellulose membrane (Amersham). The transference was performed with 10x Tris/Glycine/SDS and 20% of methanol (Fisher Chemical) under 100 V during approximately 90 minutes. To verify the efficiency of the transference process, the membrane was submerged in Ponceau S, which binds to proteins. The membrane was then washed three times with Tris buffer saline - tween (TBS-T) for 10 minutes to deplete the presence of Ponceau S. To inhibit the antibodies-unspecific bindings, the membrane was blocked with 5% of powdered milk diluted in TBS-T during 60 minutes at room temperature under shaking. In order to detect the presence of proteins of interest, immunoblotting was performed using mouse-anti P-glicoprotein (Pgp) (Sigma) at 1:500 dilution, mouse-anti XIAP (BD transduction Laboratories) at 1:1000 dilution, mouse-anti P53 (Thermo Scientific) at 1:200 dilution, rabbit-anti B-cell lymphoma extra-large (Bcl-XL) (Santa Cruz) at 1:200 dilution, mouse-anti B-cell lymphoma 2 (Bcl 2) (Dako) at 1:200 dilution (Table 2.1). All the antibody dilutions were performed with block solution. The period of antibody incubation was 60 minutes at room temperature under gently shaking. After this, the membrane was washed three times for 10 minutes with TBS-T under vigorous shaking. After exposure to the specific secondary antibodies (donkey anti-goat, goat anti-mouse and goat anti-rabbit, all from Santa Cruz), diluted 1:2000 in block solution and incubated for 60 minutes at room temperature under gentle shaking, the proteins were visualized using an electrochemiluminescence (ECL) chemiluminescent detection kit (GE Healthcare). The housekeeping protein β-actin (Santa Cruz) was used as a loading control, at 1:2000 dilution in block solution for 60 minutes incubation at room temperature under gently shaking. When necessary, a stripping process was used in order to deplete all the protein bindings to the membrane. The stripping solution was composed by β-mercaptoetanol, 10% SDS and 1 M Tris-HCl, pH 6.7.

The pictures were taken in a quemidoc system (Bio-Rad). Protein normalization was performed using the Quantity One Basic software (Bio-Rad).

Table 2.1 - List of antibodies used.

Primary antibody	Dilution	Animal Origin	Commercialized by
Pgp	1:500	Mouse	Sigma-Aldrich
XIAP	1:1000	Mouse	BD transduction Laboratories
P53	1:200	Mouse	Thermo Scientific
Bcl-XL	1:200	Rabbit	Santa Cruz
Bcl 2	1:200	Mouse	Dako
B-actin	1:2000	Goat	Santa Cruz

2.10. Gene expression analysis

2.10.1. RNA extraction

Total RNA was extracted from parental and cisplatin-resistant cells using 1 mL of TRI Reagent (Ambion) for 5-10x10^6 cells by repetitive pipetting. After cell lysis, 0.2 mL of chloroform was added and each tube shook vigorously for 15 seconds, left for 5 minutes at room temperature and centrifuged at 12,000 × *g* for 15 minutes at 4 ºC. This step allowed the separation of RNA (aqueous phase), DNA (interphase) and proteins and lipids (organic phase). The aqueous phase was transferred to a fresh tube and 0.5 mL of isopropanol added and mixed. The samples were left for 10 minutes at room temperature and then centrifuged at 12,000 x *g* for 10 minutes at 4 ºC. This step allowed the precipitation of RNA. Supernatant was carefully removed and the pellet washed with 75% of ethanol (Panreac). After this stage, the samples were vortexed and centrifuged at 7,500 x *g* for 5 minutes at 4 ºC. The RNA pellet was briefly air dried. The pellet was next dissolved in 23 µL pre-warmed (55-60 ºC) RNase/DNase-free water (Gibco) by repeated pipetting and further incubated at 55-60 ºC for 10 minutes to facilitate dissolution.

2.10.2. RNA Treatment with DNase

Possible genomic DNA contamination of RNA samples was eliminated upon DNase treatment using the TURBO DNA-free kit (Ambion), according to the manufacturer's instructions. Briefly, 10 µg RNA were incubated with 1µL TURBO DNase, TURBO DNase buffer and RNase/DNase-free water to a final volume of 50 µL. The samples were incubated at 37 ºC for 30 minutes. After the incubation period, 0.1 volume DNase inactivation reagent (Ambion) was added and mixed with the samples in order to inactivate the enzyme. The samples were incubated at room temperature during 5 minutes when the tubes were flicked 3 times to redisperse the DNase inactivation reagent. The samples were centrifuged at 10,000 x *g* for 1.5 minutes and the RNA (in supernatant) transferred to a fresh tube.

2.10.3. RNA quantification

RNA was quantified using a NanoDrop spectrophotometer (ND 1000, Thermo Scientific) with tND-1000 software (3.3.0 version). Ratios of A260/A280 were used to evaluate the purity of RNA extract and values of approximately 1.9 were considered of sufficient quality for RNA expression analysis. The formula used to calculate the concentration of RNA in µg/µL was:

$$(A260 \times 40 \times \text{dilution factor}) / 1000 = [RNA]$$

2.10.4. cDNA synthesis

After RNA sample been purified, the production of cDNA using ThermoScript for cDNA synthesis kit (ThermoSript) was the next step. A mix containing 1 µL of primer oligo d(T)20 and 1 µL of deoxyribonucleotides triphosphate (dNTPs) was added to 9 µL of each RNA sample and placed at 65 ºC for 5 minutes to denature samples, and then placed on ice. Next, a mix prepared on ice and containing 4 µL of cDNA synthesis buffer, 1 µL of 0.1 M DTT, 1 µL of RNaseOUT (40 U/µL), 1 µL of DEPC-treated water and 1 µL of thermoscript RT (15 U/µL) was added to each denatured sample and transferred to a thermal cycler (MyCycle – Bio Rad) preheated to 55 ºC for 60 minutes, for cDNA

synthesis. The reaction was terminated through sample incubation at 85 ºC for 5 minutes. 1 µL of Rnase H was added and incubated at 37 ºC for 20 minutes to eliminate the RNA.

2.10.5. Real-Time quantitative PCR

Real-time quantitative reverse transcription PCR (qRT-PCR) is one of the most sensitive and accurate methods to quantifying variations in gene expression levels. This technique involves the reverse transcription (RT) of mRNA into cDNA and uses fluorescent report molecules to measure in real-time the subsequent amplification of cDNA by polymerase chain reaction (PCR) [127]. RT-PCR was performed to corroborate the possible chemoresistance mechanisms involved in the putative CSC enriched populations and to investigate the expression of stemness-related genes by assessing multidrug resistance gene 1 (*MDR1), Bmi-1*, SRY (sex determining region Y)-box 2 (*Sox2), ABCG2* and *Hprt1* gene expression (Table 2.2). Primers for *MDR1* and *ABCG2* were designed by Almeida GM, *Bmi-1* primers were designed according to Chaurasia *et al* [128], *SOX2* primers adapted from Que *et al* [129] and *Hprt1* primers according to Almeida GM *et al*. [105].

A mix containing QuantiTect SYBR Green PCR Master Mix (Applied Biosystems), forward and reverse primers and RNase-free water was added to 1 µL of template cDNA (1:20) and dispensed into the individual wells of a 96-well plate. The primers concentration was 150 *p*M for all the tested genes with exception of SOX 2, which was 300 *p*M. The plate was briefly centrifuged and reactions conducted in a real-time cycler (7500 FAST Real-Time PCR system, Applied Biosystems). The run method used was based on 2 different stages, the holding stage and the cycling stage. In the holding stage the temperature increased from 25º C to 50º C and was maintained during 2 minutes and increased again to 95º C being maintained during 10 minutes. In the cycling stage, the temperature was maintained at 95º C for 15 seconds followed by a decrease in temperature to 60º C which was maintained for 1 minute. The number of cycles was 40. Data were analyzed using the associated 7500 software, v. 2.0.5.

Gene expression was quantified by the standard curve method [130], whereby a standard curve is constructed by amplifying known amounts of serially diluted cDNA in a parallel group of reactions run under identical conditions to the samples. Standard curves

were undertaken for each gene that was being analysed in each PCR run and was used for calculation of PCR amplification efficiency and quantification of target cDNA.

The value of both target and housekeeping genes from each sample was determined from the respective standard curve equation and the target value divided by the endogenous reference value to obtain a normalised target value independent from the starting amount or material. Non-template controls (NTC) were also used to ascertain that no DNA contamination was present in the samples. The existence of only one melting temperature/peak in all samples indicated the presence of a single amplification product. The absence of an amplification product in the NTC indicated that there was no external DNA contamination in the PCR mix and no primer dimer formation, which would also result in a fluorescence peak.

Table 2.2 - Primer sequence and expected PCR product length.

Gene	Forward Primer (5' – 3')	Reverse Primer (5'-3')	Length bp
MDR1	CCGCAATGGAGGAGCAAAGAAG	GTCAAGCCAATTTGAATAGCGAAACA	124
Bmi-1	CCACCTGATGTGTGTGCTTTG	TTCAGTAGTGGTCTGGTCTTGT	162
SOX 2	AACGGCTCGCCCACCTACAGC	AGTGGGAGGAAGAGGTAACC	130
ABCG2	GGATGTCTAAGCAGGGACGAACAAA	GCCAATAAGGTGAGGCTATCAAACAAC	91
Hprt1	GCAGACTTTGCTTTCCTTGGTCAG	GTCTGGCTTATATCCAACACTTCGTG	103

2.10. Statistical analysis

The t-test was used for the statistical analysis always to compare two averages. The values compared had equal sizes, were always independent and the variances of the two populations were equal.

3. Results

Cancer stem-like cells are believed to be partially responsible for tumour chemoresistance. The aim of the current project was to isolate and characterize lung CSCs in terms of chemoresistance mechanisms and to identify potential therapeutic targets to overcome chemoresistance in these cells.

3.1. Isolation of putative lung CSCs ($ABCG2^+$) by fluorescence activated cell sorting

As a first step, ABCG2 marker was choosen to isolate a putative lung CSC population through fluorescence activated cell sorting (FACS).

Cell line NCI-H460 was labelled with an antibody for the cell surface protein ABCG2, upon which FACS was performed to isolate the ABCG2 positive and negative sub-populations. Purity of the cell sub-populations was verified by flow cytometry immediately after FACS sorting. The two sub-populations were successfully separated although purity of the $ABCG2^+$ sub-population was only between 70 and 86% (Table 3.1) Nevertheless, a purity of around 100% was consistently obtained for the $ABCG2^-$ subpopulation. The cell sorted sub-populations were then expanded *in vitro* until sufficient cells were available to perform cell growth/viability assays to assess response to chemotherapeutic drugs.

Table 3.1 - Cell sorting performed in NCI-H460 cell line using ABCG2 antibody. Three independent cell sorting experiments were performed.

Cell sorting	ABCG2 expression	Number of $ABCG2^-$ cells	Purity of $ABCG2^-$ sorted cells	Number of $ABCG2^+$ cells	Purity of $ABCG2^+$ sorted cells
1	16 %	321 000	100%	262 000	70%
2	14 %	93 000	100%	41 900	79%
3	10 %	105 000	99%	30 500	86%

3.2. Chemosensitivity of NCI-H460 cells and $ABCG2^+$/$ABCG2^-$ sorted cell populations

After lung tumour cells being sorted, it was wanted to understand if there were differences in drug response of $ABCG2^+$, $ABCG2^-$ and NCI-H460 populations. To accomplish that, cell growth/viability assay were performed.

3.2.1. Optimization of the starting conditions for the cell growth/viability assays

Preliminary assays were performed to determine if the chosen cell growth/viability assays used were reliable (*i.e.* fluorescence/absorbance directly proportional to the number of cells) and sensitive enough (*i.e.* the range of numbers of cells for which this linearity is maintained). Cells were plated at different seeding densities and resazurin-based and SRB assays performed following 24 hours. A direct correlation was determined between fluorescence/absorbance and the number of NCI-H460 cells (Pearson correlation – 0.99), confirming the reliability of the assay. Moreover, both assays were sensitive within the range of 250 to 16,000 cells (Figure 3.1).

For determination of the optimal starting cell density, cells were plated in 96-well microplates at densities of 250 – 16,000 cells per well and left to adhere for 24 hours, as above, and processed for resazurin-based and SRB assays following a further 48 hour incubation (Figure 3.2 and 3.3, respectively). Results show that the linearity between fluorescence/absorbance measures and the number of cells is only maintained if up to 4000

cells/well are initially plated. A plateau is reached when cell seeding densities above 4000 cells/well are used, indicating that the cells have reached confluence or that the assay has saturated. Therefore, a seeding density of 2,000 cells per well was chosen for all subsequent experiments using cell growth/viability assays, in order to assure that control cells would still be in exponential growth at the end of the 48 hours of the assay.

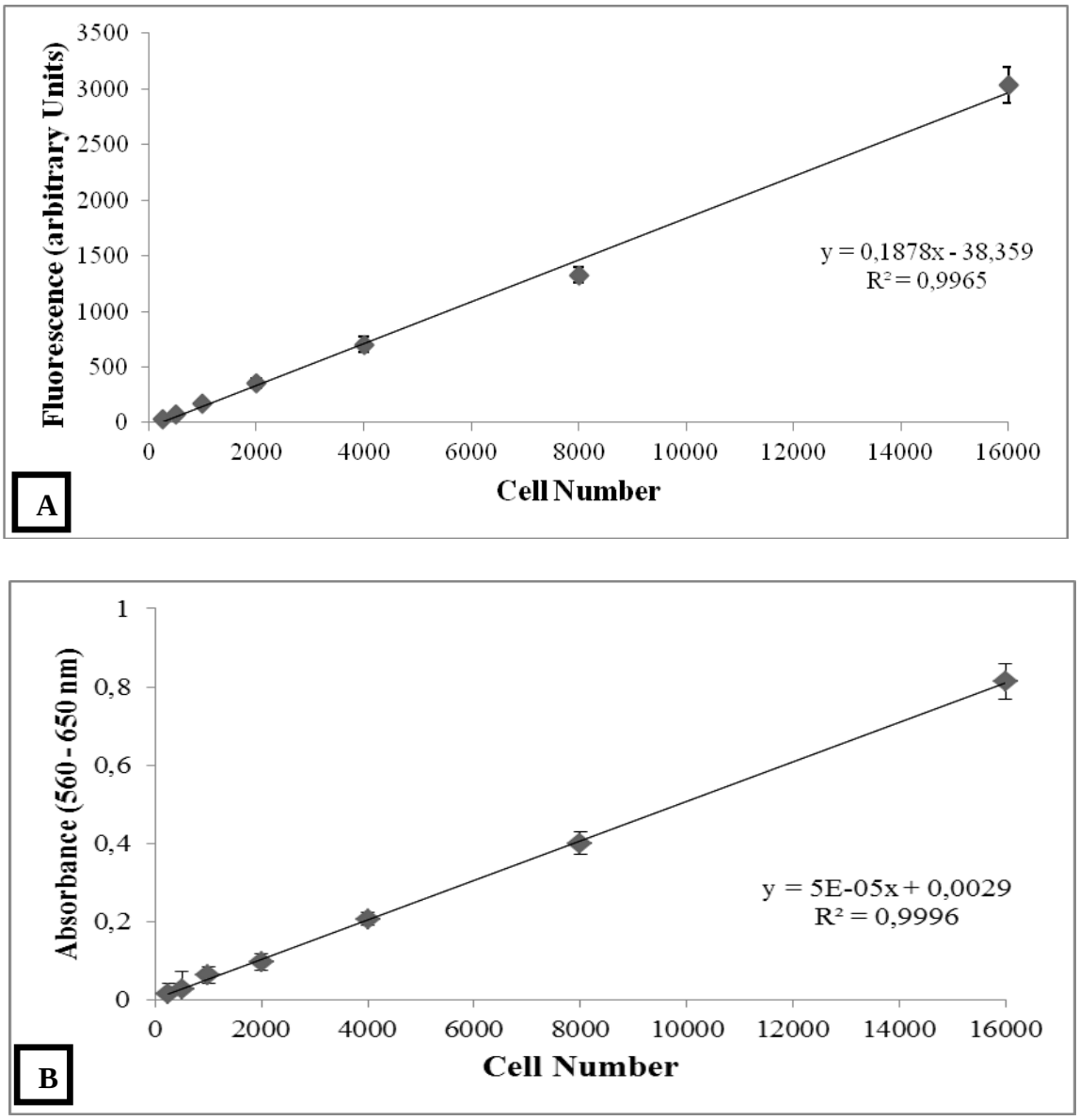

Figure 3.1- Sensitivity of the cell growth/viability assays. Cells were seeded at different densities (from 250 to 16,000 cells/well) in a 96-well plate (four replicate wells per cell density) and incubated for 24 hours prior to processing for the resazurin-based (A) and SRB (B) assays.

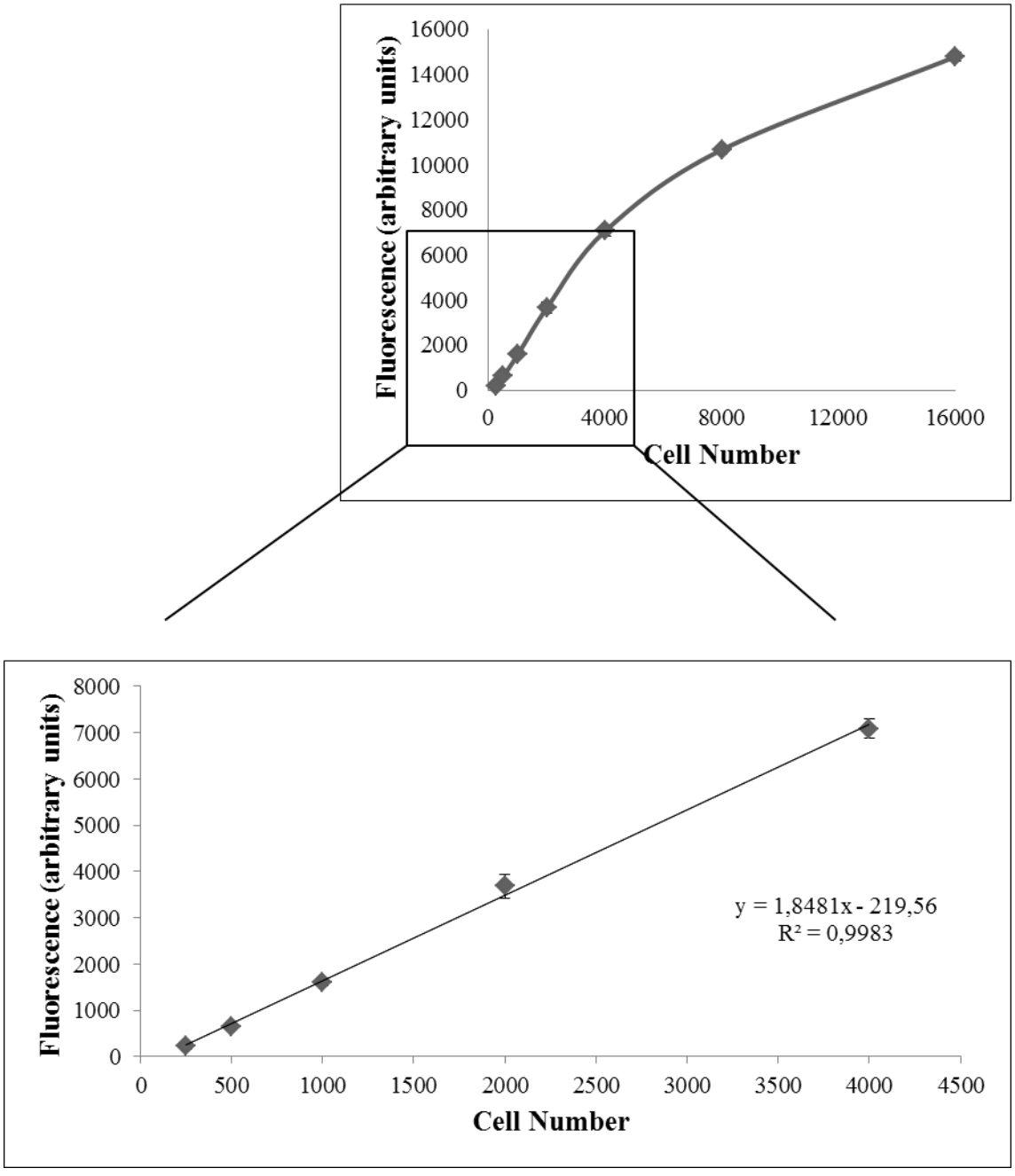

Figure 3.2 - Determination of the optimal starting cell density. Cells were seeded at different densities (from 250 to 16,000 cells) in a 96-well plate (four replicate wells per cell density) and left to adhere during 24 hours. After 48 hours resazurin-based assay was performed.

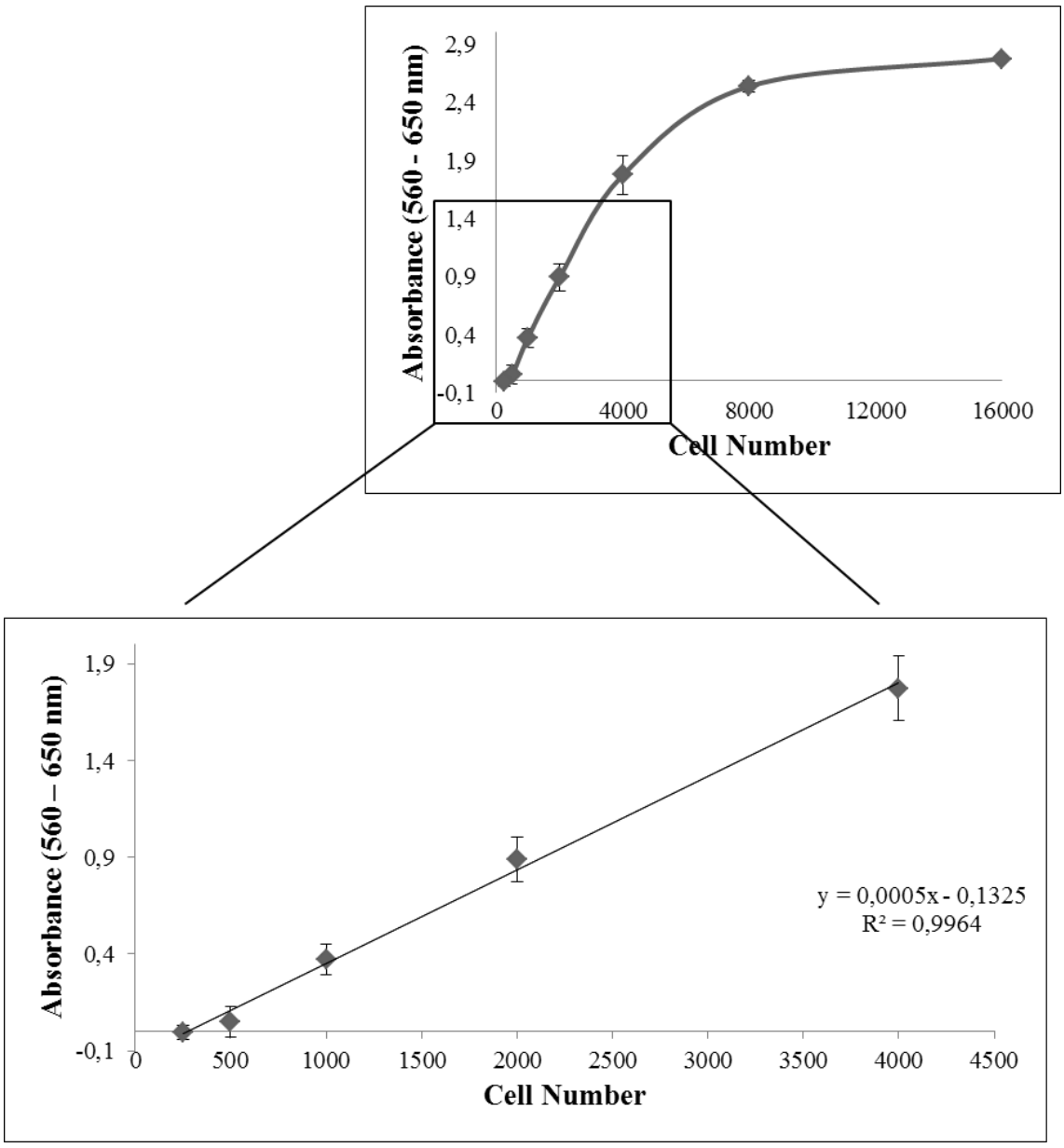

Figure 3.3 - Determination of the optimal starting cell density. Cells were seeded at different densities (from 250 to 16,000 cells) in a 96-well plate (four replicate wells per cell density) and left to adhere during 24 hours. After 48 hours SRB was performed.

3.2.2. Cell growth/viability assays

Cell growth/viability assays in response to different chemotherapeutic agents were performed in order to measure possible differences in chemoresistance between parental, ABCG2^{+} and ABCG2^{-} sub-populations of cells. No significant differences in drug response were observed between these populations of cells (Figure 3.4).

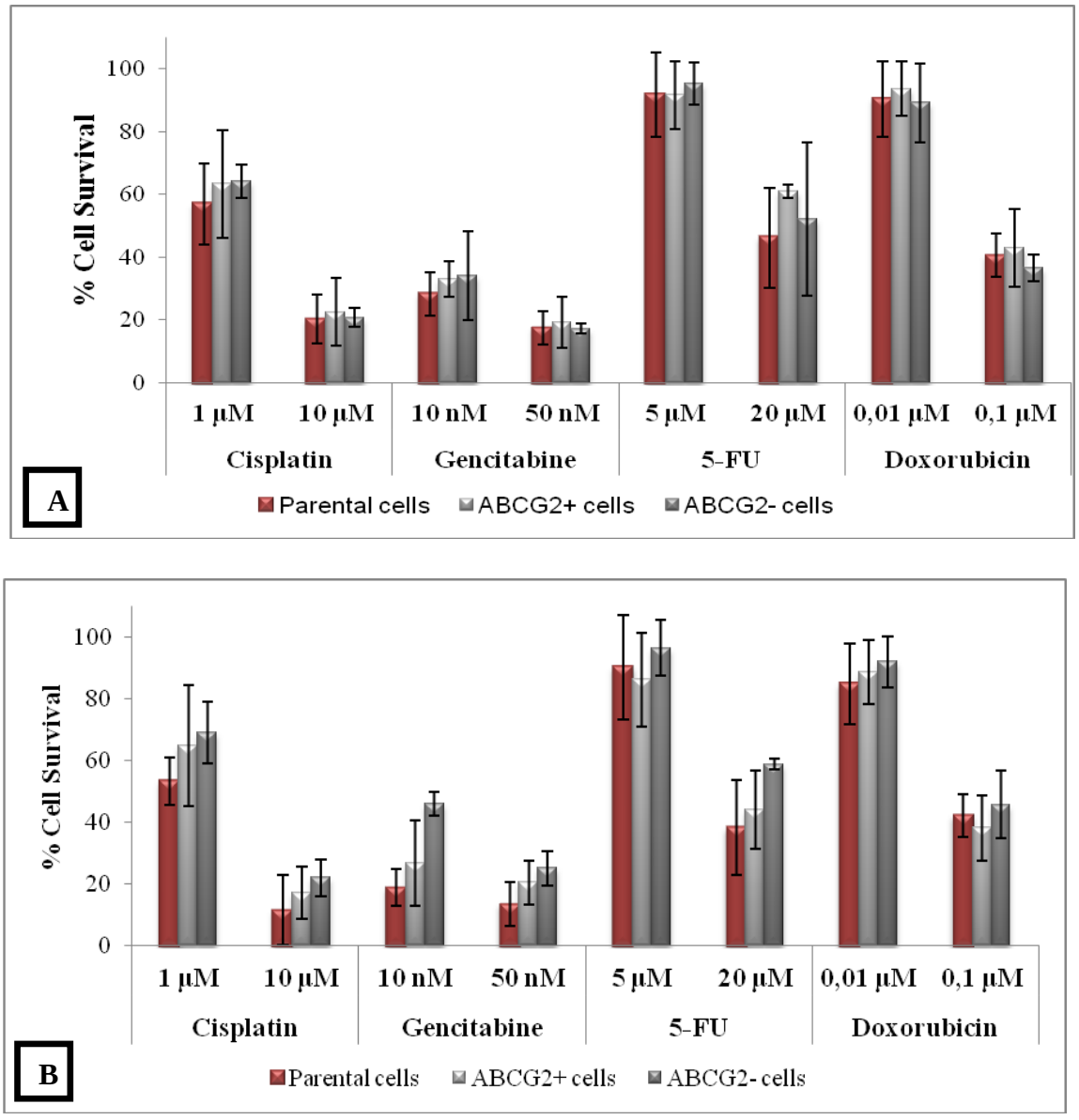

Figure 3.4 - Cell survival upon incubation with chemotherapeutic drugs (cisplatin, gemcitabine, 5-FU and doxorubicin) in NCI-H460 parental cells and the ABCG2+ and ABCG2- sub-populations, was assessed by resazurin-based (A) and SRB (B) assays. Results are the mean ± SD of three independent experiments (each from an independent cell sorting experiment).

3.2.3. Expression of ABCG2 in NCI-H460 cell sorted populations following *in vitro* expansion

To understand the evolution of sorted population, at the time of cell growth/viability assay were performed, expression of ABCG2 in the $ABCG2^+$ and $ABCG2^-$ cell sorted populations was assessed following nine days of *in vitro* expansion (after FACS). Results show that both sub-populations of sorted cells presented a similar percentage of ABCG2 expression as originally found in the parental cell line (Figure 3.5), which limits the use of this approach for subsequent studies on putative lung CSCs.

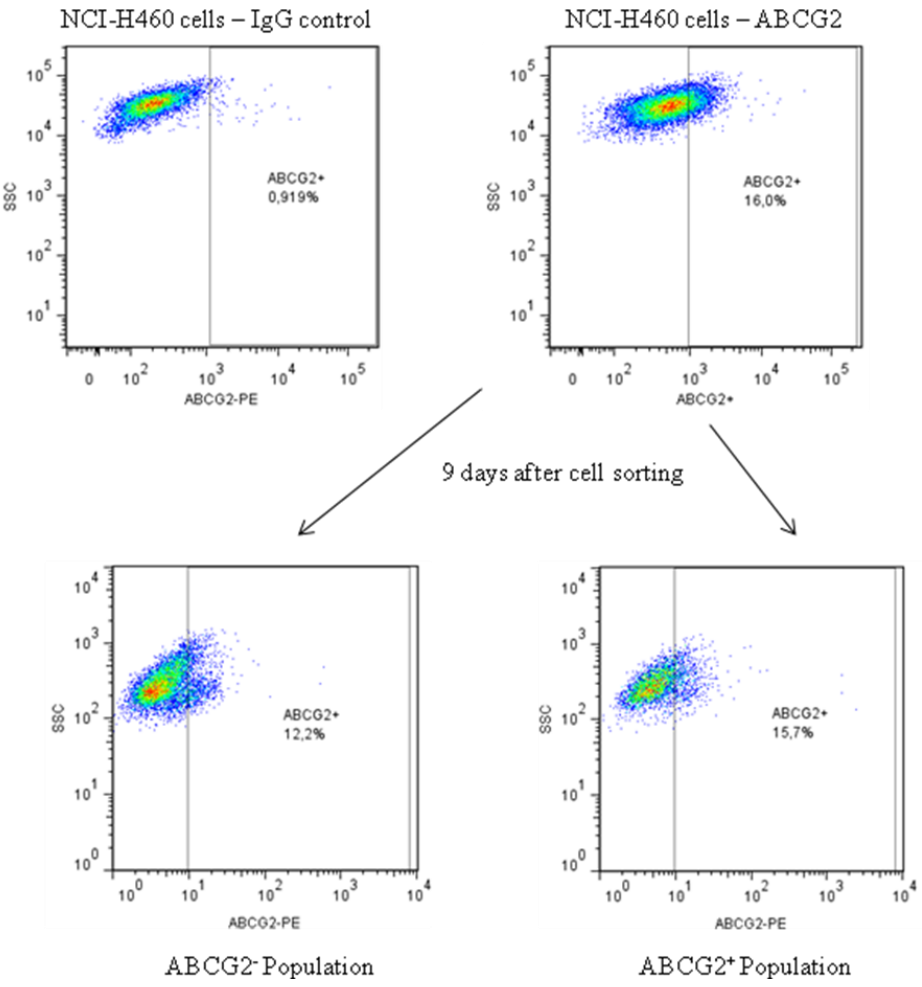

Figure 3.5 – Fluorescence activated cell sorting for the ABCG2 marker was performed in NCI-H460 cell line. ABCG2 was present in 16% of the NCI-H460 cells when compared with the IgG-PE control. Nine days upon cell sorting, the percentage of ABCG2 in each sorted sub-populations was assessed. The $ABCG2^+$ sub-population of cells possessed 15.7% of ABCG2 and the $ABCG2^-$ sub-population exhibited 12.2% of cells expressing this protein. Results shown were obtained from cell sorting experiment number 1.

3.3 Enrichment of putative lung CSCs by incubation with chemotherapeutic agents

In order to verify if incubation with chemotherapeutic drugs may result in an enrichment of cancer stem-like cells and, consequently, a more resistant sub-population of cells, two lung cancer cell lines (NCI-H460 and A549) were exposed to chemotherapeutic drugs commonly used in the clinic. The A549 lung cell line was exposed to cisplatin (10 μM) and to doxorubicin (0.1 μM) for three weeks followed by a drug-free recovery period (three to four weeks). The NCI-H460 lung cancer cell line was exposed to cisplatin (1 μM and 2 μM) and to doxorubicin (0.05 μM) for three weeks followed by a drug-free recovery period (three to four weeks).

3.3.1. Assessment of cell morphology

Cell morphology during the three week incubation time with the drugs and during the drug-free recovery period was monitored by optical microscopy. It was observed that drug treatment led to a transient alteration in cell morphology in both cell lines, whereby cells acquired a more mesenchymal-like structure at 5 to 7 days upon drug incubation, depending on the cell line and on the chemotherapeutic agent. When the drug was withdrawn, the cells re-acquired their original epithelial morphology within 6 to 14 days following drug withdrawal (Figures 3.6, 3.7, 3.8 and 3.9).

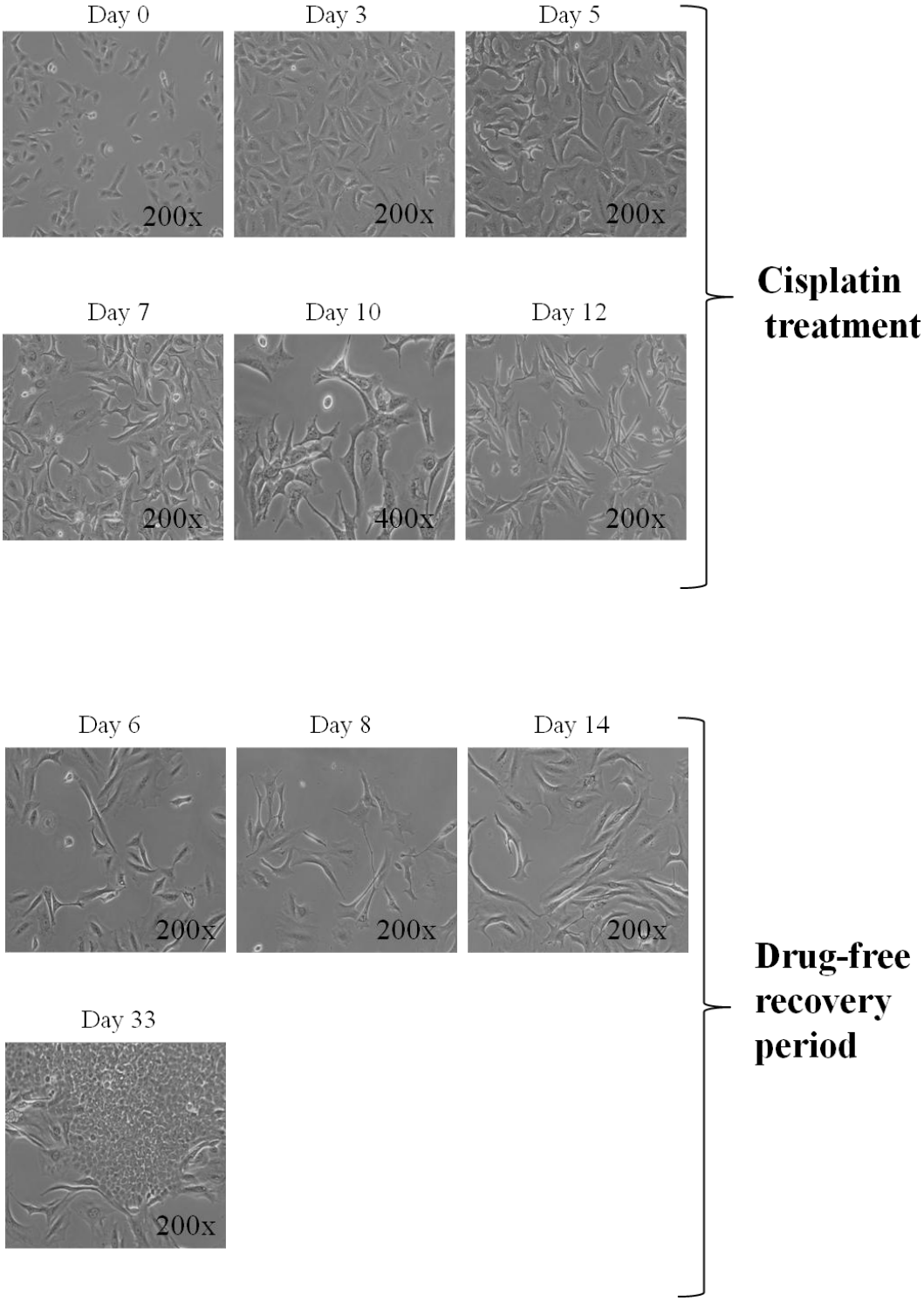

Figure 3.6 - Cell morphology changes observed upon incubation of A549 cells with 10 μM of the chemotherapeutic drug cisplatin (for three weeks) followed by a drug-free recovery period (of several weeks).

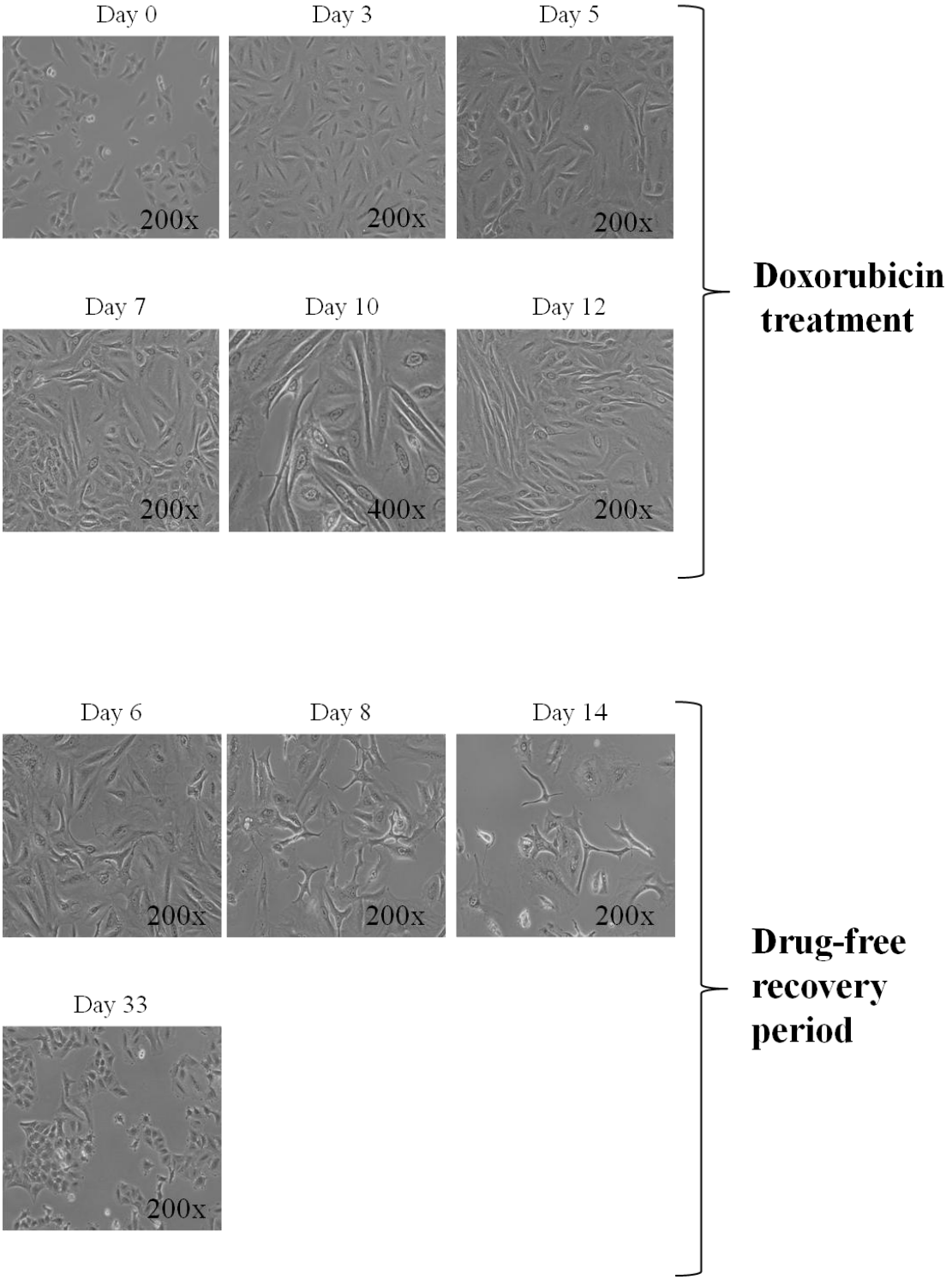

Figure 3.7 - Cell morphology changes observed upon incubation of A549 cells with 0.1 μM of the chemotherapeutic drug doxorubicin (for three weeks) followed by a drug-free recovery period (of several weeks).

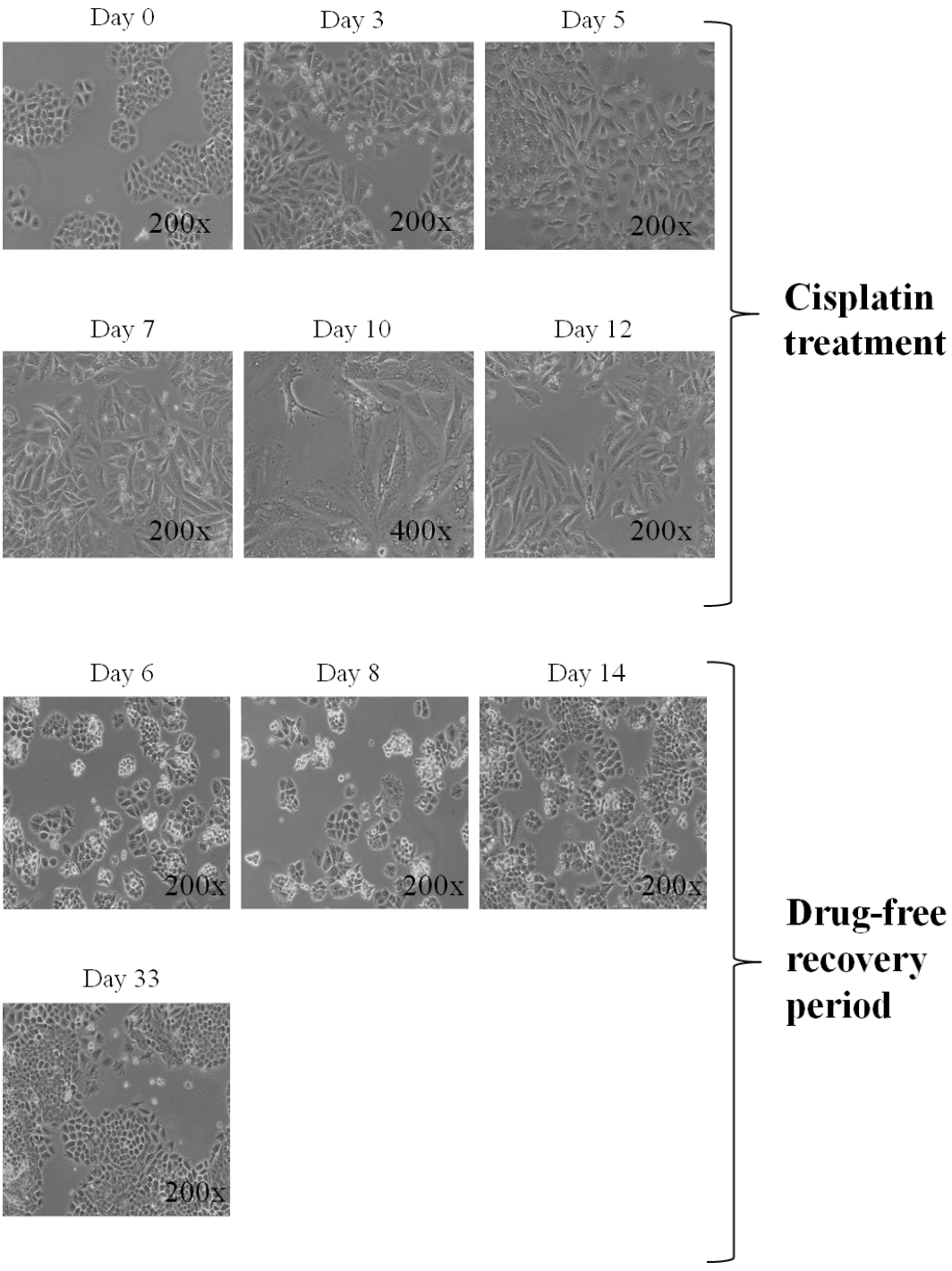

Figure 3.8 - Cell morphology changes observed upon incubation of NCI-H460 cells with 2 μM of the chemotherapeutic drug cisplatin (for three weeks) followed by a drug-free recovery period (of several weeks).

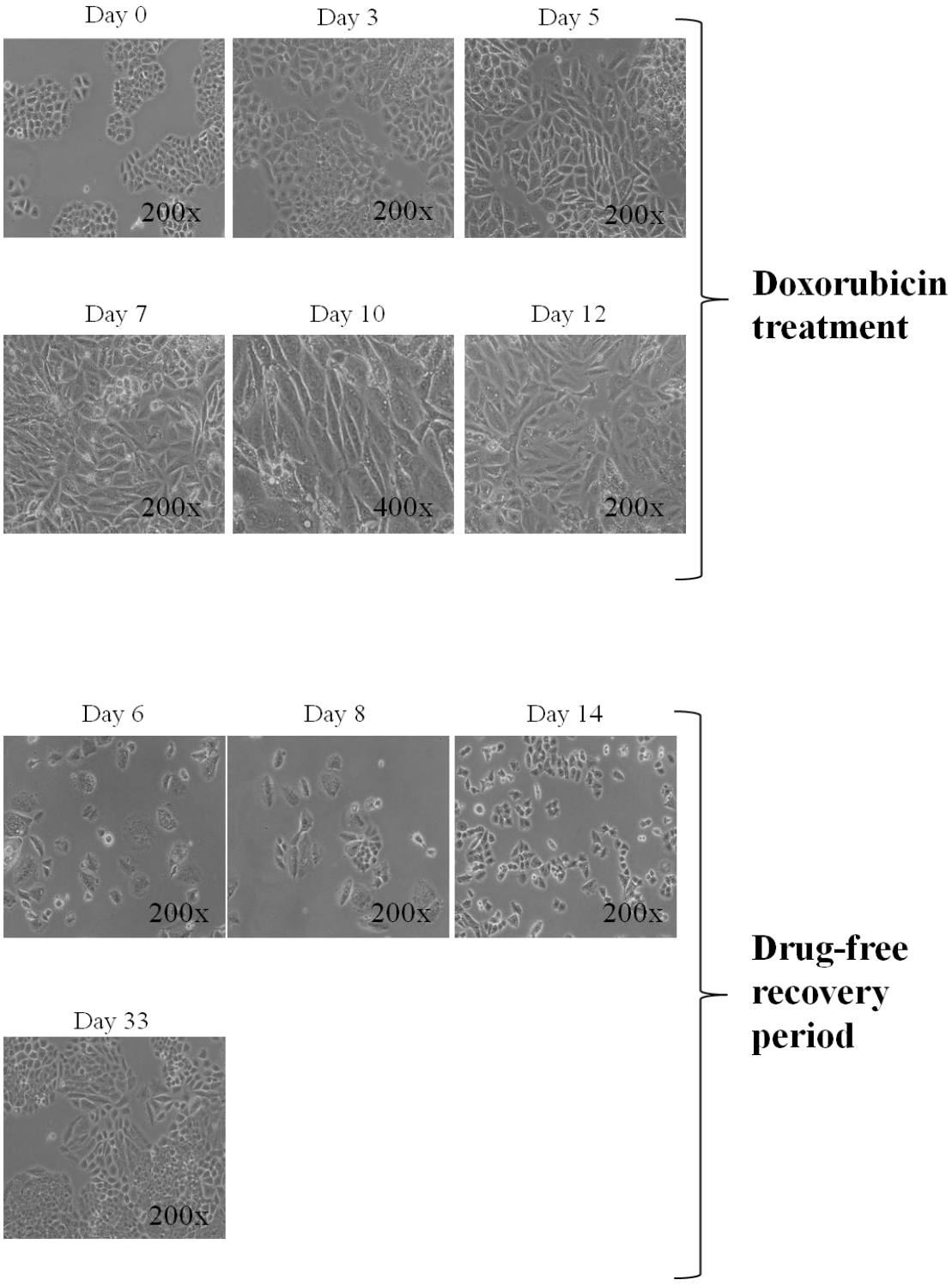

Figure 3.9 - Cell morphology changes observed upon incubation of NCI-H460 cells with 0.05 µM of the chemotherapeutic drug doxorubicin (for three weeks) followed by a drug-free recovery period (of several weeks).

3.3.2. Assessment of drug response in the drug-selected populations

Cell growth/viability assays were performed in all the drug-selected populations of cells in order to assess differential drug response when compared with the parental cell lines they originated from. All the experiences were performed after the three week drug exposure followed by the drug-free recover period. Cell growth/viability assays were always performed using both resazurin-based and SRB assays.

The drug selected A549 cells derived from long term exposure to doxorubicin (0.1 μM) did not show alterations in terms of drug response when compared with the parental cell line (Figure 3.10) after 48 hours of doxorubicin treatment (0 to 0.2 μM).

Cisplatin-selected A549 cells (10 μM) also did not show alterations in terms of drug response when compared with A549 parental cells, but only one experience was performed (data not shown).

NCI-H460 cells incubated with 0.05 μM doxorubicin for a three week period did not present increased resistance to doxorubicin (0 to 0.1 μM) during 48 hours when compared to the parental cells (Figure 3.11). However, NCI-H460 cells selected upon a long-term incubation with 1 and 2 μM of cisplatin presented a significant increase in resistance towards the selecting agent, when compared to the parental cells (Figures 3.12 and 3.13, respectively). From NCI-H460 exposure to 1 and 2 μM of cisplatin resulted what we name from now on as cisplatin resistant cell variant A (CRCVA) and cisplatin-resistant cell variant B (CRCVB), respectively.

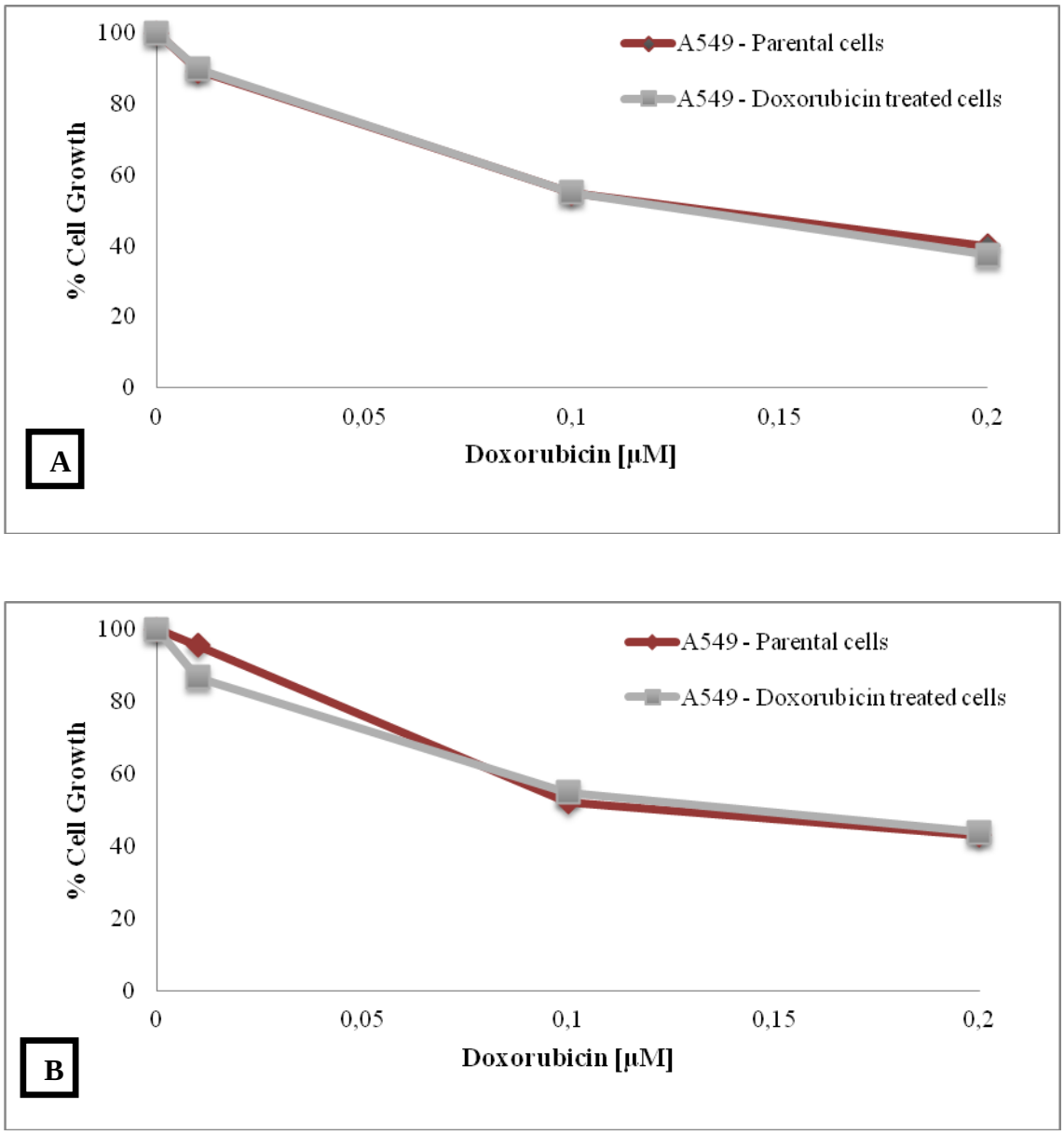

Figure 3.10 – Percentage of cell growth following 48 hour incubation with doxorubicin (0 to 0.2 µM) in A549 parental cells and doxorubicin-selected (0.1 µM) A549 cells, was assessed by resazurin-based (A) and SRB (B) assays. Results are the mean of three replicate measurements per sample, performed in two independent experiments.

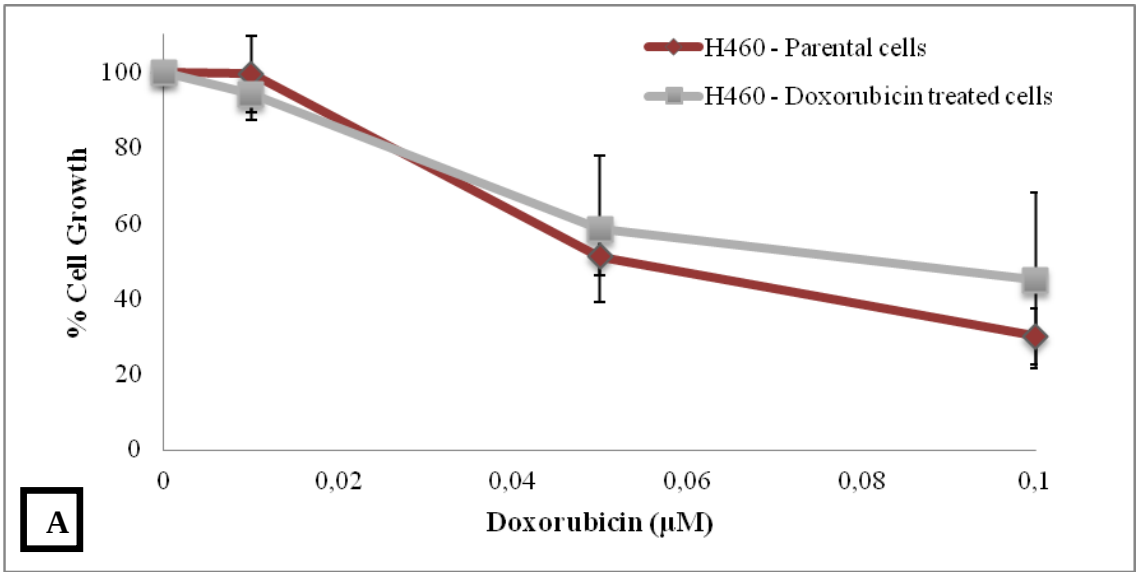

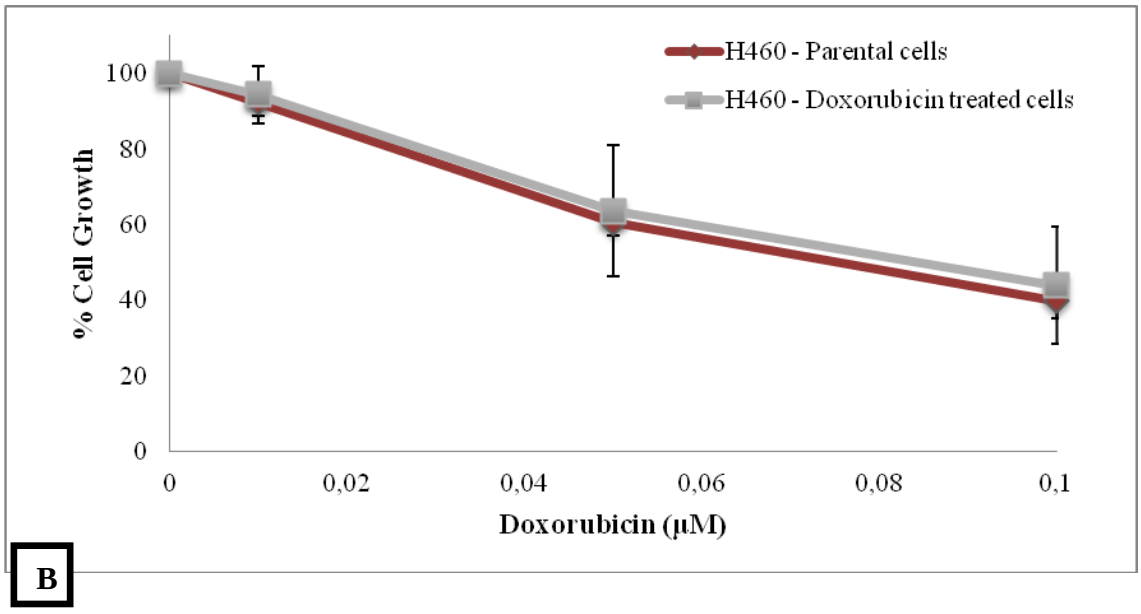

Figure 3.11 – Percentage cell growth following 48 hour incubation with doxorubicin (0 to 0.1 µM) in NCI-H460 parental cells and doxorubicin-selected (0.05 µM) NCI-H460 cells, was assessed by resazurin-based (A) and SRB (B) assays. Results are the mean of two independent experiments.

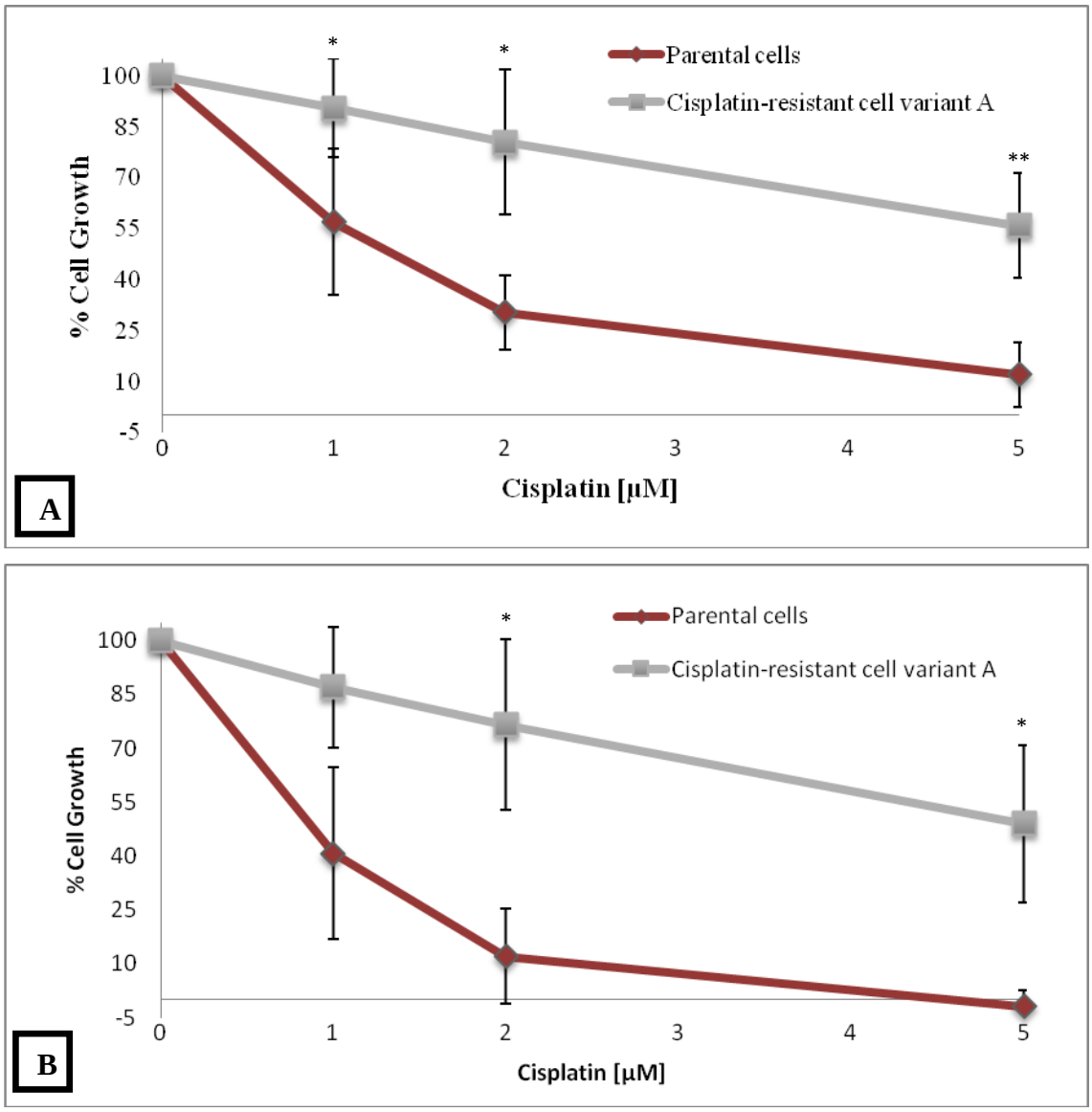

Figure 3.12 – Cisplatin-resistant cell variant A (derived from NCI-H460 when treated with 1 µM of cisplatin) and parental cells (NCI-H460) were incubated with different concentrations of cisplatin (0 to5 µM) for 48 hours. The percentage of cell growth was assessed with resazurin-based (A) and SRB (B) assays. Results are the mean ± SD of three independent experiments, * $P < 0.05$ and ** $P < 0.01$.

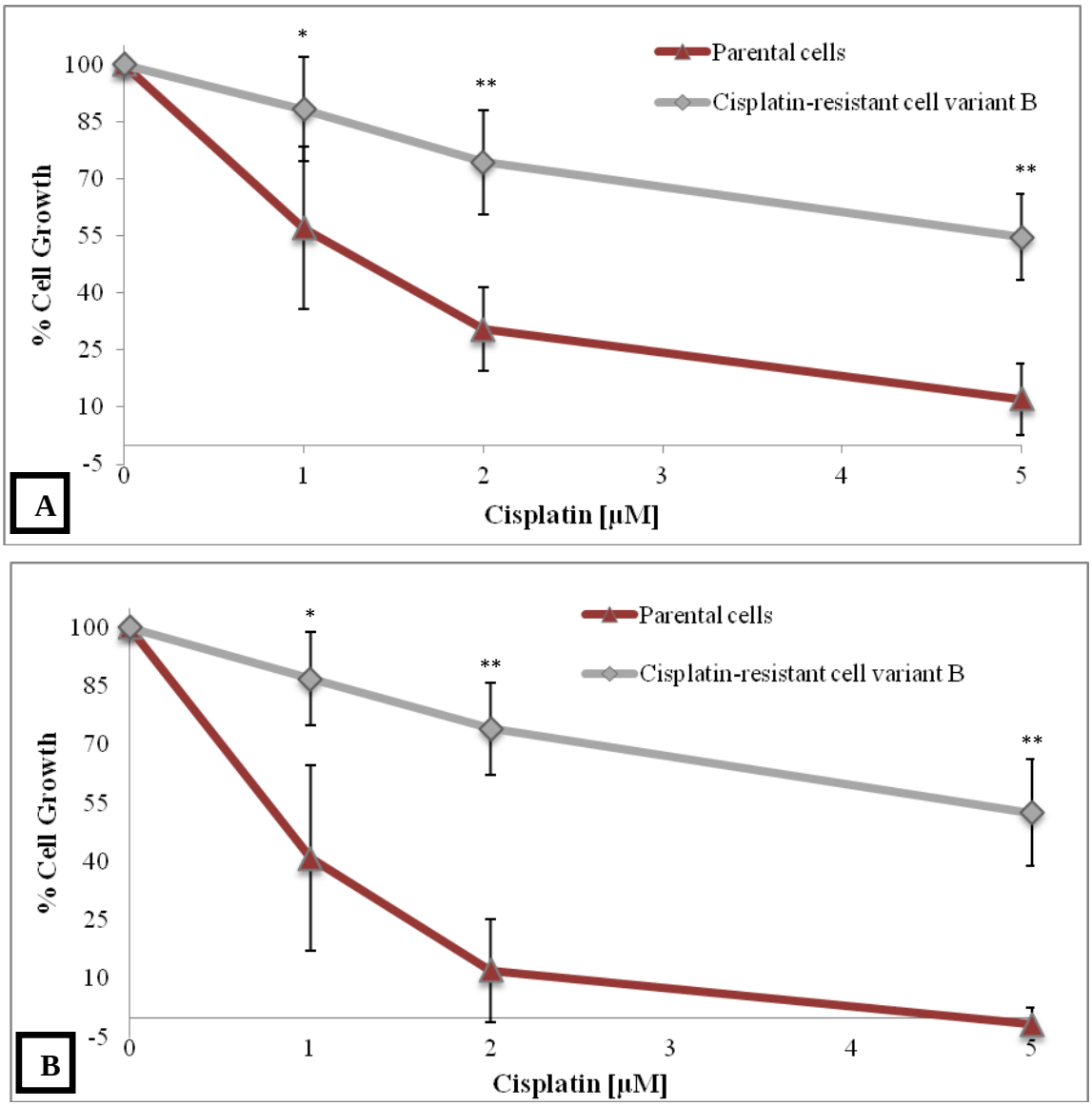

Figure 3.13 – Cisplatin-resistant cell variant B (derived from NCI-H460 when treated with 2 µM of cisplatin) and parental cells (NCI-H460) were incubated with different concentrations of cisplatin (0 to 5 µM) for 48 hours. The percentage of cell growth was assessed with resazurin-based (A) and SRB (B) assays. Results are the mean ± SD of three independent experiments, * $P < 0.05$ and ** $P < 0.01$.

Only NCI-H460 cells resulting from long-term exposure to 1 μM and 2 μM of cisplatin possessed increased survival ability towards the selecting agent when compared with the parental cells. This increased cisplatin-resistance in cisplatin-resistant cell variant B (CRCVB) was further confirmed by the clonogenic assay, whereby upon incubation with 1 μM of cisplatin the obtained % cell survival was of 5 ± 4.6 and 32 ± 6.7 for parental and CRCVB cells, respectively (average of three independent experiments, performed in triplicate). In addition, response to other chemotherapeutic agents, for which cells had not been previously exposed to, was also assessed (Figure 3.14). Results show that cisplatin long term exposure led to increased resistance towards the selecting drug but also to gemcitabine and doxorubicin (although no statistical significant difference was observed in the latter), although not for 5-FU.

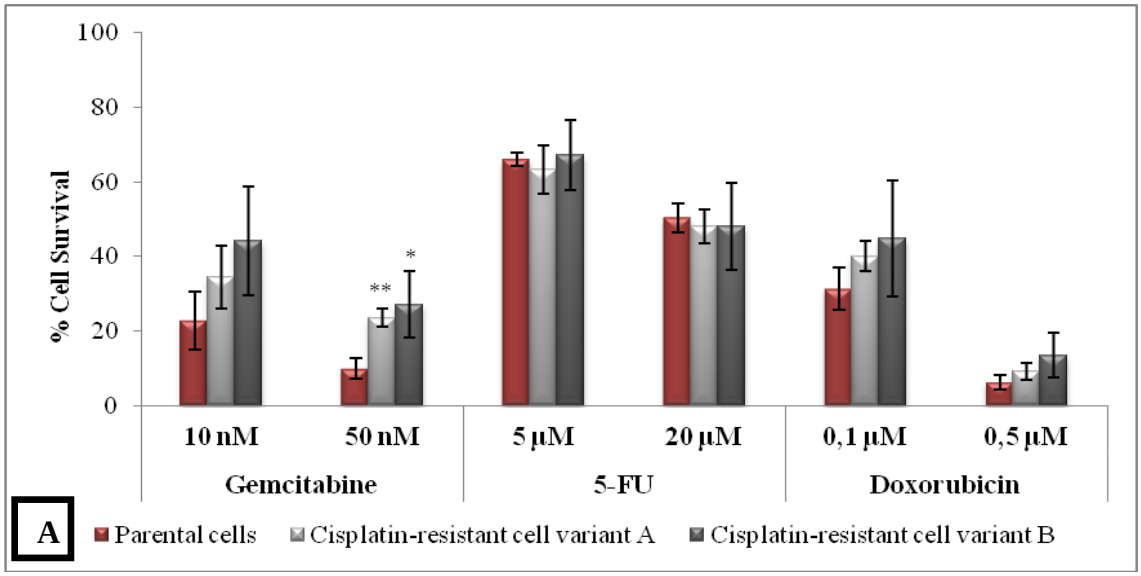

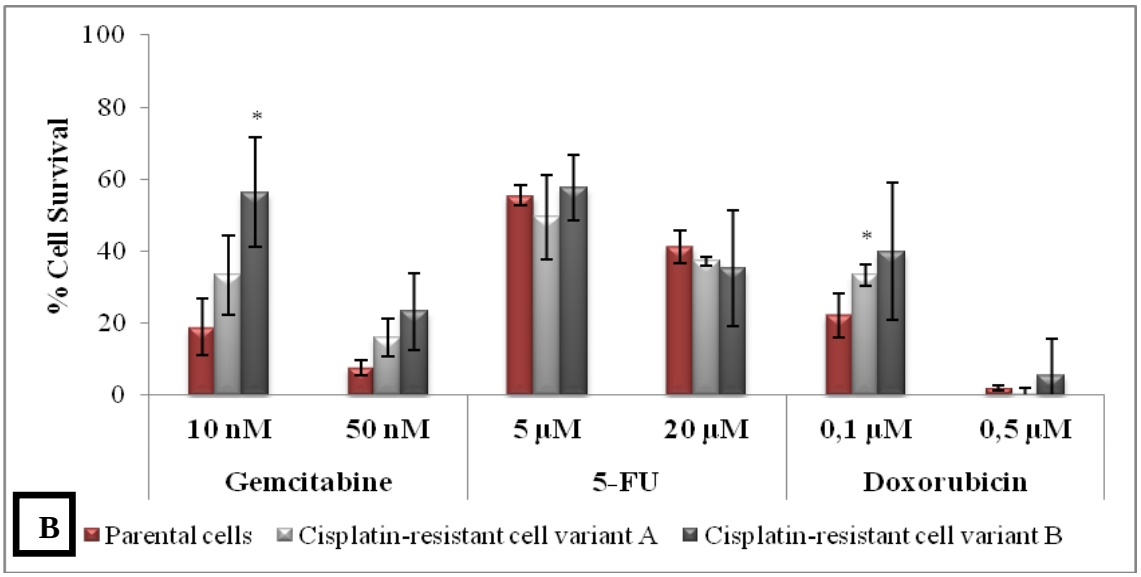

Figure 3.14 - Drug-selected and NCI-H460 parental cells were incubated with different concentrations of gemcitabine, 5-FU and doxorubicin. The percentage of cell survival was assessed with a resazurin-based (A) and the SRB (B) assays. Results are the mean ± SD of three independent experiments, * $P < 0.05$ and ** $P < 0.01$.

3.3.3. Assessment of chemoresistance upon novel drug exposure of the drug-selected cell variants

The cisplatin-resistant cell variant B and NCI-H460-doxorubicin treated (0.05 μM) cells were further exposed to a new round of incubation (three week drug exposure followed by a drug-free recover period) with chemotherapeutic agents. Cisplatin-resistant cell variant B was incubated with 5 μM of cisplatin (resulting the cisplatin-resistant cell variant C) and NCI-H460-doxorubicin treated cells with 0.1 μM of doxorubicin (resulting the doxorubicin-resistant cell variant A), for three weeks followed by a drug-free recovery period (three to four weeks). The transient alteration in cell morphology was again verified (data not shown).

The effects of these new drug-incubation and recovery periods in drug resistance were further tested. Cisplatin-resistant cell variant C showed to be characteristically more resistant than the parental cells, although very similar to the cisplatin-resistant cell variant B, from which it originated (Figure 3.15). GI50 of cisplatin was calculated to NCI-H460 parental (GI50 ≈ 1 μM), CRCVB (GI50 ≈ 4.6 μM) and CRCVC (GI50 ≈ 4.7 μM). A five times higher concentration of cisplatin was required to inhibit the cell growth of CRCVB and CRCVC in 50 % when compared to the NCI-H460 parental cells.

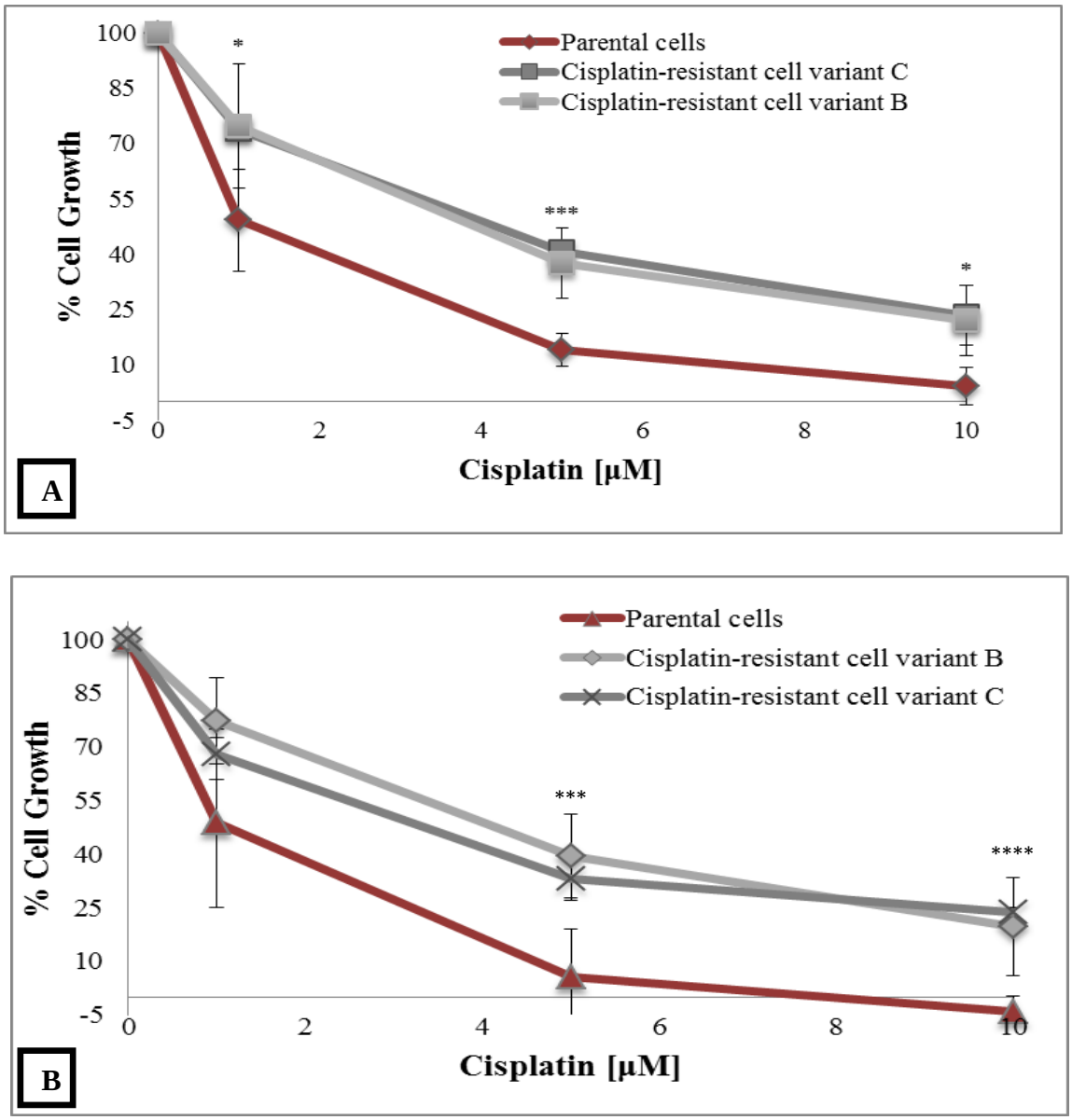

Figure 3.15 – Cisplatin-resistant cell variant C (derived from cisplatin-resistant cell variant B when treated with 5 µM of cisplatin), cisplatin-resistant cell variant B and parental cells (NCI-H460) were incubated with different concentrations of cisplatin (0 to 10 µM) for 48 hours. The percentage of cell growth was assessed with resazurin-based (A) and SRB (B) assays. Results are the mean ± SD of three independent experiments, * $P < 0.05$, *** $P < 0.001$ and **** $P < 0.0001$ (calculated between cisplatin-resistant cell variant c and parental cells).

The new cycle of therapy induced in the doxorubicin-treated cells by long-term exposure to 0.1 µM of doxorubicin resulted in a sub-population of significantly more resistant cells when compared to the parental NCI-H460 cells (Figure 3.16).

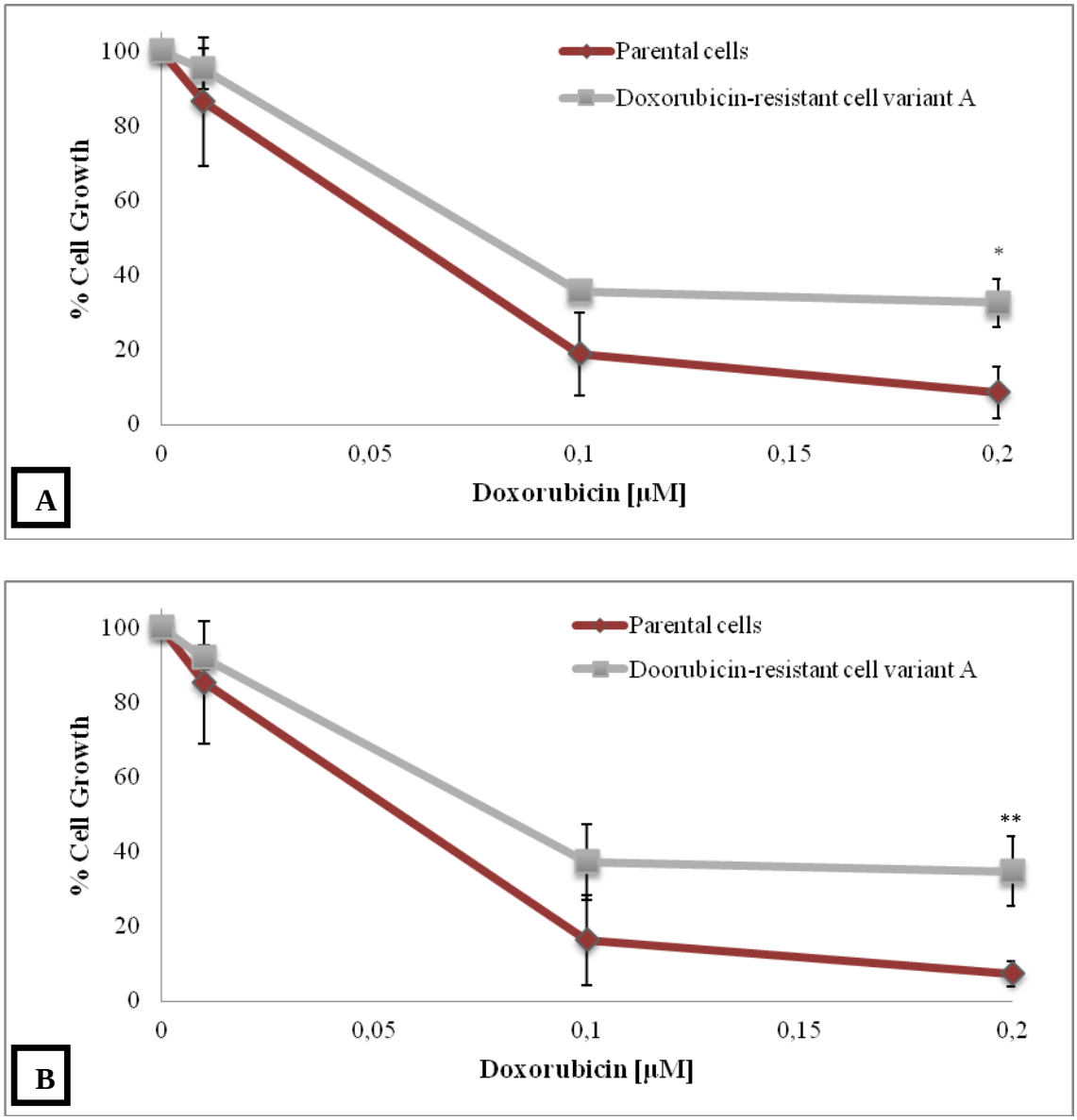

Figure 3.16 – Doxorubicin-resistant cell variant A (derived from doxorubicin-treated cells when treated with 0.1 µM of doxorubicin) and parental cells (NCI-H460) were incubated with different concentrations of doxorubicin (0 to 0.2 µM) for 48 hours. The percentage of cell growth was assessed with resazurin-based (A) and SRB (B) assays. Results are the mean ± SD of three independent experiments, * $P < 0.05$ and ** $P < 0.01$.

From all drug-selected cell variants, cisplatin-resistant cell variant A (CRCVA) and cisplatin-resistant cell variant B (CRCVB) were choosen for all subsequent studies.

3.4. Assessment of expression of proteins involved in drug resistance

In an attempt to identify the proteins conferring increased drug resistance to the resistant NCI-H460 cell variants (when compared to the parental cells), expression of proteins involved in drug resistance (Pgp, XIAP, Bcl-XL, Bcl 2) was assessed by Western blot. Increased expression of the apoptosis-related proteins Bcl-XL and XIAP in CRCVB and of the drug efflux pump P-glycoprotein (PgP) in CRCVA was verified when those populations were compared to the parental NCI-H460 cell line (figures 3.17 and 3.18).

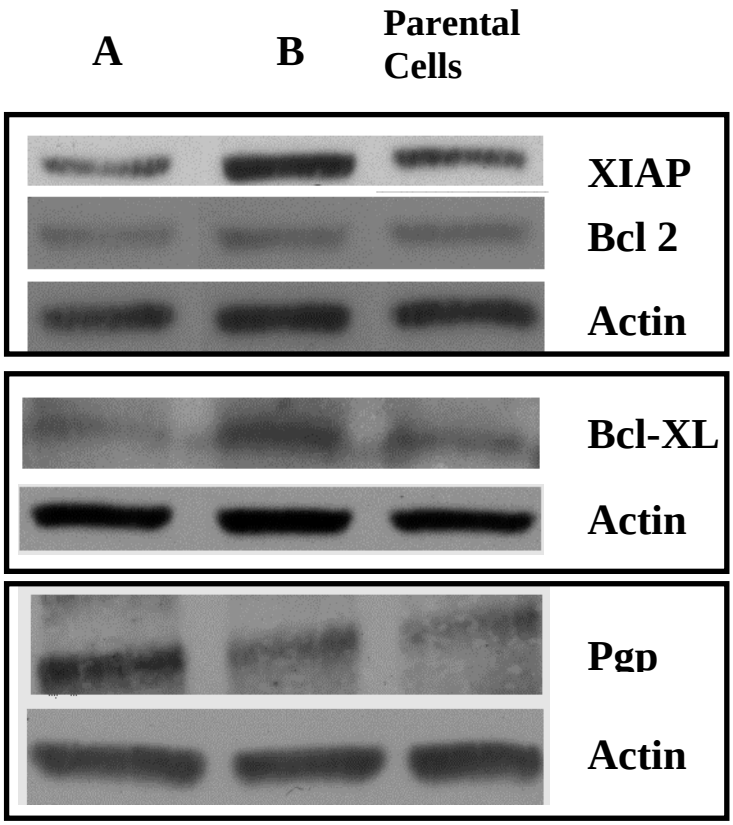

Figure 3.17 – Western blot to XIAP, Bcl 2, Bcl-XL and to Pgp were performed using two independents extractions of total protein from each population of cells (A – cisplatin-resistant cell variant A; B – cisplatin resistant cell variant B). Actin was used as a loading control.

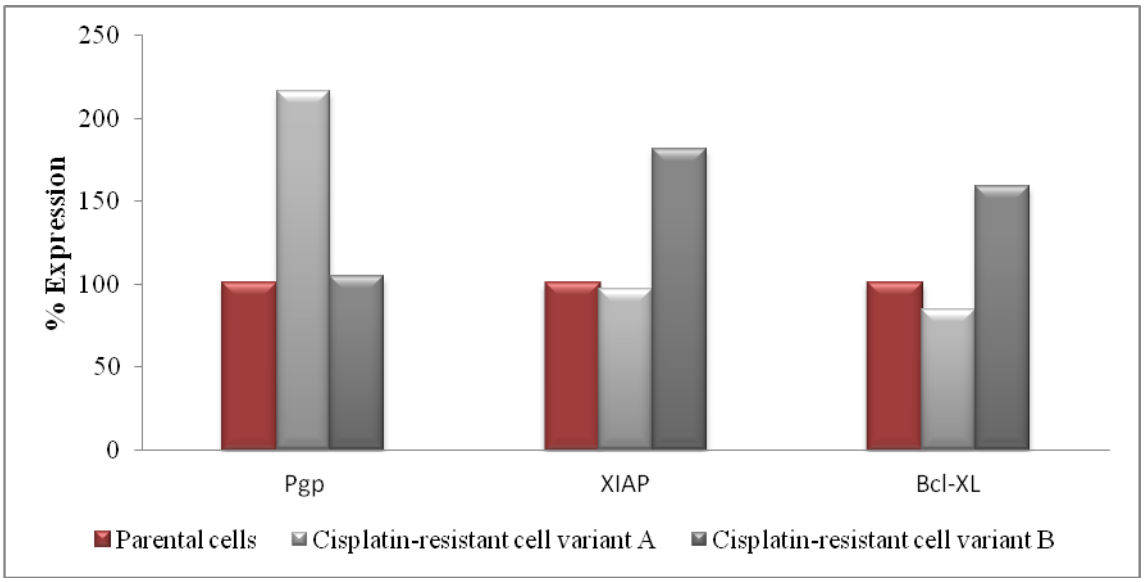

Figure 3.18 – Quantification of Pgp, XIAP and Bcl-XL expression using actin as a loading control. Each value represents the mean of two independent samples tested at least in two different occasions.

To determine how CRCVA, CRCVB and NCI-H460 parental cells responded after 24 hours of 5 µM of cisplatin exposure in terms of P53 expression and Pgp induction, the levels of P53 and Pgp were assessed by Western blot. After drug exposure, up-regulation of P53 was found in NCI-H460 parental and cisplatin resistant variants, although this response seemed increased in the parental cells when compared to CRCVA and CRCVB treated cells (Figure 3.19). Cisplatin incubation with CRCVA was capable of inducing up-regulation of Pgp, although no expression differences were found relatively to the other tested populations (Figure 3.19).

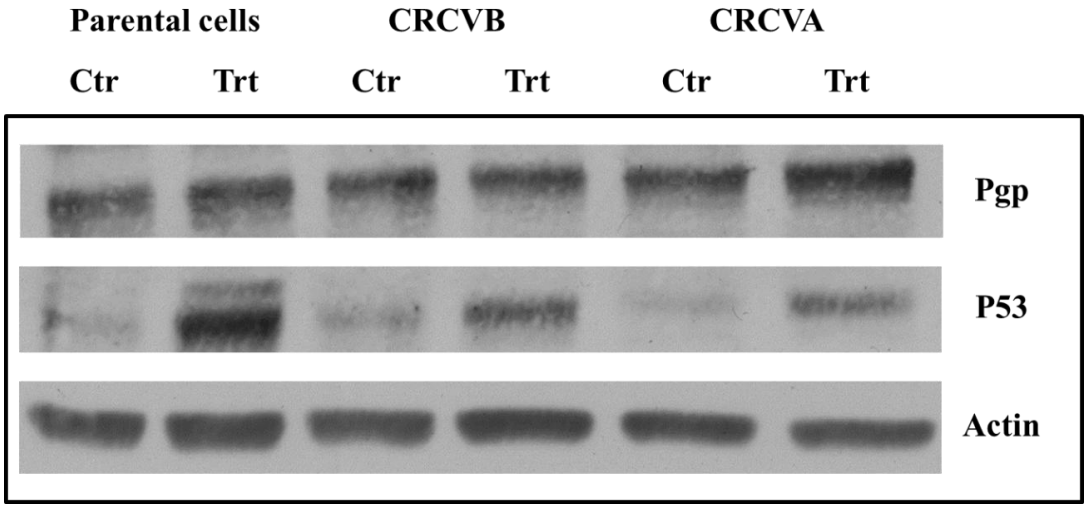

Figure 3.19 - Western blot was perfomed to P53 and Pgp proteins in CRCVA, CRCVB and NCI-H460 parental cells. After 24 hours of cisplatin exposure, all the treated populations up-regulated P53, althuogh a higher overexpression was found between the NCI-H460 parental cells. Only the CRCVA population was capable to up-regulate Pgp protein after 24 hours of drug exposure. Ctr – control cells; Trt – treated cells. Results represent one single experiment.

3.5. Stemness assessment of the cisplatin-selected cell variants

To verify if cisplatin long term exposure enriched a population with stem-like properties the presence of stem-like cell markers, such as ABCG2, CD133 and Sox 2, Bmi-1, were assessed by flow cytometry and qRT-PCR in both NCI-H460 cisplatin-resistant variants and parental cells.

3.5.1. Analysis of ABCG2 expression by flow cytometry

The percentage of expression of ABCG2 and CD133 stem cell markers was assessed by flow cytometry, to verify the presence of stem-like cell properties in the cisplatin-resistant cells (Figure 3.20). An apparent increase in the percentage of cells expressing the putative stem cell marker ABCG2 (Figure 3.20) was observed for both cell variants, although this was only statistically significant for the cisplatin-resistant cell variant B (Figure 3.21). Expression of CD133 also appeared to increase in the drug-resistant cell variants when compared to the parental cells, although the percentage of cells expressing this marker was only around 1% and may not be biologically relevant (data not shown).

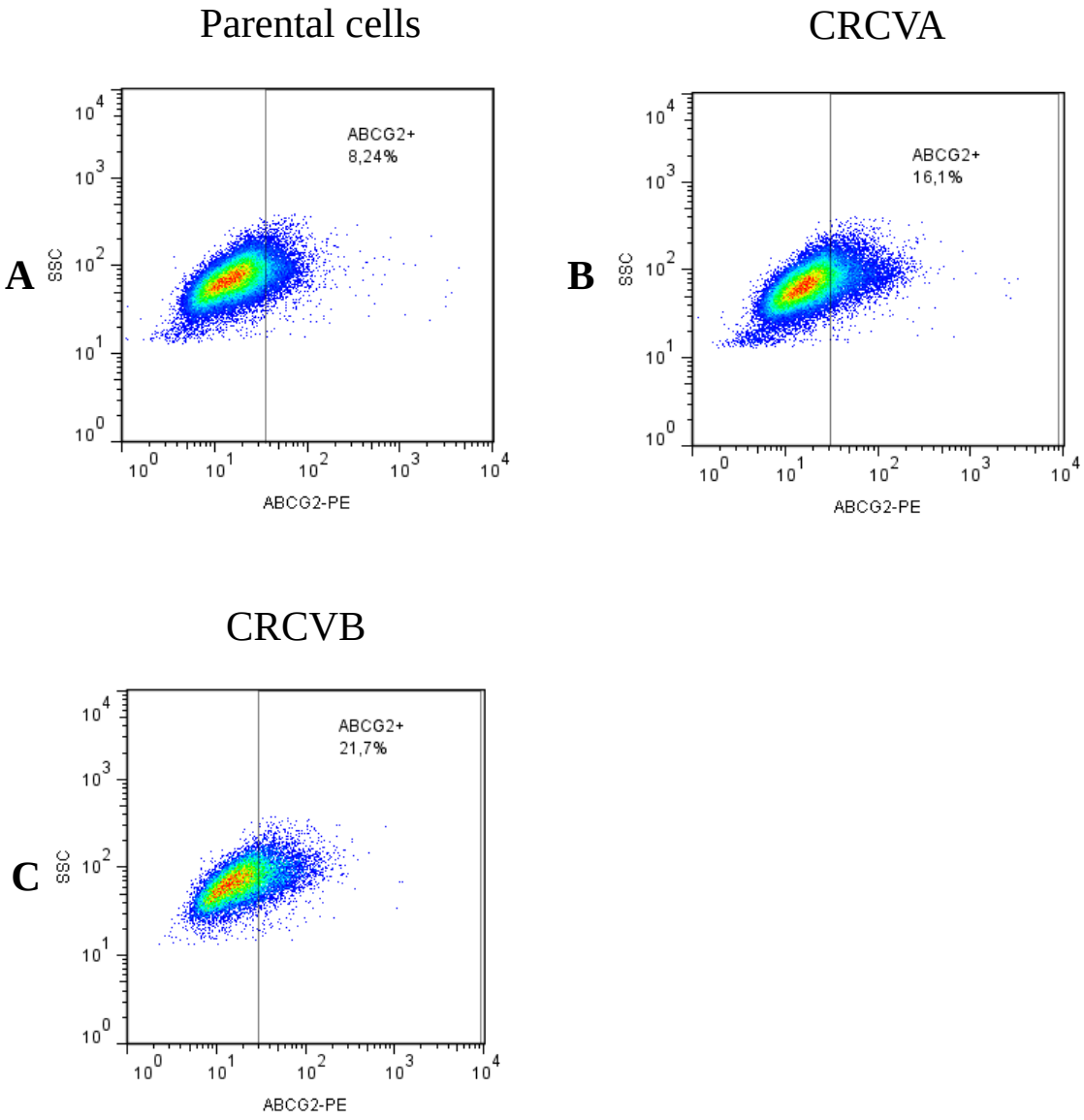

Figure 3.20 - Flow cytometry analysis for ABCG2 was performed in NCI-H460 parental cells (A), cisplatin-resistant cell variant A (B) and in cisplatin-resistant cell variant B (C). Results shown are representative of three independent experiments.

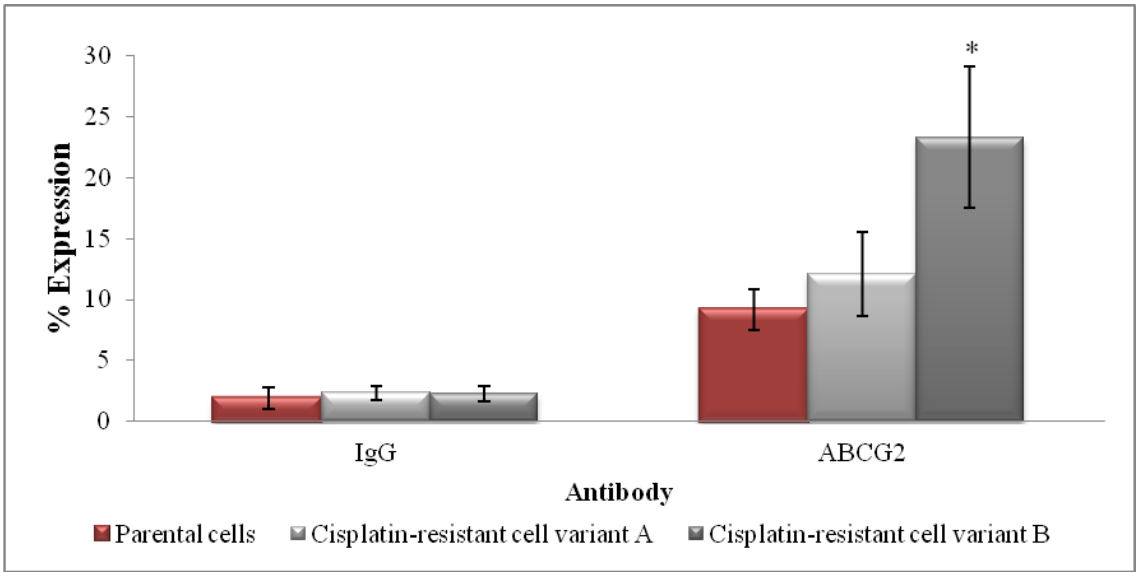

Figure 3.21 – Percentage of cells expressing ABCG2 was assessed by flow cytometry analysis in NCI-H460 parental cells and in cisplatin-resistant cell variants A and B, when compared to cells labelled with IgG-PE of each population. Results are the mean ± SD of three independent experiments, * $P < 0.05$.

3.4.2. Colony-forming assay

The colony-forming assay was perfomed to assess whether the cisplatin-resistant cells possessed enhaced stemness capacity when compared to NCI-H460 parental cells, as determined by assessing the % of plating efficiency. Plating efficiency was calculated between the number of colonies generated from each population, taking into account the initial number of cells seeded per Petri dish. Results obtained from three independent experiments (performed in triplicate) revealed only small differences in % plating efficiency between the parental and CRCVB cells (54.7 ± 3.6 and 63.1 % ± 7.6, respectively).

3.4.3. Tumourigenesis assay

An *in vivo* tumourigenesis assay, using the chicken embryo, was also performed in the NCI-H460 and CRCVB cells.

Different numbers of cells ($1x10^6$, $1x10^5$, $1x10^4$) from each CRCVB and parental population were inoculated on top of the CAM. No differences in the number of tumours

formed between CRCVB and parental cells were verified after $1x10^6$ and $1x10^5$ cells were inoculated. When $1x10^4$ cells were inoculated, CRCVB possessed capacity to generate tumours whereas NCI-H460 parental cells did not (Table 3.3). A tendency for CRCVB cells to generate bigger tumours than parental cells, after inoculation of $1x10^6$ cells, was also observed (Figure 3.22). Six chicken embryos were used for each condition, however many chicken embryos died during the experiment.

Table 3.2 - Tumourigenesis of CRCVB and NCI-H460 parental cells. The capacity of CRCVB and parental cells to generate tumours *in vivo* was assessed by CAM model. The number of chicken embryos presenting a CAM tumour 7 days after cell inoculation is represented relatively to the final numbers of surviving chicken embryos. Results are representative of one single experiment.

Condition	Inoculated cells	NCI-H460 cells	CRCVB
1	$1x10^6$	2/2	4/4
2	$1x10^5$	2/3	2/3
3	$1x10^4$	0/3	4/5

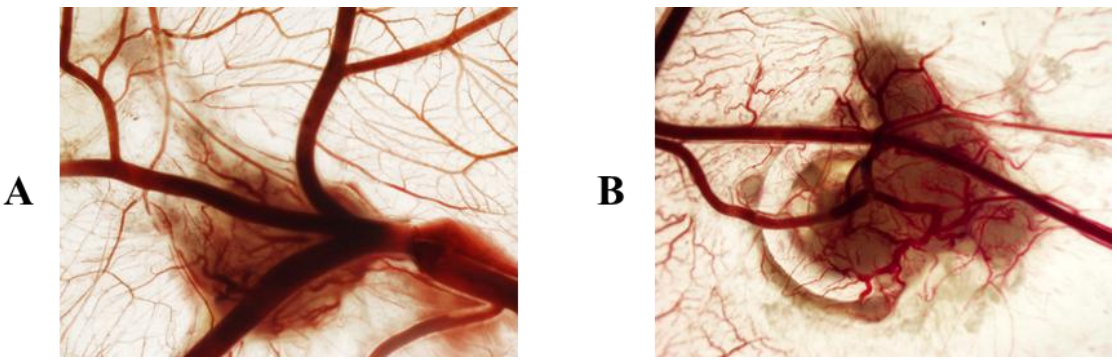

Figure 3.22 – Tumour formation in CAM tissue. Seven days after $1x10^6$ cells from NCI-H460 parental cells (A) and CRCVB (B) being inoculated on CAM, tissue was dissected and fixed and tumours observed. Images are representative of the results obtained in condition 1.

3.6. Assessment of expression of stemness and drug resistance-related genes

In order to quantify the presence of other stem cell markers in cisplatin-resistant cell variants, gene expression of *Bmi-1*, *Sox2* and *ABCG2* was assessed by RT-PCR. *MDR1* gene expression was also measured to assess whether the increased Pgp expression verified in CRCVA was due to increased mRNA expression. Fold changes (FC) > 1.7 or < –1.7 (considered biologically relevant) were observed in *ABCG2* and *MDR1* genes expression in both CRCVA and especially in CRCVB. Expression of *Sox2* was decreased in CRCVA, with a FC of -2 (Table 3.4).

Table 3.3 - Quantifications of gene expression through RT-PCR. *ABCG2*, *Sox2*, *MDR1* and *Bmi-1* genes expression was quantified in CRCVA and CRCVB relatively to the amount of all tested genes in NCI-H460 parental cells. *Hprt1* gene was used as a loading control. Results are the mean ± SD of three independent experiments.

Gene	CRCVA	CRCVB
ABCG2	1.7 ± 0.2	2.2 ± 0.1
Sox2	-2.2 ± 0.1	1.1 ± 0.5
MDR1	5.9 ± 2.6	10.2 ± 1.8
BMI1	1.5 ± 0.4	1.6 ± 0.3

4. Discussion

Tumour drug resistance is a major issue in the management of lung cancer, the worldwide leading cause of cancer-related deaths, as almost all lung tumours are either intrinsically resistant or quickly develop acquired resistance to chemotherapeutic drugs [131]. Since it is currently believed that CSCs are partially responsible for tumour drug resistance, we aimed to identify some of the drug resistance mechanisms in putative lung CSCs in order to select appropriate targets to chemosensitize those cells and improve patient survival.

The SP phenotype is described as a stem cell property that has already been successfully used to identify lung cancer cells with stem-like properties [7]. As mentioned above, SP cells can be isolated by dual-wavelength flow cytometry because of their ability to efflux Hoechst dye, being this process mediated by ABCG2 protein. In this project, expression of ABCG2 was used to identify a putative lung CSC population. Human ABCG2 is the second member of the G subfamily of ABC transporters, which use cellular ATP to drive the transport of various substrates across cell membranes including drugs, metabolites and other compounds. ABCG2 was first cloned from doxorubicin-resistant human MCF-7 breast cancer cells and named as breast cancer resistance protein (BCRP) [132]. After fluorescence activated cell sorting it was found that this transmembrane protein was present in around 10 to 16% of NCI-H460 cells (Table 3.1). There was not a well-defined $ABCG2^+$ population in the stained samples during cell sorting, making it difficult to select the appropriate gatings to identify the $ABCG2^+$ sub-population. Consequently the purity level of the positive-sorted cells was affected. A high level of purity was preferred in detriment of increased final number of cells, which meant that the cells had to be further expanded following cell sorting. At this stage it was observed that the surviving sorted cells needed time to recover, and experiments to assess cell growth/viability in response to chemotherapeutic drugs were only possible to perform at least 9 days after cell sorting. Multiwell based cell viability/cell growth assays (resazurin-based and SRB assays) were performed to assess drug response between cell sorted and parental populations. As shown in Figure 3.4, there were no differences between the NCI-H460 parental cells, $ABCG2^+$ and $ABCG2^-$ sub-populations of cells in terms of resistance to the chemotherapeutic drug tested. When cell viability assays in the presence of drugs

were performed, the percentage of ABCG2 was similar in the $ABCG2^+$ and $ABCG2^-$ cell sorted populations and the parental cells (Figure 3.5), which may explain why no differences were found between those cell populations.

After cell sorting, the sub-populations rapidly reach the levels of ABCG2 expression observed in the parental cells, impairing an appropriated study of a putative cancer-stem like cell population using this approach. It was expected that $ABCG2^+$ cells were capable to give rise to the negative population. Although, the fact that the positive fraction of cells possess contaminant $ABCG2^-$ cells (70-86% of purity) may justify the rapidly increase of $ABCG2^-$ cells in the positive population. On the other hand, the appearance of $ABCG2^+$ cells in negative-sorted population means that $ABCG2^-$ cells possessed the ability to generate $ABCG2^+$ cells, which was not expected. The same results were before observed for Patrawala *et al*, when $ABCG2^+$ prostate cancer cells could generate $ABCG2^-$ cells and $ABCG2^-$ prostate cancer cells could also generate $ABCG2^+$ cells [133]. In the present study, repopulation of the original levels of cells expressing ABCG2 in $ABCG2^+$ population impaired the study of a putative cancer-stem like cell population.

One of the major properties of CSCs is their increased ability to survive in the presence of chemotherapeutic drugs, due to the presence of a number of genetic and cellular adaptations [80]. Conventional therapies appear to be capable of eliminating most of the cells in a tumour but not CSCs [13]. Bearing this in mind, cisplatin or doxorubicin incubation was attempted as a means of enrichment of a putative CSC population. We continuously exposed A549 and NCI-H460 cell lines to cisplatin or doxorubicin using their IG50 (defined as the concentration corresponding to 50% of growth inhibition) for three weeks followed by a drug-free recovery period. The recovery period was variable from each group of treated cells (3-5 weeks) and during this time the cells seemed to have a very low rate of cell divisions. Cell morphology was monitored and recorded throughout the experiment. It was observed that cells acquired a mesenchymal-like structure when exposed to the drugs and recovered their initial morphology after the chemotherapeutic agent was withdrawn (Figures 3.6, 3.7, 3.8 and 3.9). The observed morphological changes are consistent with EMT, a process by which epithelial cells undergo morphological changes such as acquire an elongated fibroblastic phenotype [134]. EMT induced by chemotherapy has already been described in the literature, being preferentially related with

ionising radiation or reactive oxygen species capable of inducing changes in morphology, cell adhesion and cell motility in a process that seems to be linked with radiation-induced fibrosis [112]. Recent studies correlated EMT induction by chemotherapy. Enhanced invasiveness and motility after cisplatin treatment were reported and specific microRNAs were linked with such regulation [135]. Some reports strongly suggest that EMT could generate stem-like cells, however the molecular mechanisms responsible for that process are not fully understood. CSCs share some characteristics with cells that have undergone EMT, like invasiveness and metastatic potential and drug resistance [136]. In fact, EMT and drug resistance phenotype seem to be extremely correlated. In some cases, the suppression of transcription factors involved in EMT resulted in chemo-sensitivity [137]. In other studies, cells that were particularly chemo-resistant possessed increased EMT markers [116]. The mechanism by which EMT confers resistance to therapy seems to be correlated with protecting the cells from undergoing apoptosis [138]. The presence of EMT has not yet been confirmed in our cells, although some indications of a possible epithelial-to-mesenchymal transition through the acquisition of an elongated mesenchymal-like structure have been recorded.

Response towards chemotherapeutic drugs was assessed in the drug-selected cell populations (following a three to five week drug-free recovery period) and compared with their respective parental cells. During the treatment time the majority of the parental cells died and only a subpopulation of cells survived. Even so, the A549 cells resulting from long term exposure to cisplatin (data not shown) or doxorubicin (Figure 3.10) did not show an enhanced resistance capacity to the selecting agent when compared to the parental cell line. Possibly, a more resistant population was enriched, although when cells recovered from drug treatment and started to proliferate they rapidly resemble the original population. Cisplatin exposure on NCI-H460 cells resulted in cisplatin-resistant cell variant A (CRCVA; exposed to 1μM of cisplatin) and cisplatin-resistant cell variant B (CRCVB; exposed to 2 μM of cisplatin) with significant increased resistance towards the selecting drug (Figures 3.12, 3.13, respectively) but also resistance to doxorubicin and gemcitabine, although not for 5-FU (Figure 3.14). The mechanism of action of all these drugs is related with impairment of DNA replication and consequently cell death by apoptosis. The only difference is that 5-FU most described mechanism of action does not interact directly with DNA, but by inhibition of the key enzyme of pyrimidine synthesis, TS [110]. Results

suggest that the mechanisms behind resistance to the chemotherapeutic drugs observed in the NCI-H460 drug selected cells are insufficient to confer resistance towards 5-FU. Drug resistance of cisplatin-selected cell variants A and B were assessed and confirmed, by cell growth/viability assays, to be maintained over a period of time of approximately 4 months. However, 6 months later, when colony-forming assay was performed, CRCVB plated cells possessed increased capacity to survive to cisplatin treatment (32.3 % ± 6.7) than NCI-H460 parental cells (5 % ± 4.6). These results corroborated the capacity of CRCVB to survive to cisplatin already assessed before by short-term cell growth/viability assays. In the case of NCI-H460-doxorubicin treated cells a very slight tendency to resist to the selecting drug than the parental population was verified, especially in resazurin-based assay (Figure 3.11). To test if this tendency was real NCI-H460-doxorubicin treated cells were exposed to a new cycle of therapy. The results revealed that the new period of therapy in NCI-H460-doxorubicin treated cells induced doxorubicin resistance when the resulted population (doxorubicin-resistant cell variant A - DRCVA) was compared to the original cells (Figure 3.16). We also exposed CRCVB to a new period of drug treatment to determine whether the resulting cell populations were even more drug resistant. The resulting cell population (cisplatin-resistant cell variant C - CRCVC) did not show increased resistance to cisplatin when compared to cisplatin-resistant cell variant B (Figure 3.15).

Resistance to therapy can be intrinsic or acquired. When tumours possess the capacity to survive therapy from the start of chemotherapy they are considered as intrinsically resistant. When tumour developed drug resistance during therapy, their resistance has been acquired [139]. Accounting to obtained results, chemotherapy induced tumour resistance. Cisplatin treatment resulted in an enrichment of a more cisplatin-resistant population than before, suggesting that resistance was acquired. However, it is not possible to understand if cisplatin treatment is responsible for enriching a pre-resistant sub-population, or if incubation with cisplatin induced adaptable changes in the most unstable cells, acquiring mechanism of resistance. CRCVA and CRCVB were the populations chosen as models to proceed with the rest of work since they showed to possess increased capacity to survive to chemotherapeutic agents.

In an attempt to verify if the cisplatin-resistant cell variants possess stem-like properties, expression of ABCG2 and CD133 stem cell related markers were assessed.

$CD133^+$ population and SP marked by ABCG2 are the most two important determinants of CSC phenotype for NCSLC [3, 7, 8]. In the present work, an increase in the % of cells expressing ABCG2 was found in both CRCVA and CRCVB when compared with NCI-H460 parental cells, although this was only statistically significant for CRCVB (Figure 3.21). The % of cells expressing CD133 also increased in CRCVB and CRCVA compared to parental cells, although these values were too low to attribute any relevant biological meaning. However, the percentage of cells expressing ABCG2 protein in CRCVA and especially in CRCVB after cisplatin exposure was found to be relevantly increased comparing the NCI-H460 parental cells (Figure 3.20). This was also confirmed when analysing ABCG2 gene expression levels by real-time qRT-PCR revealed to be up-regulated both in CRCVA (1.7 ± 0.2 FC) and especially in CRCVB (2.2 ± 0.1 FC) (Table 3.3). Hsieh *et al*, have already reported that cisplatin-resistant lung cancer cells possessed higher percentage of ABCG2 gene expression than the parental cell line. It is important to note that, in our study, different doses of cisplatin treatment resulted in different percentages of cells expressing ABCG2 protein.

Accounting that ABCG2 expression by itself is not sufficient to validate a population with stem-like properties, other stem markers were evaluated in this study. The gene expression of *Bmi-1*, *Sox2* and *ABCG2* were assessed by qRT-PCR. Bmi-1, a transcriptional repressor from polycomb family, is required for the self-renewal and post-natal maintenance of hematopoietic stem cells [140] and neural stem cells [141]. *Bmi-1* gene expression was found to be identically regulated between both resistant population and parental cells (Table 3.3). Sox2, an embryonic stem cell marker, was found to be up-regulated in a lung carcinoma SP comparing to non-SP [142]. The same group also reported that knocking down Sox2 expression resulted in a markedly decrease in the percentage of lung cancer-SP cells and in cells ability to migrate, suggesting that Sox2 plays an important role in the maintenance of CSC characteristics. [142]. In our study, *Sox2* gene expression was found to be identical between CRCVB and parental cells and down-regulated in CRCVA (-2.2±0.2 FC) (Table 3.3). Therefore, CRCVA and CRCVB did not show increased expression of the studied stemness related genes. It may, however, be important to assess expression of additional relevant genes.

Colony-forming assay was performed to evaluate if CRCVB possessed an enhanced capacity to generate tumour cell colonies than parental cells. It has already been reported

that a cisplatin-resistant population (created by cisplatin exposure) was enriched in stem-like cells and possessed the ability to generate larger colonies and in a greater number than parental cells [139]. However, our study revealed no statistically significant differences between the number of tumour colonies formed from CRCVB (63.1 % ± 7.6) and NCI-H460 parental cells (54.7 % ± 3.6), providing no evidence that the cisplatin-selected populations were enriched in stem-like cells.

An *in vivo* assay was also performed to measure the tumourigenecity of NCI-H460 parental cells and CRCVB, by inoculating three different numbers of cells in the CAM. Six chicken embryos were used for each condition, $1x10^6$, $1x10^5$ and $1x10^4$ inoculated cells for each population, however not all of them survived until the end of experiment, making it difficult to compare the tumourigenicity of both populations. Even so, it was possible to note that both populations possessed tumourigenicity ability when $1x10^6$ and $1x10^5$ cells were inoculated, however only CRCVB demonstrated ability to generate tumours when $1x10^4$ cells were inoculated in the CAM (Table 3.2). A tendency for CRCVB cells to generate bigger tumours than NCI-H460 parental cells was observed (Figure 3.22), although the fact that only one experiment was performed and that there were high levels of chicken embryo mortality, compromised the reliability of the obtained data. In order to diminish chicken embryo mortality it will be required to decrease the number of days between tumour cell inoculation in the CAM and dissection and tissue fixation. So far, results obtained indicate that the drug-selected cells may have increased tumourigenic capacity (as assessed when $1x10^4$ cells were inoculated in the CAM), and hence stem-like cell properties, although additional studies are required to confirm this.

Bearing this in mind, it seems reasonable to question whether increased ABCG2 expression found in both cisplatin-resistant cells was associated with a chemoresistance mechanism and not related to an indication of stemness properties. Hsieh *et al* already linked the ABCG2 protein as responsible to cisplatin efflux out of the cell and acquired resistance towards cisplatin therapy [139].

Nevertheless, even if we are not in the presence of cells with stem-like features, the results clearly show that chemotherapy enriched a population with higher ability to survive than before. Clinically, drug resistance means an important obstacle and reduces the survival rate of patients. Platinum-base chemotherapy, especially in combination with other drugs, is a common regimen to treat NSCLC [143]. Generally, the mechanism by

which cisplatin induces cell death is related to mitochondria mediated apoptosis. To verify if anti-apoptotic proteins were involved in the mechanism developed for cells after cisplatin exposure, Western blot to Bcl2, Bcl-XL and XIAP were performed. Bcl2 family of proteins can both promote (Bax, Bak, Bad, Bid, and Bcl-Xs dependent) or inhibit (Bcl2 and Bcl-XL) apoptosis through regulation of mitochondrial permeability and cytochrome c release [144]. XIAP, a member of IAP family proteins, also possesses the ability to inhibit apoptosis pathway by inhibition of caspases 3, 7 and 9 [145]. Both Bcl-2 and Bcl-XL were reported before as responsible to represses cell death triggered by cisplatin and to develop multidrug-resistance of human ovarian cancer cell lines [146]. Liu *et al*, in 2011 reported that XIAP gene silencing increased apoptosis and restricted the growth of NSCLC cells, resulting in increased chemosensitivity of those cells to cisplatin [147]. After Western blot analysis, an up-regulation of both Bcl-XL and XIAP proteins were observed in CRVCB but no alterations were observed in CRCVA comparing to NCI-H460 parental cells (Figures 3.17 and 3.18). No Bcl2 expression differences were detected between CRCVA, CRCVB and parental cells (Figure 3.17). It seems that after 2 μM of cisplatin treatment for three weeks followed by a drug-free recovery period induced cisplatin resistance and up-regulation of Bcl-XL and XIAP proteins (Figures 3.17 and 3.18), which probably reflects the developed mechanism of those cells to survive the selecting agent. However, when cells were exposed to the same conditions but using a lower dose of cisplatin (1 μM), the mechanism developed by cells to resist was different. Interestingly, the degree of chemoresistance of both cisplatin-resistant populations was found to be exactly the same (Figures 3.12, 3.13, respectively). Accounting that both populations possessed multi-drug resistance (Figure 3.14) the levels of both Pgp protein and *MDR1* gene expression were evaluated by western blot and RT-PCR, respectively. It was interesting to note that Pgp was 100% up-regulated in CRCVA comparing both to NCI-H460 parental cells and CRCVB as determined by Western blot analysis (Figure 3.18). Although Pgp protein has never be associated with a mechanism by which cells can have increased resistance to cisplatin, it has been considered to exert an important role in resistance to a wide range of cytotoxic drugs [148]. RT-PCR to *MDR1* gene, which encode to Pgp protein, was found to be enhanced in CRCVA (5.9 ± 2.6 FC) when compared to parental cells and even more up-regulated in CRCVB (10.2 ± 1.8 FC) comparing with parental cells (Table 3.3). The up-regulation of *MDR1* in CRCVB does not correspond to the levels of Pgp as determined by

Western blot, in the same population of cells. Pgp protein seemed to be underling the mechanism by which CRCVA resists therapy, although its increased presence in CRCVB was questionable after known that corresponding gene was up-regulated in those cells. In an attempt to investigate the possible role of Pgp protein in both populations, NCI-H460 parental cells, CRCVA and CRCVB were exposed to cisplatin during 24 hours and the expression of Pgp and P53 proteins were than assessed by Western blot. The results revealed no Pgp expression differences between NCI-H460 control and treated parental cells and CRCVB control and treated cells (Figure 3.19). This may mean that Pgp-mediated resistance was not activated in CRCVB when cells were exposed to the selecting agent. Although, the Pgp was found to be over-expressed in CRCVA treated cells when compared to CRCVA untreated cells (Figure 3.19). This suggested that Pgp protein really was behind the mechanisms by which these cells resist to therapy, being rapidly up-regulated after cells contacted with drug. It is, however, important to note that these results represent only a sing experience. It was not possible to understand the reason why CRCVB possessed enhanced basal levels of *MDR1* gene expression but equal levels of Pgp protein comparing to parental cells. This means that is not possible to conclude whether Pgp protein is responsible for drug efflux. It can be hypothesized that *MDR1* mRNA translation was being down-regulated, meaning that Pgp protein were not enhanced in CRCVB. It also may be possible that a post-transcriptional alteration occurred, such as protein targeting to degradation, or even alteration in the epitope recognized by Pgp antibody. In the last case, it is possible that Pgp is playing a role in drug efflux out of the cell. P53 expression results revealed that after cisplatin treatment the cells activate P53 protein (Figure 3.19). As CRCVA and CRCVB were significant more resistant to cisplatin than NCI-H460 parental cells, up-regulation of P53 was found to be lower in both resistant population when compared to parental cells.

5. Conclusions and future perspectives

Cancer treatment is often hampered by tumor resistance towards chemo and radiotherapy, being the CSCs partially responsible for that phenotype. The isolation and study of these cells is necessary to understand their properties and regulation, providing a way to identify possible targets to render them more sensitive to the chemotherapeutic drugs used in the clinic. In this project we aimed to isolate and characterize lung CSC populations taking into account the chemoresistance mechanisms of these cells and to identify potential therapeutic targets to overcome CSCs chemoresistance.

It was found that ABCG2 protein is present in about 10-16 % of the entire population of NCI-H460 cell line. This allowed the isolation of an $ABCG2^+$ population after fluoresce activated cell sorting been performed. Even so, it has been impossible to study the putative CSC population isolated because both $ABCG2^+$ and $ABCG2^-$ cells were rapidly capable to ressemble the original population.

Cisplatin or doxorubicin exposure during three weeks led to a transient alteration in cell morphology in A549 and NCI-H460 cell lines, acquiring a mesenchymal-like structure. After chemotherapeutic drugs were withrawn the initial morphology was regained. However only in NCI-H460 cells, cisplatin or doxorubicin treatment resulted in an acquired resistance towards the selecting agent when compared with the parental cells. Indeed, cisplatin treatment induced significant increased resistance towards the selecting drug but also resistance to doxorubicin and gemcitabine, although not for 5-FU.

Cisplatin treatment also enriched a population expressing higher levels of ABCG2 markers than before. Although, the increased number of cells expressing ABCG2 protein after 2 μM of drug exposure seemed to be the only one with biological relevance. It is not possible to conclude whether cisplatin was able to enrich a cell population with stem-like properties. It would be required to perform additional *in vivo* assays to measure the tumourigenesis of cisplatin-resistant and NCI-H460 parental cells.

Different doses of cisplatin treatment in the same cell line select different populations, however their capacity to resist to the selecting agent is identical. Anti-apoptotic proteins, such as Bcl-XL and XIAP, and drug efflux pumps, like *MDR1* gene and ABCG2, although not Pgp protein, were up-regulated after 2 μM cisplatin treatment. This possibly indicates that, in our cisplatin-resistant cells, Bcl-XL and XIAP proteins are

responsible for cell survival against cisplatin therapy. Pgp may also be partially responsible for the increased drug resistance although only up-regulation was observed in gene expression and not in protein expression. A post-transcriptional alteration could have affected the epitope recognized by Pgp antibody. Performing the rhodamine-based assay would clarify if Pgp function is enhanced in the CRCVB. Rhodamine is a fluorescent Pgp substrate widely used as a transporter dye to study multidrug transporters [149]. A more elucidative method would be silencing of Bcl-XL, XIAP or Pgp proteins and verify if cells reversed their resistant phenotype. Pgp protein and *MDR1* gene expression were both enhanced after 1μM of cisplatin treatment, but no signal of up-regulation of anti-apoptotic proteins were found. P-glycoprotein is normally related with a mechanism by which cells efflux drugs, although cisplatin has never been reported to be one of them. Silencing Pgp expression in this population and confirm that it sensitized those cells is also the best approach to validate Pgp protein as mechanism of cisplatin acquired resistance.

Besides Western bolt approaches, it would be extremely important to find out the global profile of the proteins present in the parental and resistant cells. 2-D electrophoresis is a powerful method used for the analysis of complex protein mixtures extracted from cells, tissues, or other biological samples. This technique allows the separation of proteins according to two independent properties in two different steps. Thousands of different proteins can thus be separated, and information such as the protein pI, the apparent molecular weight, and the amount of each protein can be obtained. We have already began this kind of experience and using this it would be possible to cross over the protein pattern distribution of NCI-H460 parental and resistant cells, which may provide the opportunity to discover new proteins involved in regulation of a more aggressive phenotype.

In summary, cisplatin treatment enriched resistant lung cancer cells that have increased drug resistance. It would be extremely important to understand the mechanisms underlying the chemoresistance phenotype in order to be able to overcome tumour resistance and relapse. Bcl-XL, XIAP and Pgp proteins appear to be potential therapeutic targets to chemosensitize lung cancer tumour cells, although this requires validation in future experiments. Therefore, RNA interference studies with siRNAs targeting the expression of these genes (independently or in combination) will be performed soon. The cells developed during this research may be used as models to develop specific therapeutic targets to overcome chemoresistance in lung cancer and improve patient survival.

6. References

1. Rapp, U.R., F. Ceteci, and R. Schreck, *Oncogene-induced plasticity and cancer stem cells.* Cell Cycle, 2008. **7**(1): p. 45-51.
2. Rivera, C., et al., *Lung cancer stem cell: new insights on experimental models and preclinical data.* J Oncol, 2011. **2011**: p. 549181.
3. Chen, Y.C., et al., *Oct-4 expression maintained cancer stem-like properties in lung cancer-derived CD133-positive cells.* Plos One, 2008. **3**(7): p. e2637.
4. Eramo, A., T.L. Haas, and R. De Maria, *Lung cancer stem cells: tools and targets to fight lung cancer.* Oncogene, 2010. **29**(33): p. 4625-35.
5. Levina, V., et al., *Drug-selected human lung cancer stem cells: cytokine network, tumorigenic and metastatic properties.* Plos One, 2008. **3**(8): p. e3077.
6. Jiang, F., et al., *Aldehyde dehydrogenase 1 is a tumor stem cell-associated marker in lung cancer.* Mol Cancer Res, 2009. **7**(3): p. 330-8.
7. Ho, M.M., et al., *Side population in human lung cancer cell lines and tumors is enriched with stem-like cancer cells.* Cancer Res, 2007. **67**(10): p. 4827-33.
8. Eramo, A., et al., *Identification and expansion of the tumorigenic lung cancer stem cell population.* Cell Death Differ, 2008. **15**(3): p. 504-14.
9. Tirino, V., et al., *The role of CD133 in the identification and characterisation of tumour-initiating cells in non-small-cell lung cancer.* Eur J Cardiothorac Surg, 2009. **36**(3): p. 446-53.
10. Klonisch, T., et al., *Cancer stem cell markers in common cancers - therapeutic implications.* Trends Mol Med, 2008. **14**(10): p. 450-60.
11. Sung, J.M., et al., *Characterization of a stem cell population in lung cancer A549 cells.* Biochem Biophys Res Commun, 2008. **371**(1): p. 163-7.
12. Li, F., H. Zeng, and K. Ying, *The combination of stem cell markers CD133 and ABCG2 predicts relapse in stage I non-small cell lung carcinomas.* Med Oncol, 2011. **28**(4): p. 1458-62.
13. Reya, T., et al., *Stem cells, cancer, and cancer stem cells.* Nature, 2001. **414**(6859): p. 105-11.
14. Bonnet, D. and J.E. Dick, *Human acute myeloid leukemia is organized as a hierarchy that originates from a primitive hematopoietic cell.* Nat Med, 1997. **3**(7): p. 730-7.
15. Al-Hajj, M., et al., *Prospective identification of tumorigenic breast cancer cells.* Proc Natl Acad Sci U S A, 2003. **100**(7): p. 3983-8.
16. Lapidot, T., et al., *A cell initiating human acute myeloid leukaemia after transplantation into SCID mice.* Nature, 1994. **367**(6464): p. 645-8.
17. Wicha, M.S., S. Liu, and G. Dontu, *Cancer stem cells: an old idea--a paradigm shift.* Cancer Res, 2006. **66**(4): p. 1883-90; discussion 1895-6.
18. Park, C.Y., D. Tseng, and I.L. Weissman, *Cancer stem cell-directed therapies: recent data from the laboratory and clinic.* Mol Ther, 2009. **17**(2): p. 219-30.
19. Scadden, D.T., *The stem-cell niche as an entity of action.* Nature, 2006. **441**(7097): p. 1075-9.
20. Alison, M.R. and S. Islam, *Attributes of adult stem cells.* J Pathol, 2009. **217**(2): p. 144-60.
21. Zhu, X., et al., *Cancer stem cell, niche and EGFR decide tumor development and treatment response: A bio-computational simulation study.* J Theor Biol, 2011. **269**(1): p. 138-49.
22. Clarke, M.F. and M. Fuller, *Stem cells and cancer: two faces of eve.* Cell, 2006. **124**(6): p. 1111-5.
23. Kitamura, H., et al., *Cancer stem cell: implications in cancer biology and therapy with special reference to lung cancer.* Lung Cancer, 2009. **66**(3): p. 275-81.

24. Lobo, N.A., et al., *The biology of cancer stem cells.* Annu Rev Cell Dev Biol, 2007. **23**: p. 675-99.
25. Yang, Y.M. and J.W. Chang, *Current status and issues in cancer stem cell study.* Cancer Invest, 2008. **26**(7): p. 741-55.
26. Li, L., L. Borodyansky, and Y. Yang, *Genomic instability en route to and from cancer stem cells.* Cell Cycle, 2009. **8**(7): p. 1000-2.
27. Price, J.E. and D. Tarin, *Low incidence of tumourigenicity in agarose colonies from spontaneous murine mammary tumours.* Differentiation, 1989. **41**(3): p. 202-7.
28. Sabbath, K.D., et al., *Heterogeneity of clonogenic cells in acute myeloblastic leukemia.* J Clin Invest, 1985. **75**(2): p. 746-53.
29. Bruce, W.R. and H. Van Der Gaag, *A Quantitative Assay for the Number of Murine Lymphoma Cells Capable of Proliferation in Vivo.* Nature, 1963. **199**: p. 79-80.
30. Park, C.H., D.E. Bergsagel, and E.A. McCulloch, *Mouse myeloma tumor stem cells: a primary cell culture assay.* J Natl Cancer Inst, 1971. **46**(2): p. 411-22.
31. Alison, M.R., S.M. Lim, and L.J. Nicholson, *Cancer stem cells: problems for therapy?* J Pathol, 2011. **223**(2): p. 147-61.
32. Coussens, L.M. and Z. Werb, *Inflammation and cancer.* Nature, 2002. **420**(6917): p. 860-7.
33. Alison, M.R., S. Lim, and J.M. Houghton, *Bone marrow-derived cells and epithelial tumours: more than just an inflammatory relationship.* Curr Opin Oncol, 2009. **21**(1): p. 77-82.
34. Nowell, P.C., *The clonal evolution of tumor cell populations.* Science, 1976. **194**(4260): p. 23-8.
35. Visvader, J.E. and G.J. Lindeman, *Cancer stem cells in solid tumours: accumulating evidence and unresolved questions.* Nat Rev Cancer, 2008. **8**(10): p. 755-68.
36. Chen, R., et al., *A hierarchy of self-renewing tumor-initiating cell types in glioblastoma.* Cancer Cell, 2010. **17**(4): p. 362-75.
37. Lonardo, E., P.C. Hermann, and C. Heeschen, *Pancreatic cancer stem cells - update and future perspectives.* Mol Oncol, 2010. **4**(5): p. 431-42.
38. Hermann, P.C., M.T. Mueller, and C. Heeschen, *Pancreatic cancer stem cells--insights and perspectives.* Expert Opin Biol Ther, 2009. **9**(10): p. 1271-8.
39. Graeber, T.G., et al., *Hypoxia-mediated selection of cells with diminished apoptotic potential in solid tumours.* Nature, 1996. **379**(6560): p. 88-91.
40. Brown, N.S. and R. Bicknell, *Hypoxia and oxidative stress in breast cancer. Oxidative stress: its effects on the growth, metastatic potential and response to therapy of breast cancer.* Breast Cancer Res, 2001. **3**(5): p. 323-7.
41. Wouters, B.G., et al., *Targeting hypoxia tolerance in cancer.* Drug Resist Updat, 2004. **7**(1): p. 25-40.
42. Garvalov, B.K. and T. Acker, *Cancer stem cells: a new framework for the design of tumor therapies.* J Mol Med (Berl), 2011. **89**(2): p. 95-107.
43. Pang, R., et al., *A subpopulation of CD26+ cancer stem cells with metastatic capacity in human colorectal cancer.* Cell Stem Cell, 2010. **6**(6): p. 603-15.
44. Mani, S.A., et al., *The epithelial-mesenchymal transition generates cells with properties of stem cells.* Cell, 2008. **133**(4): p. 704-15.
45. Woodhouse, E.C., R.F. Chuaqui, and L.A. Liotta, *General mechanisms of metastasis.* Cancer, 1997. **80**(8 Suppl): p. 1529-37.
46. Iwatsuki, M., et al., *Epithelial-mesenchymal transition in cancer development and its clinical significance.* Cancer Sci, 2010. **101**(2): p. 293-9.
47. Stylianou, S., R.B. Clarke, and K. Brennan, *Aberrant activation of notch signaling in human breast cancer.* Cancer Res, 2006. **66**(3): p. 1517-25.
48. Nishii, T., et al., *Cancer stem cell-like SP cells have a high adhesion ability to the peritoneum in gastric carcinoma.* Cancer Sci, 2009. **100**(8): p. 1397-402.

49. Hennessy, B.T., et al., *Characterization of a naturally occurring breast cancer subset enriched in epithelial-to-mesenchymal transition and stem cell characteristics.* Cancer Res, 2009. **69**(10): p. 4116-24.
50. Malanchi, I., et al., *Cutaneous cancer stem cell maintenance is dependent on beta-catenin signalling.* Nature, 2008. **452**(7187): p. 650-3.
51. Clement, V., et al., *HEDGEHOG-GLI1 signaling regulates human glioma growth, cancer stem cell self-renewal, and tumorigenicity.* Curr Biol, 2007. **17**(2): p. 165-72.
52. Richardson, G.D., et al., *CD133, a novel marker for human prostatic epithelial stem cells.* J Cell Sci, 2004. **117**(Pt 16): p. 3539-45.
53. Yu, S., et al., *Isolation and characterization of the CD133+ precursors from the ventricular zone of human fetal brain by magnetic affinity cell sorting.* Biotechnol Lett, 2004. **26**(14): p. 1131-6.
54. Mizrak, D., M. Brittan, and M.R. Alison, *CD133: molecule of the moment.* J Pathol, 2008. **214**(1): p. 3-9.
55. Schatton, T., et al., *Identification of cells initiating human melanomas.* Nature, 2008. **451**(7176): p. 345-9.
56. Cox, C.V., et al., *Characterization of acute lymphoblastic leukemia progenitor cells.* Blood, 2004. **104**(9): p. 2919-25.
57. Ishikawa, F., et al., *Chemotherapy-resistant human AML stem cells home to and engraft within the bone-marrow endosteal region.* Nat Biotechnol, 2007. **25**(11): p. 1315-21.
58. Prince, M.E., et al., *Identification of a subpopulation of cells with cancer stem cell properties in head and neck squamous cell carcinoma.* Proc Natl Acad Sci U S A, 2007. **104**(3): p. 973-8.
59. Patrawala, L., et al., *Highly purified CD44+ prostate cancer cells from xenograft human tumors are enriched in tumorigenic and metastatic progenitor cells.* Oncogene, 2006. **25**(12): p. 1696-708.
60. Li, C., et al., *Identification of pancreatic cancer stem cells.* Cancer Res, 2007. **67**(3): p. 1030-7.
61. Singh, S.K., et al., *Identification of a cancer stem cell in human brain tumors.* Cancer Res, 2003. **63**(18): p. 5821-8.
62. O'Brien, C.A., et al., *A human colon cancer cell capable of initiating tumour growth in immunodeficient mice.* Nature, 2007. **445**(7123): p. 106-10.
63. Ricci-Vitiani, L., et al., *Identification and expansion of human colon-cancer-initiating cells.* Nature, 2007. **445**(7123): p. 111-5.
64. Todaro, M., et al., *Colon cancer stem cells dictate tumor growth and resist cell death by production of interleukin-4.* Cell Stem Cell, 2007. **1**(4): p. 389-402.
65. Hermann, P.C., et al., *Distinct populations of cancer stem cells determine tumor growth and metastatic activity in human pancreatic cancer.* Cell Stem Cell, 2007. **1**(3): p. 313-23.
66. Bao, S., et al., *Glioma stem cells promote radioresistance by preferential activation of the DNA damage response.* Nature, 2006. **444**(7120): p. 756-60.
67. Chen, K.L., et al., *Highly enriched CD133(+)CD44 (+) stem-like cells with CD133.* Clin Exp Metastasis, 2011. **28**(8): p. 751-63.
68. Armstrong, L., et al., *Phenotypic characterization of murine primitive hematopoietic progenitor cells isolated on basis of aldehyde dehydrogenase activity.* Stem Cells, 2004. **22**(7): p. 1142-51.
69. Hess, D.A., et al., *Functional characterization of highly purified human hematopoietic repopulating cells isolated according to aldehyde dehydrogenase activity.* Blood, 2004. **104**(6): p. 1648-55.
70. Hess, D.A., et al., *Selection based on CD133 and high aldehyde dehydrogenase activity isolates long-term reconstituting human hematopoietic stem cells.* Blood, 2006. **107**(5): p. 2162-9.

71. Cheung, A.M., et al., *Aldehyde dehydrogenase activity in leukemic blasts defines a subgroup of acute myeloid leukemia with adverse prognosis and superior NOD/SCID engrafting potential.* Leukemia, 2007. **21**(7): p. 1423-30.
72. Pearce, D.J., et al., *Characterization of cells with a high aldehyde dehydrogenase activity from cord blood and acute myeloid leukemia samples.* Stem Cells, 2005. **23**(6): p. 752-60.
73. Ginestier, C., et al., *ALDH1 is a marker of normal and malignant human mammary stem cells and a predictor of poor clinical outcome.* Cell Stem Cell, 2007. **1**(5): p. 555-67.
74. Dylla, S.J., et al., *Colorectal cancer stem cells are enriched in xenogeneic tumors following chemotherapy.* Plos One, 2008. **3**(6): p. e2428.
75. Ding, X.W., J.H. Wu, and C.P. Jiang, *ABCG2: a potential marker of stem cells and novel target in stem cell and cancer therapy.* Life Sci, 2010. **86**(17-18): p. 631-7.
76. Wu, C. and B.A. Alman, *Side population cells in human cancers.* Cancer Lett, 2008. **268**(1): p. 1-9.
77. Hirschmann-Jax, C., et al., *A distinct "side population" of cells in human tumor cells: implications for tumor biology and therapy.* Cell Cycle, 2005. **4**(2): p. 203-5.
78. Hirschmann-Jax, C., et al., *A distinct "side population" of cells with high drug efflux capacity in human tumor cells.* Proc Natl Acad Sci U S A, 2004. **101**(39): p. 14228-33.
79. Louie, E., et al., *Identification of a stem-like cell population by exposing metastatic breast cancer cell lines to repetitive cycles of hypoxia and reoxygenation.* Breast Cancer Res, 2010. **12**(6): p. R94.
80. Morrison, R., et al., *Targeting the mechanisms of resistance to chemotherapy and radiotherapy with the cancer stem cell hypothesis.* J Oncol, 2011. **2011**: p. 941876.
81. Li, T., et al., *ALDH1A1 is a marker for malignant prostate stem cells and predictor of prostate cancer patients' outcome.* Lab Invest, 2010. **90**(2): p. 234-44.
82. Chen, Y.C., et al., *Aldehyde dehydrogenase 1 is a putative marker for cancer stem cells in head and neck squamous cancer.* Biochem Biophys Res Commun, 2009. **385**(3): p. 307-13.
83. Eyler, C.E. and J.N. Rich, *Survival of the fittest: cancer stem cells in therapeutic resistance and angiogenesis.* J Clin Oncol, 2008. **26**(17): p. 2839-45.
84. Woodward, W.A., et al., *WNT/beta-catenin mediates radiation resistance of mouse mammary progenitor cells.* Proc Natl Acad Sci U S A, 2007. **104**(2): p. 618-23.
85. Mueller, M.T., et al., *Combined targeted treatment to eliminate tumorigenic cancer stem cells in human pancreatic cancer.* Gastroenterology, 2009. **137**(3): p. 1102-13.
86. Frosina, G., *DNA repair in normal and cancer stem cells, with special reference to the central nervous system.* Curr Med Chem, 2009. **16**(7): p. 854-66.
87. Diehn, M., et al., *Association of reactive oxygen species levels and radioresistance in cancer stem cells.* Nature, 2009. **458**(7239): p. 780-3.
88. Vlashi, E., W.H. McBride, and F. Pajonk, *Radiation responses of cancer stem cells.* J Cell Biochem, 2009. **108**(2): p. 339-42.
89. Dean, M., *ABC transporters, drug resistance, and cancer stem cells.* J Mammary Gland Biol Neoplasia, 2009. **14**(1): p. 3-9.
90. Gatti, L., et al., *ABC transporters as potential targets for modulation of drug resistance.* Mini Rev Med Chem, 2009. **9**(9): p. 1102-12.
91. Saelens, X., et al., *Toxic proteins released from mitochondria in cell death.* Oncogene, 2004. **23**(16): p. 2861-74.
92. LaCasse, E.C., et al., *IAP-targeted therapies for cancer.* Oncogene, 2008. **27**(48): p. 6252-75.
93. Vellanki, S.H., et al., *Small-molecule XIAP inhibitors enhance gamma-irradiation-induced apoptosis in glioblastoma.* Neoplasia, 2009. **11**(8): p. 743-52.
94. Ji, Q., et al., *MicroRNA miR-34 inhibits human pancreatic cancer tumor-initiating cells.* Plos One, 2009. **4**(8): p. e6816.

95. Shiras, A., et al., *Spontaneous transformation of human adult nontumorigenic stem cells to cancer stem cells is driven by genomic instability in a human model of glioblastoma.* Stem Cells, 2007. **25**(6): p. 1478-89.
96. Pang, R.W. and R.T. Poon, *From molecular biology to targeted therapies for hepatocellular carcinoma: the future is now.* Oncology, 2007. **72 Suppl 1**: p. 30-44.
97. Campos, B., et al., *Differentiation therapy exerts antitumor effects on stem-like glioma cells.* Clin Cancer Res, 2010. **16**(10): p. 2715-28.
98. Artavanis-Tsakonas, S., M.D. Rand, and R.J. Lake, *Notch signaling: cell fate control and signal integration in development.* Science, 1999. **284**(5415): p. 770-6.
99. Phillips, T.M., W.H. McBride, and F. Pajonk, *The response of CD24(-/low)/CD44+ breast cancer-initiating cells to radiation.* J Natl Cancer Inst, 2006. **98**(24): p. 1777-85.
100. Scharpfenecker, M., et al., *Ionizing radiation shifts the PAI-1/ID-1 balance and activates notch signaling in endothelial cells.* Int J Radiat Oncol Biol Phys, 2009. **73**(2): p. 506-13.
101. Fan, X., et al., *Notch pathway inhibition depletes stem-like cells and blocks engraftment in embryonal brain tumors.* Cancer Res, 2006. **66**(15): p. 7445-52.
102. Fan, X., et al., *NOTCH pathway blockade depletes CD133-positive glioblastoma cells and inhibits growth of tumor neurospheres and xenografts.* Stem Cells, 2010. **28**(1): p. 5-16.
103. Zhao, C., et al., *Hedgehog signalling is essential for maintenance of cancer stem cells in myeloid leukaemia.* Nature, 2009. **458**(7239): p. 776-9.
104. Gazdar, A.F., et al., *Establishment of continuous, clonable cultures of small-cell carcinoma of lung which have amine precursor uptake and decarboxylation cell properties.* Cancer Res, 1980. **40**(10): p. 3502-7.
105. Almeida, G.M., et al., *Multiple end-point analysis reveals cisplatin damage tolerance to be a chemoresistance mechanism in a NSCLC model: implications for predictive testing.* Int J Cancer, 2008. **122**(8): p. 1810-9.
106. Zalatnai, A. and J. Molnar, *Review. Molecular background of chemoresistance in pancreatic cancer.* In Vivo, 2007. **21**(2): p. 339-47.
107. Siddik, Z.H., *Cisplatin: mode of cytotoxic action and molecular basis of resistance.* Oncogene, 2003. **22**(47): p. 7265-79.
108. Mini, E., et al., *Cellular pharmacology of gemcitabine.* Ann Oncol, 2006. **17 Suppl 5**: p. v7-12.
109. Carvalho, C., et al., *Doxorubicin: the good, the bad and the ugly effect.* Curr Med Chem, 2009. **16**(25): p. 3267-85.
110. Noordhuis, P., et al., *5-Fluorouracil incorporation into RNA and DNA in relation to thymidylate synthase inhibition of human colorectal cancers.* Ann Oncol, 2004. **15**(7): p. 1025-32.
111. Polyak, K. and R.A. Weinberg, *Transitions between epithelial and mesenchymal states: acquisition of malignant and stem cell traits.* Nat Rev Cancer, 2009. **9**(4): p. 265-73.
112. Jung, J.W., et al., *Ionising radiation induces changes associated with epithelial-mesenchymal transdifferentiation and increased cell motility of A549 lung epithelial cells.* Eur J Cancer, 2007. **43**(7): p. 1214-24.
113. Ngan, C.Y., et al., *Quantitative evaluation of vimentin expression in tumour stroma of colorectal cancer.* Br J Cancer, 2007. **96**(6): p. 986-92.
114. Kowalski, P.J., M.A. Rubin, and C.G. Kleer, *E-cadherin expression in primary carcinomas of the breast and its distant metastases.* Breast Cancer Res, 2003. **5**(6): p. R217-22.
115. Peinado, H., D. Olmeda, and A. Cano, *Snail, Zeb and bHLH factors in tumour progression: an alliance against the epithelial phenotype?* Nat Rev Cancer, 2007. **7**(6): p. 415-28.
116. Kajiyama, H., et al., *Chemoresistance to paclitaxel induces epithelial-mesenchymal transition and enhances metastatic potential for epithelial ovarian carcinoma cells.* Int J Oncol, 2007. **31**(2): p. 277-83.

117. Thomson, S., et al., *Epithelial to mesenchymal transition is a determinant of sensitivity of non-small-cell lung carcinoma cell lines and xenografts to epidermal growth factor receptor inhibition.* Cancer Res, 2005. **65**(20): p. 9455-62.
118. Blobe, G.C., W.P. Schiemann, and H.F. Lodish, *Role of transforming growth factor beta in human disease.* N Engl J Med, 2000. **342**(18): p. 1350-8.
119. Batlle, E., et al., *The transcription factor snail is a repressor of E-cadherin gene expression in epithelial tumour cells.* Nat Cell Biol, 2000. **2**(2): p. 84-9.
120. Park, S.M., et al., *The miR-200 family determines the epithelial phenotype of cancer cells by targeting the E-cadherin repressors ZEB1 and ZEB2.* Genes Dev, 2008. **22**(7): p. 894-907.
121. Ma, L., J. Teruya-Feldstein, and R.A. Weinberg, *Tumour invasion and metastasis initiated by microRNA-10b in breast cancer.* Nature, 2007. **449**(7163): p. 682-8.
122. Vichai, V. and K. Kirtikara, *Sulforhodamine B colorimetric assay for cytotoxicity screening.* Nat Protoc, 2006. **1**(3): p. 1112-6.
123. Ribatti, D., *The Chick Embryo Chorioallantoic Membrane as an In Vivo Assay to Study Angiogenesis.* Pharmaceuticals, 2010. **3**: p. 482-513.
124. Hagedorn, M., et al., *Accessing key steps of human tumor progression in vivo by using an avian embryo model.* Proc Natl Acad Sci U S A, 2005. **102**(5): p. 1643-8.
125. Prazeres, H., et al., *Chromosomal, epigenetic and microRNA-mediated inactivation of LRP1B, a modulator of the extracellular environment of thyroid cancer cells.* Oncogene, 2011. **30**(11): p. 1302-17.
126. Burnette, W.N., *"Western blotting": electrophoretic transfer of proteins from sodium dodecyl sulfate--polyacrylamide gels to unmodified nitrocellulose and radiographic detection with antibody and radioiodinated protein A.* Anal Biochem, 1981. **112**(2): p. 195-203.
127. Bustin, S.A., et al., *Quantitative real-time RT-PCR--a perspective.* J Mol Endocrinol, 2005. **34**(3): p. 597-601.
128. Chaurasia, P., D. Berenzon, and R. Hoffman, *Chromatin-modifying agents promote the ex vivo production of functional human erythroid progenitor cells.* Blood, 2011. **117**(17): p. 4632-41.
129. Que, J., et al., *Multiple dose-dependent roles for Sox2 in the patterning and differentiation of anterior foregut endoderm.* Development, 2007. **134**(13): p. 2521-31.
130. Rutledge, R.G. and C. Cote, *Mathematics of quantitative kinetic PCR and the application of standard curves.* Nucleic Acids Res, 2003. **31**(16): p. e93.
131. Stewart, D.J., *Tumor and host factors that may limit efficacy of chemotherapy in non-small cell and small cell lung cancer.* Crit Rev Oncol Hematol, 2010. **75**(3): p. 173-234.
132. Doyle, L.A., et al., *A multidrug resistance transporter from human MCF-7 breast cancer cells.* Proc Natl Acad Sci U S A, 1998. **95**(26): p. 15665-70.
133. Patrawala, L., et al., *Side population is enriched in tumorigenic, stem-like cancer cells, whereas ABCG2+ and ABCG2- cancer cells are similarly tumorigenic.* Cancer Res, 2005. **65**(14): p. 6207-19.
134. Thiery, J.P. and J.P. Sleeman, *Complex networks orchestrate epithelial-mesenchymal transitions.* Nat Rev Mol Cell Biol, 2006. **7**(2): p. 131-42.
135. Sun, L., et al., *MiR-200b and miR-15b regulate chemotherapy-induced epithelial-mesenchymal transition in human tongue cancer cells by targeting BMI1.* Oncogene, 2012. **31**(4): p. 432-45.
136. Singh, A. and J. Settleman, *EMT, cancer stem cells and drug resistance: an emerging axis of evil in the war on cancer.* Oncogene, 2010. **29**(34): p. 4741-51.
137. Zhuo, W.L., et al., *Short interfering RNA directed against TWIST, a novel zinc finger transcription factor, increases A549 cell sensitivity to cisplatin via MAPK/mitochondrial pathway.* Biochem Biophys Res Commun, 2008. **369**(4): p. 1098-102.

138. Valdes, F., et al., *The epithelial mesenchymal transition confers resistance to the apoptotic effects of transforming growth factor Beta in fetal rat hepatocytes.* Mol Cancer Res, 2002. **1**(1): p. 68-78.
139. Hsieh, J.L., et al., *Acquisition of an enhanced aggressive phenotype in human lung cancer cells selected by suboptimal doses of cisplatin following cell deattachment and reattachment.* Cancer Lett, 2012. **321**(1): p. 36-44.
140. Lessard, J., Baban, S. &Sauvangeau, G., *Stage-specific expression of Polycomb group genes in human bone narrow cells.* Blood, 1999. **91**: p. 1216-1224.
141. Molofsky, A.V., et al., *Bmi-1 dependence distinguishes neural stem cell self-renewal from progenitor proliferation.* Nature, 2003. **425**(6961): p. 962-7.
142. Xiang, R., et al., *Downregulation of transcription factor SOX2 in cancer stem cells suppresses growth and metastasis of lung cancer.* Br J Cancer, 2011. **104**(9): p. 1410-7.
143. Mirshahidi, H.R. and C.T. Hsueh, *Updates in non-small cell lung cancer--insights from the 2009 45th annual meeting of the American Society of Clinical Oncology.* J Hematol Oncol, 2010. **3**: p. 18.
144. Gross, A., J.M. McDonnell, and S.J. Korsmeyer, *BCL-2 family members and the mitochondria in apoptosis.* Genes Dev, 1999. **13**(15): p. 1899-911.
145. Salvesen, G.S. and C.S. Duckett, *IAP proteins: blocking the road to death's door.* Nat Rev Mol Cell Biol, 2002. **3**(6): p. 401-10.
146. Yu, L. and Z. Wang, *Difference in expression of Bcl-2 and Bcl-xl genes in cisplatin-sensitive and cisplatin-resistant human in ovarian cancer cell lines.* J Huazhong Univ Sci Technolog Med Sci, 2004. **24**(2): p. 151-3.
147. Liu, Y., et al., *Silencing of X-linked inhibitor of apoptosis decreases resistance to cisplatin and paclitaxel but not gemcitabine in non-small cell lung cancer.* J Int Med Res, 2011. **39**(5): p. 1682-92.
148. Childs, S. and V. Ling, *The MDR superfamily of genes and its biological implications.* Important Adv Oncol, 1994: p. 21-36.
149. Shapiro, A.B. and V. Ling, *The mechanism of ATP-dependent multidrug transport by P-glycoprotein.* Acta Physiol Scand Suppl, 1998. **643**: p. 227-34.